DEVELOPMENT AND VALIDATION OF A DRY-FIBER BUNDLE TEST METHOD

by

Dallas Warren Parkins Jr.

A thesis submitted in partial fulfillment
of the requirements for the degree

of

Master of Science

in

Chemical Engineering

MONTANA STATE UNIVERSITY – BOZEMAN
Bozeman, Montana

May 2000

APPROVAL

of a thesis submitted by

Dallas Warren Parkins Jr.

This thesis has been read by each member of the thesis committee and has been found to be satisfactory regarding content, English usage, format, citations, bibliographic style, and consistency, and is ready for submission to the College of Graduate Studies.

Dr. Douglas Cairns _____ _____
(Signature) Date

Dr. John Sears _____ _____
(Signature) Date

Approved for the Department of Chemical Engineering

Dr. John Sears _____ _____
(Signature) Date

Approved for the College of Graduate Studies

Dr. Bruce McLeod _____ _____
(Signature) Date

STATEMENT OF PERMISSION TO USE

In presenting this thesis in partial fulfillment of the requirements for a master's degree at Montana State University-Bozeman, I agree that the Library shall make it available to borrowers under rules of the Library.

If I have indicated my intention to copyright this thesis by including a copyright notice page, copying is allowable only for scholarly purposes, consistent with "fair use" as prescribed in the U.S. Copyright Law. Requests for permission for extended quotation from or reproduction of this thesis in whole or in parts may be granted only by the copyright holder.

Signature_____

Date_____

ACKNOWLEDGEMENTS

The author wishes to acknowledge the assistance and support of several individuals and companies in the completion of this research. Dr. Doug Cairns provided much appreciated guidance throughout the course of this project. The Office of Naval Research funded a large portion of this research. Hexcel® Corporation provided carbon-fiber samples and the epoxy matrix materials used, along with other technical support. Amoco® Polymers provided certified carbon-fiber samples. Henkel Adhesives provided sample quantities of Macromelt® 6300 hot melt glue. Dr. E. M. Wu provided his expertise and suggestions about theoretical and statistical matters. Dan Samborsky aided with test equipment setup and training, and provided some statistical assistance. Gunder and Sue McCombs, owners of Hi-Tech Motor Sports in Billings, Montana, allowed full use of their shop facilities when needed. This allowed research to be completed in a timelier manner. Dallas and Marlene Parkins, parents of the author and owners of Farm Aid Equipment Company in Billings, Montana, contributed immeasurable support and complete use of their business and shop facilities. This enabled completion of the research in a far more expedient manner than would have been realized otherwise.

Each of these individuals and companies contributed in varying degrees to the completion of this research project. The author gratefully acknowledges each contributor and offers his sincere thanks.

TABLE OF CONTENTS

TABLE OF CONTENTS -- Continued

TABLE OF CONTENTS -- Continued

LIST OF TABLES

LIST OF TABLES Continued

LIST OF FIGURES

LIST OF FIGURES - Continued

LIST OF FIGURES - Continued

LIST OF FIGURES - Continued

ABSTRACT

It is desirable to use the constitutive properties of the carbon fibers and matrix materials to model carbon-fiber composite primary structures. A database of reliable constitutive properties for carbon-fiber bundles is needed. However, in the hierarchy of analysis for carbon fibers, dry bundle testing has been essentially cast aside or ignored because of inherent difficulties associated with it. Substantial efforts have been put into theoretical aspects of fibers grouped as bundles. Much of this work has involved theoretical and experimental results of unidirectional composites that were correlated to represent dry-fiber bundles. Results from a reliable dry-fiber bundle test method could be used to directly find strength distribution functions for dry-fiber bundles rather than indirectly correlating impregnated-fiber bundle test results.

The parameters needed for ideal dry-fiber bundle testing were explored and established. A dry-fiber bundle test method was developed to meet the necessary parameters as ideally as possible. The method incorporated test fixtures that were used to mold tabs onto the fiber-bundle ends as well as maintain the alignment and integrity of the specimens through final testing. The test fixtures were designed to insure alignment of the specimens in the test machine and yet cause no interference during testing. Over 600 dry-fiber bundle tests were completed using sized and unsized samples of Hexcel® AS-4 and Amoco® T300 fibers.

A method was developed to impregnate the carbon-fiber bundles with Hexcel® 3501-6 and 8552 epoxies in a laboratory. The method used a plate press that used both air pressure and vacuum to produce high quality impregnated specimens. Testing the cured specimens incorporated the test fixtures that were used for the dry-fiber bundle tests. Each of the fiber types that were tested as dry bundles was separately impregnated with both 3501-6 and 8552 epoxies. Over 600 impregnated-fiber bundle specimens were prepared and tested.

The groups of test results were analyzed for relevant information. The coefficients of variation indicated that variability in the test results was due to variability of the samples and apparently not induced by the test method. The corresponding dry and impregnated test results were compared statistically. The test method appeared successful.

CHAPTER 1

INTRODUCTION

Composites and other advanced materials are being used for modern primary structures to achieve superior performance. Before advanced materials can be used for primary structure in applications such as aircraft and aerospace, the materials must be qualified for use by undergoing substantial testing. For composites, the constituent components and the processing procedures both induce significantly different constitutive behaviors and strength properties. Consequently, qualification of a composite necessitates characterization from either the perspective of analyzing the composite or the perspective of analyzing the constituent materials. The constituent components of the composites of interest here are fiber and matrix. A database of properties must be compiled whether characterization is achieved through analysis of the composite or analysis of the constituents. However, if characterization is achieved by analysis of the constituents, further analysis may be necessary to relate constitutive and strength properties to those of a composite.

Composites of continuous fiber and polymer matrix form an important class of advanced materials for primary structure. These are especially important in high-performance applications, such as aircraft and aerospace structures. Due to excellent strength-to-weight ratios, fiber-reinforced-polymer-matrix composites are able to provide

superior performance in many areas. The typical hierarchical approach to application of these materials begins with material property characterization of the constituents and carries through to the characterization of structural test articles and analysis of in-service data. The overall intention of this research is to identify and quantify more meaningful parameters to enhance understanding of each hierarchical level. This aids in the characterization of constituent materials as well as their composites.

This research is a component of the first phase of a two-phase project, which entails fiber and resin characterization through laminate characterization of fiber dominated strength properties. The first phase primarily involves characterization of fiber and matrix properties. This is then extended as the materials are combined for composite tests. One of the goals of Phase I is the development of the second phase program as an extension of foundation work completed during Phase I to be employed for structural qualification of composites.

The materials that are central to this research are Amoco® T300 and Hexcel® AS-4, both of which are carbon fibers. The hierarchy of analysis for carbon fibers is (*i*) internal carbon structure, (*ii*) crystalline orientation within single filaments, (*iii*) single filament tensile tests, (*iv*) dry bundle tensile tests, (*v*) impregnated bundle tests, (*vi*) composite tests, (v*ii*) representative part tests, either small or full scale, and (*viii*) analysis of in-service data. Of these, dry bundle testing has been essentially cast aside or ignored because of inherent difficulties associated with it. Single filament tests yield useful information, but are tedious and require a great deal of care. Furthermore, many tests must be conducted to obtain a statistically significant database. A dry bundle test method that produces reliable results that could be correlated with single filament test results

would be quite useful. Dry bundle tests could be implemented to reliably collect useful constitutive information in industrial test facilities as well as in research test facilities.

Substantial efforts have been put into theoretical aspects of fibers grouped as bundles. Much of this work has involved theoretical and experimental results of impregnated-fiber bundles or unidirectional composites. These results were then correlated through theory to obtain results for dry-fiber bundles. This approach requires assumptions and other considerations to account for the effects contributed by the matrix and processing variables. Development of a reliable dry bundle test method would provide empirical results to eliminate the induction such of assumption-based problems. The interface between theoretical and experimental results would benefit by elimination of these assumption-based problems. The need for reliable dry-bundle test results provides the impetus of the present research.

Research Objective

The rather broad scope of this research is encompassed by the following research objective:

> Develop a dry-bundle test and validate it experimentally by comparison to impregnated-bundle tests.

The main research objective includes the following five sub-objectives due to the broad scope of this research:

1. Develop a reliable dry-bundle test method for carbon fiber bundles.
2. Verify the reliability of the dry-bundle test method.
3. Develop and verify an impregnated-bundle test method

4. Statistically compare dry and impregnated test results
5. Compile dependable material properties for Hexcel® AS-4 and Amoco® T300 carbon fiber bundles.

Each of these sub-objectives will be discussed next with the additional information necessary to clarify the extents of the sub-objectives and the required tasks involved. There is naturally some amount of overlap among the sub-objectives due to their combined focus on the overall objective.

Develop a Reliable Dry-Bundle Test Method for Carbon Fiber Bundles

This first objective required research of the existing test methods for fiber bundles to find what methods were in use and their basic principles. It was also necessary to explore the most basic aspects of dry-bundle testing to find areas where problems could potentially lead to unreliable results. Development was based on idealizing as many parameters as possible and the methods were designed to adhere to the idealistic parameters within realistic reason.

Verify the Reliability of the Dry-Bundle Test Method

Verification of the reliability of the method was a matter of actual testing both dry and impregnated bundles of carbon fibers to obtain data using the test methods. Statistical analysis of the data was necessary to determine if the test method yielded results with a minimum of test-related scatter. It was essential to keep in mind the variability that is inherent to carbon fiber, regardless of it being a single filament, a dry bundle or part of a composite material. Constitutive and failure properties were explored, including dissipated strain energy density.

Develop and Verify an Impregnated-Bundle Test Method

There was a need to develop a method to impregnate and test fiber bundles in the laboratory to effectively explore the behaviors of different fiber and matrix combinations. This was important because using only pre-impregnated fibers prepared by their respective manufacturers could limit the fiber and matrix combinations that could be tested. It is understandable that a company that produces fibers and matrix materials would be apprehensive about impregnating their fiber product with a competitor's matrix product or vice versa. Also, setting up a process to impregnate the small amount of impregnated fiber needed for research purposes would be an incredible inconvenience for a large production facility. Another problem with the inability to produce impregnated fibers in the laboratory would be availability of the pre-impregnated fiber bundles within a reasonable timeframe. The flexibility necessary for research to be conducted in a timely manner would be greatly hampered if the research were dependent on industrial production schedules. Clearly, it was necessary to develop a laboratory method to produce impregnated-fiber bundles.

The test method was a matter of developing methods that could incorporate the equipment available for use. Statistical methods were used for verification of the impregnated test methods.

Statistically Compare Dry and Impregnated Test Results

It was important to statistically compare the test results of the testing of dry and impregnated bundles. One motivation for the comparison was that much of the theoretical background work correlates impregnated-bundle test results to theoretical dry-

bundle results through various assumptions. A statistically significant amount of test data for both dry and impregnated specimens of the same fibers would allow validation of some of the theoretical methods that exist. This sub-objective is also incorporated as part of the second sub-objective.

Compile Dependable Material Properties for Hexcel® AS-4 and Amoco® T300 Carbon Fiber Bundles

It was desired to compile statistically dependable material properties for Hexcel® AS-4 and Amoco® T300 carbon fiber bundles in both the dry and impregnated form. These material properties could be used to find a relationship between bundle properties and material properties of full-sized composite structures.

CHAPTER 2

BACKGROUND

The background for this research essentially involves three interrelated areas, fiber and matrix composite materials, dry-fiber bundle theory and testing, and impregnated-fiber bundle theory and testing. Dry-fiber bundle theory and testing is of primary concern to this research. However, since little direct dry-fiber bundle testing has been done for carbon fiber, most of the information pertains to theoretical aspects of dry carbon fiber bundles and is correlated through tests and theory of carbon-fiber composites or impregnated carbon fiber bundles. It is therefore necessary to first delve into the subject of fiber and matrix composite materials first to understand much of the theoretical work that involves dry-fiber bundles.

Composite Materials

The composite materials of concern to this project have constituent components of fibers and matrix. From here forth, references to composites or composite materials refer to continuous fiber reinforced polymer composite materials, unless otherwise noted. The fibers of a composite provide the bulk of the strength while the matrix acts as a binder to hold the fibers in position and transfer loads between fibers. Common fiber materials used in these composites are glass fibers and carbon fibers. The matrix

materials are typically polyesters, vinylesters, polyurethanes, or epoxies, depending on the particular application. The application dictates which combination of fiber and matrix material is used. Widely used, glass fiber and polyester composites are cost effective and structurally sufficient for a broad variety of applications. There are many applications, however, that have far more stringent strength and weight requirements. Many of these applications are in the aircraft and aerospace industry and require the properties of carbon fiber and epoxy composites regardless of the greater expense. These carbon fiber and epoxy composites are the ones of interest with regard to this research.

Even though there are differences in material properties in the range of fiber and matrix composites, they all behave similarly in tension. Much effort has been expended for statistical modeling of unidirectional composites. Talreja [1] stated that this effort is justified since the basic element of laminates is a unidirectional layer, which facilitates the determination of the final failure event. Uniaxial tension is a tensile load parallel with the fiber direction of a unidirectional composite. When a unidirectional composite is subjected to uniaxial tension, it is assumed that the strain throughout the composite is uniform until fibers break at weak or flawed areas. When individual fibers break, they become ineffective as load carriers in the immediate vicinity of the break. The broken fibers' share of the load is transferred through the fiber/matrix interphase and matrix to neighboring fibers. As more failures occur throughout the composite and fiber lengths become shorter, the composite becomes more dependent on the ability of the matrix to bridge the areas where fiber breaks have appeared. Therefore, a shear failure of the fiber/matrix interphase or the matrix results in the overall failure of the composite. A model known as the "chain of bundles model" was developed by Rosen [2] to describe

the behavior of fiber composites in tension and has been used by many researchers since. This model treats each fiber as a chain of fiber links. The length of each link is defined as the length that is required for the load to be transferred around the broken area of the fiber. This length is called the ineffective length δ and is illustrated in Figure 2.1. Gao and Reifsnider [3] state that the ineffective length δ is fundamentally dependent on the properties of the fibers, the matrix, and the interphase region. A larger unidirectional

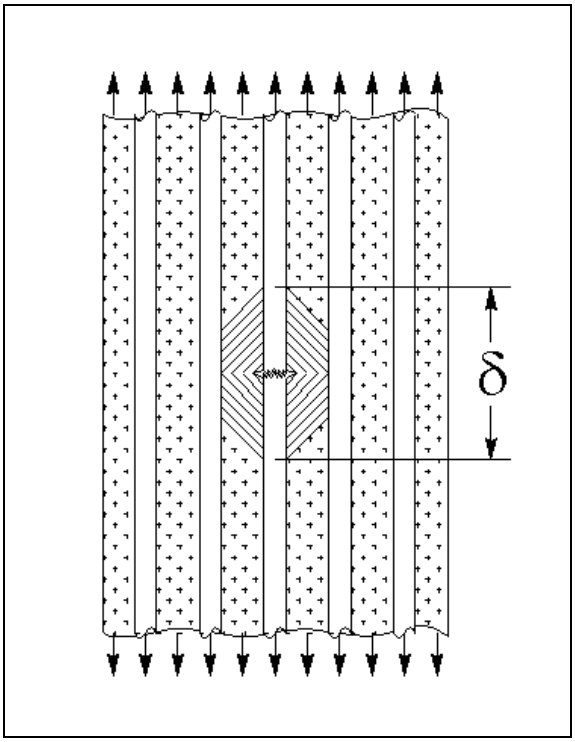

Figure 2.1. The ineffective length, δ, as defined by Rosen's chain of bundles model

composite can be thought of as many of these chains side-by-side, all having links of length δ. Each layer is considered a bundle of the fiber links. The statistical strength distribution of the links is considered to be equivalent to the statistical distribution of

flaws in the fibers. This means that longer chains of fibers have a higher probability of having a weaker link than shorter chains. This not only makes sense intuitively, Rosen [2] states that it also agrees with experimental results.

When a fiber within a bundle breaks, the remaining fibers must share the load that is no longer sustained by the broken fiber. Two load sharing rules have been examined extensively, the equal load-sharing rule (ELS rule), and the local load-sharing rule (LLS rule). The ELS considers the case in which all of the surviving fibers equally bear a share of the load no longer taken by the broken fiber. The LLS considers the more realistic case where the load that had been supported by the fiber before the breaks is transferred to fibers in the locality of the fiber break. The LLS was proven to be more realistic than the ELS for authentic material properties and geometries by both theoretical and experimental means. It was shown that the majority of the load of a single broken fiber is shifted to the immediate lateral neighbors. The second closest neighbors bear a small portion of the shifted load and increasingly insignificant amounts of the load are shifted to the more distant neighbors. The load shifting factors were dependent on the properties of the matrix, the strength of the fiber-matrix interphase, and the fiber spacing as discussed by Harlow and Phoenix [4]. The implications are that poor matrix properties, weak fiber-matrix interphases, and greater fiber spacing will reduce the load shifting ability within a composite. Conversely, better composites have increased load shifting ability due to superior matrix properties, strong fiber-matrix interphase regions, and less space between fibers, i.e., higher fiber volume.

Fiber composite materials have an intrinsic variability with respect to strength, since the fibers themselves exhibit considerable variability in tensile strength. The

strength of individual fibers is commonly assumed to follow a Weibull distribution. Harlow and Phoenix [4] state that the variability associated with the fibers is attributed to random variation of severity and location of flaws along the fiber. Experimental observations have shown that the variability in composite strength is far less than that of the fibers alone. Also, Harlow and Phoenix [5] point out that as fiber strength variability increases, bundle and composite strengths decrease markedly.

Dry Bundle Theory

Dry fiber bundles have been examined to various degrees by many researchers. The chain of bundles model, which was developed by Rosen for composites, is still used with special considerations for dry bundles of fibers under ELS. Prior to Rosen, Daniels [6] and Coleman [7] both worked with statistical theory that involved the ELS strength of dry fiber bundles. The ELS model is intuitively more reasonable for dry bundles of fibers since there is no matrix to transfer the load locally. It is reasonable to assume that in an ideally loaded fiber bundle, initially all of the fibers equally share the load. After individual constituent fibers fail under increasing load, the load is shared equally by the surviving fibers. Beyerlein and Phoenix [8] reviewed prior work using Rosen's model, which they referred to as the "chain-of-ELS-bundles model." Rosen's model considered a composite of n parallel fibers with length l, which is treated as a chain of $m = l/\delta_R$ short ELS bundles. Each of the m bundles has n fiber elements with a characteristic length δ_R defined as

$$\delta_R \equiv (1/\sigma)\int_{-\infty}^{\infty}\{\sigma - \sigma_0(x;\sigma)\}dx = 2\hat{\delta} \qquad (1)$$

where $\sigma_0(x;\sigma)$ is the stress along a broken fiber given by

$$\sigma_0(x;\sigma) \approx \sigma f(x/\hat{\delta}) \equiv \sigma\{1-\exp(-|x|/\hat{\delta})\} \quad (2)$$

where $\hat{\delta} = \pi\delta_e / 4$ (3)

$$\delta_e \approx d\sqrt{\overline{E}_{xx} / \overline{G}_{xy}} \quad (4)$$

$\overline{E}_{xx}$ is the longitudinal stiffness of the composite and $\overline{G}_{xy}$ is the shear stiffness approximated by

$$\overline{E}_{xx} \approx V_f E_f + (1-V_f)E_m \quad (5)$$

and

$$\overline{G}_{xy} \approx 1/[(1-V_f)/G_m + V_f / G_f] \quad (6)$$

V_f is the fiber volume of the composite and G_m and G_f are the shear moduli of the matrix and fibers respectively. Beyerlein and Phoenix's δ_R is analogous to Rosen's ineffective length δ. The assumption is made that all *n* fiber elements contribute in ELS in a composite cross-section. The total number of bundles in the composite is taken to be *m* times the effective number of bundles in each cross-section. In order to consider the behavior of a fiber bundle, the matrix is excluded as a tensile load sustaining part of the composite and the effective composite stress becomes

$$\overline{\sigma} = V_f \sigma \quad (7)$$

where σ is the average fiber stress within a bundle.

This assumption is commonly made because data from unidirectional composites are used instead of direct dry-bundle data. A statistically significant amount of dry-bundle

test data compiled by a reliable test method would allow many researchers to check the validity of these types of assumptions.

A bundle of n continuous fibers held between two clamps in a perfect manner is considered. All fibers have equal length δ_R, stiffness E_f, and cross-sectional area A_f. Their strengths $S_1, S_2, \ldots, S_n$, are in units of stress and are independent and identically distributed random variables. The strengths have mutual distribution functions $F_\delta(\sigma)$, $\sigma/0$, where the applied bundle stress is σ. The applied bundle stress is the total force acting on the bundle divided by the total cross-sectional area nA_f. The ELS model of a fiber bundle assumes that during failure progression, surviving fibers equally share the applied load and broken fibers carry no load. Following this model, if i of the n fibers fail with applied bundle stress σ, the actual stress s supported by each fiber is

$$s = n\sigma/(n\text{-}I) \tag{8}$$

Let σ_n^* be the strength of a fiber bundle, the maximum stress, σ, the fiber bundle can support, and let $G_n(\sigma)$, $\sigma/0$, be its distribution function, that is, $G_n(\sigma)$ gives the probability that $nZ_n \leq \sigma$, where nZ_n is the bundle strength. The random variable Z_n is the per fiber strength of the bundle and is found by letting $S_{(1)}' S_{(2)}' \ldots ' S_{(n)}$ be the strengths of the individual fibers in ascending order, with

$$Z_n = \max\left\{S_{(1)}, \frac{n-1}{n} S_{(2)}, \ldots, \frac{2}{n} S_{(n-1)}, \frac{1}{n} S_{(n)}\right\} \tag{9}$$

It is desirable to know $G_n(\sigma)$, the distribution function of the fiber bundle, in terms of $F_\delta(\sigma)$, the distribution function of the individual fibers, n, the size of the bundle,

and with consideration of the ELS model. Where n is small, a recursion relationship for $G_n(\sigma)$ is given by

$$G_n(\sigma) = \sum_{i=1}^{n} (-1)^{i+1} \frac{n!}{(n-i)!i!} F_\delta(\sigma)^i G_{n-1}\left(\frac{n\sigma}{n-1}\right), x \geq 0 \tag{10}$$

where $G_0(\sigma) \equiv 1$.

Beyerlein and Phoenix [8] and Harlow and Phoenix [4] show essentially the result given by Daniels [6] with various notational differences for n = 1~5 as follows in equations (11) through (15):

$$G_1(\sigma) = F_\delta(\sigma), \tag{11}$$

$$G_2(\sigma) = 2F_\delta(2\sigma)\, F_\delta(\sigma) - F_\delta(\sigma)^2, \tag{12}$$

$$\begin{aligned} G_3(\sigma) = {} & 6F_\delta(\sigma)\, F_\delta(3\sigma/2)\, F_\delta(3\sigma) - 3F_\delta(3\sigma/2)^2\, F_\delta(\sigma) \\ & - 3F_\delta(\sigma)^2\, F_\delta(3\sigma) + F_\delta(\sigma)^3, \end{aligned} \tag{13}$$

$$\begin{aligned} G_4(\sigma) = {} & 24F_\delta(\sigma)\, F_\delta(4\sigma/3)\, F_\delta(2\sigma)\, F_\delta(4\sigma) - 12F_\delta(\sigma)\, F_\delta(4\sigma/3)\, F_\delta(2\sigma)^2 \\ & - 12F_\delta(\sigma)\, F_\delta(4\sigma/3)^2\, F_\delta(4\sigma)\, F_\delta(4\sigma) + 4F_\delta(\sigma)\, F_\delta(4\sigma/3)^3 \\ & - 12F_\delta(\sigma)^2\, F_\delta(2\sigma)\, F_\delta(4\sigma) + 6F_\delta(\sigma)^2\, F_\delta(2\sigma)^2 \\ & + 4F_\delta(\sigma)^3\, F_\delta(4\sigma) - F_\delta(\sigma)^4, \end{aligned} \tag{14}$$

$$\begin{aligned} G_5(\sigma) = {} & 120F_\delta(\sigma)\, F_\delta(5\sigma/4)\, F_\delta(5\sigma/3)\, F_\delta(5\sigma/2)\, F_\delta(5\sigma) \\ & - 60F_\delta(\sigma)\, F_\delta(5\sigma/4)\, F_\delta(5\sigma/3)\, F_\delta(5\sigma/2)^2 \\ & - 60F_\delta(\sigma)\, F_\delta(5\sigma/4)\, F_\delta(5\sigma/3)^2\, F_\delta(5\sigma) \\ & + 20F_\delta(\sigma)\, F_\delta(5\sigma/4)\, F_\delta(5\sigma/3)^3 - 60F_\delta(\sigma)\, F_\delta(5\sigma/4)^2\, F_\delta(5\sigma/2)\, F_\delta(5\sigma) \\ & + 30F_\delta(\sigma)\, F_\delta(5\sigma/4)^2\, F_\delta(5\sigma/2)^2 - 20F_\delta(\sigma)\, F_\delta(5\sigma/4)^3\, F_\delta(5\sigma) \\ & - 5F_\delta(\sigma)\, F_\delta(5\sigma/4)^4 - 60F_\delta(\sigma)^2\, F_\delta(5\sigma/3)\, F_\delta(5\sigma/2)\, F_\delta(5\sigma) \\ & + 30F_\delta(\sigma)^2\, F_\delta(5\sigma/3)^2\, F_\delta(5\sigma/2)^2 + 30F_\delta(\sigma)^2\, F_\delta(5\sigma/3)^2\, F_\delta(5\sigma) \\ & - 10F_\delta(\sigma)^2\, F_\delta(5\sigma/3)^3 + 20F_\delta(\sigma)^3\, F_\delta(5\sigma/2)\, F_\delta(5\sigma) \\ & - 10F_\delta(\sigma)^3\, F_\delta(5\sigma/2)^2 - 5F_\delta(\sigma)^4\, F_\delta(5\sigma)\, F_\delta(\sigma)^5, \end{aligned} \tag{15}$$

It is evident that computing $G_n(\sigma)$ when n is large is a considerable task, since there are 2^{n-1} terms. Beyerlein and Phoenix [8] state that this recursion works well up about $n = 50$ and offer another procedure that works well up to about $n = 600$. A statistically significant group of dry-fiber bundle tensile test data would enable distribution functions of fiber bundles to be developed from actual data. This would allow realistic values of n (3000, 6000, etc.,) to be used for development of distribution functions. The importance of this ability is that it is unlikely that fiber bundles as small as 600 filaments would be used on a regular basis, whereas fiber bundles of 3000, 6000, and greater filaments are regularly used in composites. Accurate distribution functions for these large fiber bundles would be of greater use for modeling of composites.

A Weibull distribution may be considered for $F_\delta(\sigma)$ where

$$F_\delta(\sigma) = 1 - \exp\{-(\sigma/\sigma_\delta)^\rho\},\ \sigma/0 \tag{16}$$

where

$$\sigma_\delta = \sigma_{l_0}(\delta / l_0)^{-1/\rho} \tag{17}$$

where l_0 is a reference length or typical test length and σ_δ is the scale parameter at length δ_R and ρ is the Weibull shape parameter.

Assuming this Weibull distribution and a power law approximation based on lower tail behavior, Beyerlein and Phoenix [8] used

$$F_\delta(\sigma) \approx (\sigma/\sigma_\delta)^\rho,\ 0 \le \sigma \le \sigma_\delta \tag{18}$$

to arrive at expressions that are no less complex for $G_n(\sigma)$, but yield significant asymptotic forms for small and large σ. These asymptotic forms of $G_n(\sigma)$ are given by

$$G_n(\sigma) \approx \begin{cases} 1-\exp\{-n(\sigma/\sigma_\delta)^\rho\}, & \sigma_\delta << \sigma \\ \left(\sigma/\sigma_1^{(n)}\right)^{n\rho}, & 0 \le \sigma << \sigma_\delta \end{cases} \tag{19}$$

where

$$\sigma_1^{(n)} = \sigma_\delta \left\{ (-1)^{n+1} + \sum_{i=1}^{n-1} (-1)^{i+1} \frac{n!}{(n-i)!\,i!} \left(\frac{n\sigma_\delta}{(n-i)\sigma_1^{n-i}} \right)^{(n-i)\rho} \right\}^{-1/(n\rho)} \tag{20}$$

which gives

$$\sigma_1^{(2)} = \sigma_\delta (2^{\rho+1} - 1)^{-1/(2\rho)} \tag{21}$$

$$\sigma_1^{(3)} = \sigma_\delta \{6(3/2)^\rho 3^\rho - 3(3/2)^{(2\rho)} - 3(3)^\rho + 1\}^{-1/(3\rho)} \tag{22}$$

The upper approximation for $G_n(\sigma)$ is a "weakest-link" approximation and the lower approximation for $G_n(\sigma)$ is a "power-law" approximation that accounts for load sharing.

The approximation given for the lower tail of $G_n(\sigma)$ is also the lower tail of the Weibull distribution. This lower tail approximation for $G_n(\sigma)$ gives important indications of why the fibers of a composite tend to fit a Weibull distribution for strength, as well as why composites experimentally show considerably less variability in strength than the constituent fibers themselves. Fiber load sharing effectively causes local redundancies, which lead to increases in the effective Weibull shape parameter of the composite over that of the fiber in approximate proportion to n, the bundle size. The approximation for larger bundles, however, is too conservative because $\sigma_1^{(n)}$ constantly decreases below σ_δ until it approaches zero as $n \to \infty$. Daniels [6] found that the bundle strength asymptotically follows a Gaussian distribution as the bundle sized increases. Coleman [7] assumed a Weibull distribution for $F_\delta(\sigma)$, the fiber strength, and examined the asymptotic results. Beyerlein and Phoenix [8] presented improvements to the Gaussian distribution and combined them with some of Coleman's asymptotic terms and achieved results that worked well with small values of n, as well as the infinite bundle size.

Though much theoretical work has been completed, there are voids between the theoretical work and the final composite structures. This is disconcerting and tends to place much of the theoretical work on an esoteric plane, far removed from the actual constituents and composites that are theoretically represented. While researching background material, many publications were reviewed that presented work involving strength distribution functions. These distribution functions were for individual fibers, fiber bundles, or composites. It is clear that volumes of work have been done wherein these distribution functions were central to the statistical modeling of the work. However, in the publications reviewed for this research, most of which involved dry-fiber bundles to some extent, no actual distribution function was presented as more than a variable that represented a distribution function. The value of generalizing this type of work is recognized, but it truly appears that the reason for generalization is due to lack of empirical data, rather than in the interest of completeness. Enough composite testing has been done that abundant data is available. This, along with the difficulties involved with dry-fiber bundle testing, has lead to modeling of dry-fiber bundles from impregnated-fiber bundle and composite data. This indirect method yields no true representation of a fiber bundle that can be verified. There is a need for a statistically significant amount of dry-fiber bundle test data to allow verification of the large amount of mathematical work that has already been done. Actual dry-fiber bundle data would allow calculation of strength distribution functions for different types of fibers. The Weibull scale and shape parameters shown in equations (16) and (17) could also be calculated to provide a link between distribution functions of individual fibers and distribution functions of fiber bundles. The empirical dry-fiber bundle data could lead to important bridges in

understanding the connections from individual fibers to dry-fiber bundles to impregnated-fiber bundles and their relationships to final composite structures. A database of reliable dry-fiber bundle specifications could provide the ability to try different matrix materials with various fibers to model full-sized composite structures. This could lead to greatly reduced design costs because preliminary designs could be changed easily before building any actual molds or production equipment.

Dry Bundle Tensile Tests

Dry-bundle tensile tests have presented a challenge and have earned a reputation for giving unreliable results due to the variability in the collected data. It has been established that brittle fibers exhibit a large amount of variability in tensile strength with coefficients of variation in the 5 to 25 percent range Phoenix [9]. Chiao and Moore [10] developed a tensile test method for fibers, but commented that the data from dry bundle tests are often not representative of fiber tensile strength and vary much more than data from epoxy impregnated fiber bundles. They recommended that testing dry fibers should be avoided. Due to the difficulties of maintaining test conditions that are consistent and as ideal as possible, some of the variability associated with the fibers may be introduced during testing. The test methods must therefore be well chosen to avoid previous problems.

Hancock and Swanson [11] considered the three most critical problems with testing composites to be: (*i*) failure in the test gage section, (*ii*) accurate alignment, and (*iii*) valid tests with economically small specimens. In the same context, when dry bundles are considered, the specimen size is of little concern; however, valid tests that are

representative of or can be correlated to full sized composites are important. In addition, it is important to have a test method that economically enables enough specimens to be tested so the results are statistically significant. The economical considerations include time requirements involved with tests as well as actual material costs. This is important because a significant time expenditure on a per test basis could potentially inhibit the testing of a large enough group to be statistically significant.

Little information was found that involved specific dry fiber bundle test procedures. Daniels [6] discusses "A group of parallel threads of equal length, clamped at each end so that all threads extend equally under tension…" and Beyerlein and Phoenix [8] mention "a bundle of *n* continuous fibers held perfectly between two

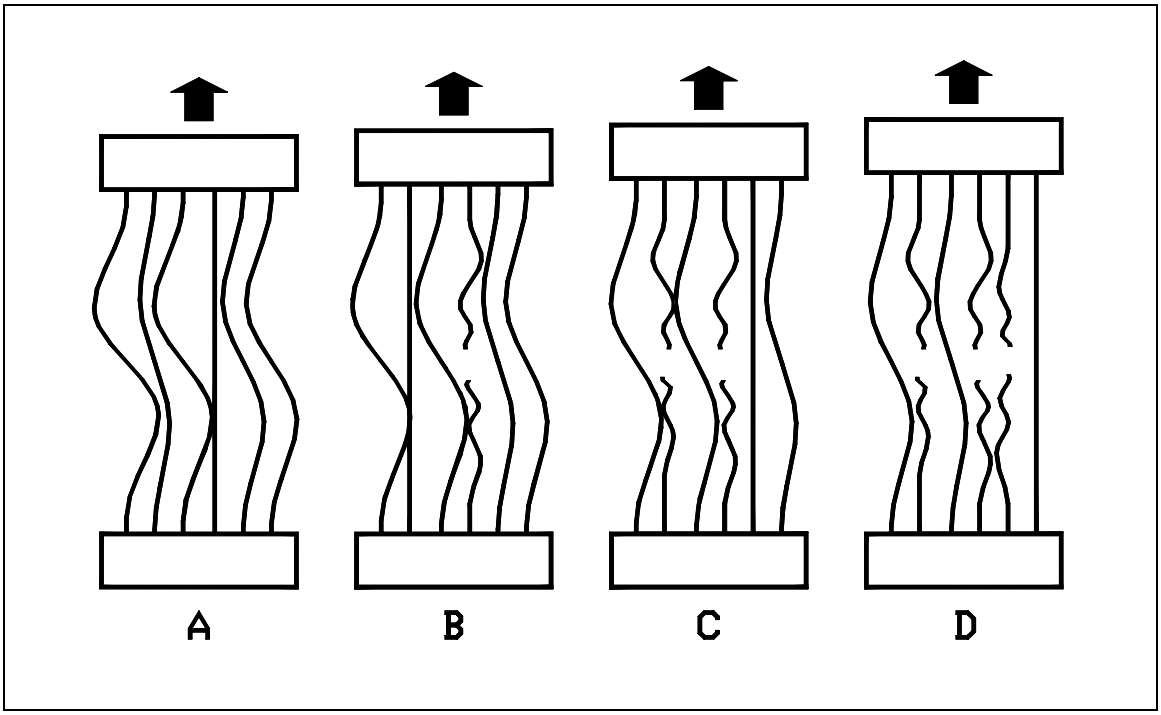

Figure 2.2. Fiber-load progression as load is applied to an unevenly loaded fiber bundle

clamps," but no methods were given to achieve these theoretical and ideal states. These requirements and the effects of achieving them may be considered. For dry fiber bundle tests, the fibers in a bundle must be collimated, that is, all be the same length and must be parallel, to obtain an accurate representation of the bundle's capability. Otherwise, the shortest fiber breaks first, the next shortest then breaks, and the sequence repeats through the fiber bundle as shown in Figure 2.2. This assumes that all of the fibers have identical properties. Since the longer fibers are not bearing their share of the load, the strength value resulting from the test would be lower, representing only the shorter fiber's strength value. This lower strength value obviously misrepresents the true capabilities of an evenly loaded bundle of fibers. Uneven loading can be caused by improper sample

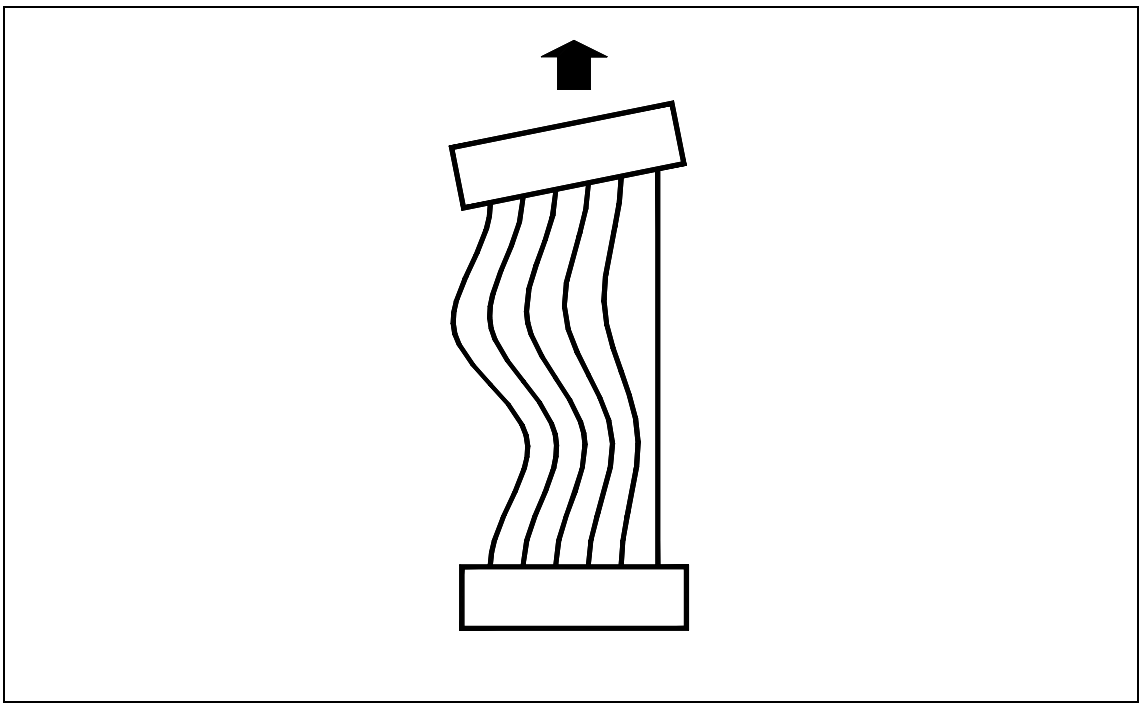

Figure 2.3. Top of properly prepared specimen clamped at angle, causing uneven fiber loading

preparation or incorrect testing of a properly prepared specimen. An example of this is shown in Figure 2.3, where the top end of a properly prepared specimen is incorrectly clamped at an angle into the test equipment. This causes essentially the same problem as before, uneven fiber loading resulting in misleading test results. Due to the flexible and fragile natures of the carbon-fiber bundles, proper specimen preparation and test setup are essential to maintain that the fibers in a bundle are the same length as well as straight andparallel. Another problem is handling of the specimen to perform the tests. Carbon fibers are relatively brittle and can be damaged by handling. It is important to minimize the amount of handling of the fibers before testing. The bundles tested are only about 0.53 mm (0.021 in.) in diameter, but have 3000 individual fibers. Simply handling the bundles can cause individual fibers to catch on dry skin, resulting in a frayed area in the fiber bundle. The damaged area would cause erroneous results if used for testing. An excess of bending and similar manipulations could break fibers or cause entanglements of fibers inside the bundle, which would also influence test results. Therefore, handling and manipulations must be minimized from the time that the fiber bundle comes off the spool through completion of the testing.

Gage length of the test specimens is another parameter that must be considered. Referring to the realism of the correlation between dependence of fiber strength on fiber length, Rosen [2] explained that longer chains have a higher probability of having a weaker link than shorter chains. That is, in two populations of links there is a higher probability within a larger population that one of the links is weaker than all of the links in the smaller population, causing the larger population, i.e. the longer fiber, to ultimately be weaker. Wu and Robinson [12] discussed the experimentally documented dependence

of fiber strength on test sample gage length. It is important to consider why it would be of interest to change the specimen gage length used for fiber tensile tests. The issues involved when considering gage length with respect to fiber bundle tensile tests are: (*i*) possible entanglements of the fibers within the bundle and (*ii*) possible changes resulting in differences of fiber lengths within a bundle. Entanglement requires a fiber to be nonparallel from the rest of the fibers, causing part of it to be located where it can interact with other fibers around it. A short gage length reduces the possibility of fiber entanglement because a slight degree of nonparallel nature has little effect on the path of a fiber over a short distance. That is, the short gage length reduces the opportunity for a fiber to move far from the parallel path. A longer gage length has just the opposite effect, increasing the opportunity for the fiber to stray farther from its parallel path and become entangled or otherwise interfere with neighboring fibers. The second consideration, possible changes that might result in differences in fiber lengths, refers to something that could potentially occur during the process of preparing the specimens or test setup that would inherently cause minute differences in the fiber lengths within a specimen. This is an elementary case of percentages where the potential change of lengths would be fixed, but the gage length can change. For example, consider a case where a difference in fiber length of 0.01mm is inherent to some stage of the test. If a gage length of 25mm were used, the difference is 0.04 percent of the gage length, whereas the difference would be 0.004 percent of a 250mm gage length. Longer gage lengths could lead to less variability of the data if the second consideration is a potential issue in testing.

Impregnated Bundle Tests

Impregnated carbon fiber bundles are essentially unidirectional composites. This means that one can think of the impregnated fiber bundle as a chain of bundles of fiber links, the same as a larger unidirectional composite structure. It is important to note, however, that there are differences between small composite specimens and much larger composite structures. Batdorf and Ghaffarian [13] discussed the theory that implies that large composites have smaller variances in failure stress than small composites, with the variance of very large composites approaching zero. They added, however, that there was a considerable discrepancy between the theoretical and experimental results, with the experimental results reaching a lower limit that was non-zero. Batdorf [14] later developed a relation that correlated the theoretical and experimental results with considerably better accuracy. It should be stressed that the properties of an impregnated fiber bundle might not be directly correlated with those of a full sized composite structure. The relationships would have to be established with a high degree of certainty before the results could be deemed reliable.

An additional bibliography of useful background sources has been compiled in Appendix A. These sources provided valuable information about composites that did not pertain directly to this research. They were of interest, however, to enhance one's general understanding of composites. The sources also include general statistical methods references.

CHAPTER 3

DRY-BUNDLE TEST METHOD

From the background work, ideal dry-bundle test requirements were established. Known information about impregnated-bundle testing was also considered in the development of the dry-bundle test procedures, due to the general similarities involved. One requirement was that the fiber bundles must be collimated, and methods to achieve this were explored. After examining the options available, collimation of the fiber bundles by drawing them through pigtail orifices was chosen as the best method. Requirements and methods of constructing pigtail orifices were scrutinized and discussion of the best methods follows in this chapter. The need for orifice lubrication was established and various orifice lubricants were tried. Acetone was chosen as the best option as an orifice lubricant. Many aspects of dry-bundle tests were considered and it was decided to try to develop a test fixture, in which the specimens were both prepared and tested. This showed clear advantages.

In the following narrative, a discussion follows about the details of development and design considerations of the test fixtures. Finally, developed procedures for proper dry-bundle specimen preparation are presented. These procedures are to insure that tests yield consistent results.

Dry-Bundle Test Method

Since impregnated fiber bundles are tested often, the methods used were examined to find if similar methods would apply to dry-bundle testing. The fiber bundles are usually bathed in resin, drawn through an orifice or squeegee to remove excess resin, and placed on a rack with a weight to maintain tension while the resin cures. Then, tabs must be attached to the ends of the specimen. Tabs enable the test equipment to clamp onto the specimen without causing damage to the specimen. The tabs may be molded or bonded onto the specimen. For molded tabs, the specimen is placed in a mold and resin or glue is poured into the mold, which form the tabs on the ends of the specimen. When tabs are bonded, the ends of the specimen are sandwiched between two pieces of material, such as a fiberglass composite, with appropriate cement to bond it all together. Proper tabbing ideally has no effect on the specimen within the gage length. An improper tab can cause a stress concentration at the specimen-tab interface, resulting in the specimen prematurely failing at the specimen-tab interface rather than within the gage length as desired.

The best test method was sought, first to find a method to collimate the fibers, and second to keep the prepared fibers collimated through testing. Fiber bundles are usually drawn through a properly sized orifice with a viscous lubricant to collimate them. The orifice must be smooth to avoid fiber damage and can be drilled and machined, or it can be a “pigtail orifice.” A pigtail orifice is constructed from round wire, which is wound around a drill rod in a helical manner. The drilled and machined orifice can be produced with greater precision, but requires much more time to make than a pigtail orifice. In

addition, starting the fiber bundle through a machined orifice is more difficult than with the pigtail orifice, especially if the orifice is snug around the fiber bundle. A helical groove could be machined into a drilled orifice to facilitate starting the fiber bundle, but the production time would increase substantially. Since the exact orifice size was unknown, the pigtail orifice was the best choice for this application because pigtail orifices can be constructed quickly and are relatively simple to make.

Making Pigtail Orifices

The first requirement to make a pigtail orifice is to use smooth wire to ensure that the orifice is smooth and will cause no fiber damage. The wire must be strong enough to retain its shape while the fibers are pulled through. This leaves steel wire as the logical choice, eliminating aluminum and copper as the other readily available choices. The first three orifices were wound from smooth galvanized steel tie wire that measured 0.889mm (0.035”) in diameter. Three different sizes, 0.635mm (0.025”), 0.711mm (0.028”), and 0.813mm (0.032”) were wound around torch tip cleaners. Only the first half-inch of the tip cleaners can be used for winding, since beyond that the round rods have raised rings around them similar to a file’s surface. An alternative would be to use the shank of an appropriately sized drill bit held in a pin vise, however the tip cleaners were on hand and worked sufficiently well. It is important to produce a correct pitch between the windings to insure the correct gap between windings because the carbon fiber bundles are wound through the gap to get the bundle started through the center of the orifice. Originally, the method of winding the orifices included winding the wire to the desired pitch as the orifice was wound. This produced slight irregularities in the pitches, which most likely

would not affect the function of the orifice. The first three orifices were too large and attempts at winding smaller orifices using the galvanized steel tie wire resulted in bending the smaller sized tip cleaner. Smaller wire was required to wind a smaller orifice. Steel wire-feed welding wire was readily available in small diameters, is smooth, and worked well for making orifices. The size used was 0.024 inch in diameter, since smaller diameters will not withstand the pull of the fibers drawn through them without bending. This is a consideration, since the orifice must be supported during use by the same wire from which it is wound. The 0.610mm (0.024") wire could be wound around a 0.533mm (0.021") tip cleaner without bending the tip cleaner. If the original winding method was used, this would limit the smallest orifice diameter to .533mm (0.021"), which initial 3k (3000 fibers) bundle tests indicated would possibly be too large. A smaller orifice can be achieved, however, as shown in the steps of Figure 3.1. The wire, from which the orifice is to be wound, held by a needle-nosed set of Vise Grip® pliers is shown in Frame 1. The tip cleaner was held against the side of the Vise Grip® jaws as the first wrap of the orifice was started as shown in Frame 2 of Figure 3.1. The wire was wrapped tightly around the tip cleaner, leaving no space between wraps, as shown in frame 3. Then, the tightly wrapped coil was gripped from the "tails" of wire on each end and pulled to stretch it, as shown in frame 4 of Figure 3.1. This causes the inner diameter of the coil to decrease while it also produces a uniform pitch of the coils. The stretching has a tendency to cause the tails to bend and partially obstruct a clear path through the orifice. Therefore, the tails must be bent out of the path of the orifice. Care must be exercised while bending the tails so that the pliers do not mar the wire. If the orifice wire is marred, it could damage a fiber bundle as it is drawn through the orifice. Once the

orifice is stretched and the tails are properly bent out of the way, the size of the orifice can be checked with an appropriately sized tip cleaner or drill rod. A finished pigtail orifice is shown in frame 5 of Figure 3.1. This method proved to be the best method to produce small diameter orifices.

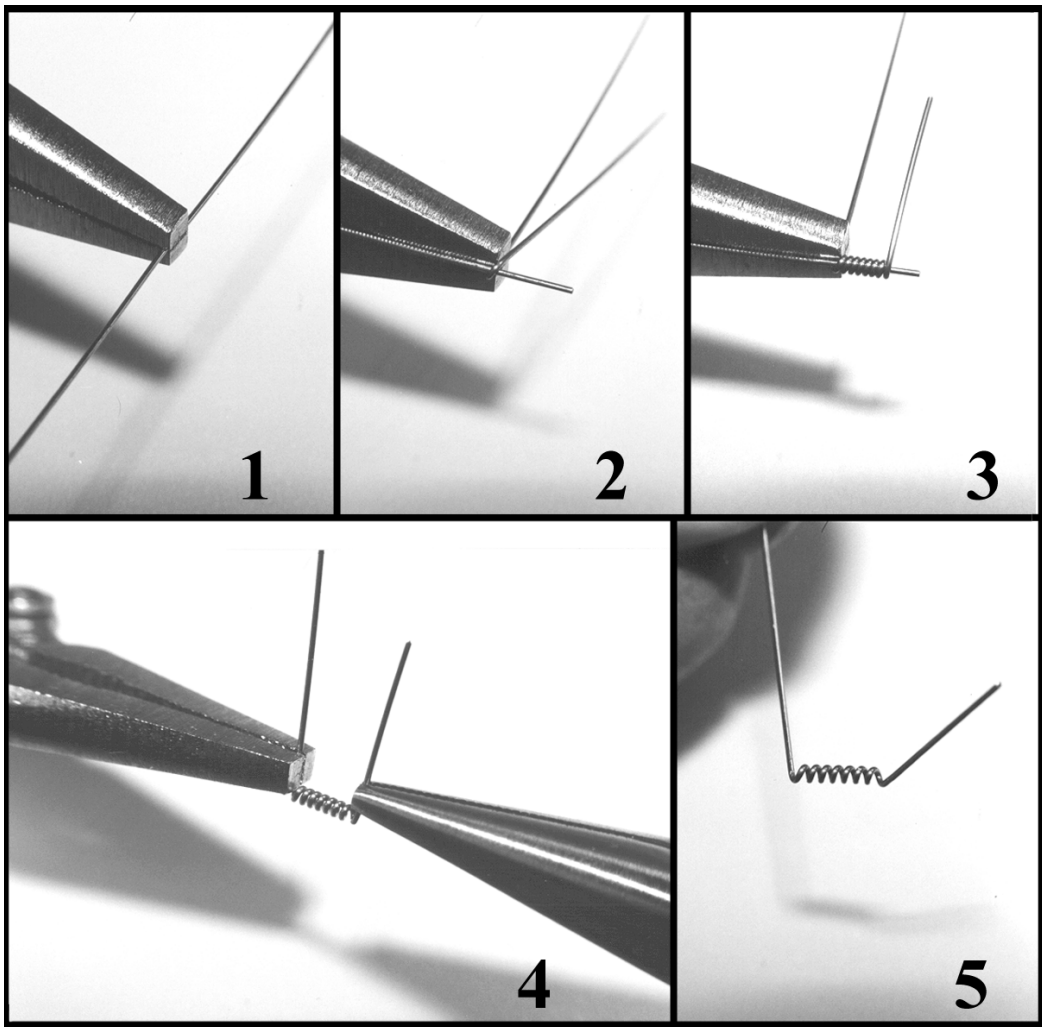

Figure 3.1. Steps to make precision, small pigtail orifices

In the early stages of orifice development, different orifice pitches were tried to see if the pitch of the windings of a pigtail orifice was of concern. The minimum pitch

that can be used is logically one that will just allow the fiber bundle between the windings of the orifice. The maximum pitch tried was one with only about three wraps around the 0.711mm (0.028") tip cleaner in about 13mm (1/2"). This orifice was used with some unsized fibers that had been taken from a production line as a sample. During sampling, two 3k carbon-fiber bundles were wound parallel onto a sample roll and initially unrolled as one large 6k bundle. This larger bundle was pulled through the long-pitched orifice and was a snug fit. The result was that the wire of the orifice had a tendency to press into the fiber bundle, similar to a thread on a bolt. This caused the fiber bundle to twist as it was pulled through the orifice. The twisting, of course, rendered the fibers useless as test specimens, since they were not straight and parallel. The same tendency was exhibited using orifices with less extreme, yet long, pitches. The pitch of the orifice was not critical to specimen preparation as long as it was no greater than the necessary dimension that would allow the fibers to be easily wound between the wire wraps of the orifice. The orifices that were used after the initial orifice research were all made from 0.61mm (0.024") wire and had pitch dimensions of 0.97mm (0.038") to1.41mm (0.055") measured from center to center of the orifice windings.

Orifice Lubrication

Once usable orifices were produced, it was necessary to find a lubricant for the fiber bundle as it was pulled through an orifice to provide a constant viscous drag while lubricating enough to eliminate damage to the fibers in the bundle. Hexcel® recommended contacting Kelmar Industries about silane oil or a similar product to serve this purpose. Initial testing was conducted using acetone as the lubricant since it

evaporates rapidly and would therefore cause no problems with molding the tabs onto the end of the fiber bundles. The acetone served its purpose adequately, providing enough lubrication to keep the fibers from being damaged. It was apparent that the acetone had a solvating effect on the sizing on the carbon fiber bundles. This was evident by the gel of excess sizing that gathered on the orifice as the fibers were drawn through and by the stiff character that the fiber bundle exhibited once the acetone had evaporated.

Sizing is a preparation that is similar to a matrix material. It is often used to stiffen fabric or fibers. After carbon fiber bundles are produced, they are bathed in sizing to reduce the fuzzy nature of the fibers. The sizing essentially affixes stray fiber ends, and mitigates further damage. If the fibers are too fuzzy, they are difficult to weave because the fuzz collects on parts of the weaving equipment. Specific sizes are also used to improve the interaction between the carbon fibers and the matrix materials. A better bond between the matrix and the fibers creates a composite material with better properties. Examples of sized and unsized fiber bundles can be seen in Figure 3.2. The

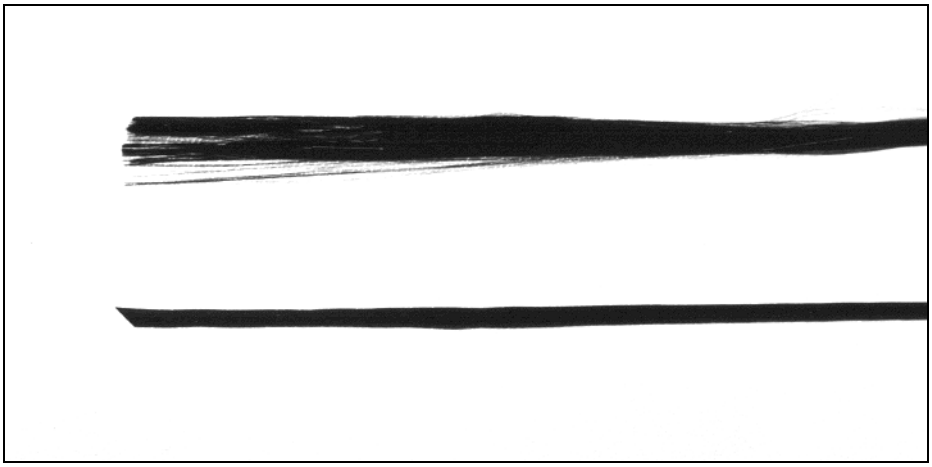

Figure 3.2. Photo of unsized fiber bundle along side a sized fiber bundle

fiber on the top is unsized, allowing the fibers to spread out loosely. The sizing on the bottom fiber bundle holds the fibers together, making the bundle much easier to manage.

Water was also tried as an orifice lubricant. Again, there was a solvating effect on the sizing shown by the same indications as with acetone. The test results showed little difference between the specimens prepared with acetone and the specimens prepared with water. Since water evaporates slower than acetone, and would have more of a tendency to remain between the fibers of the bundles due their hygroscopic nature, there was no beneficial reason to use water over acetone. If fact, water could have a detrimental effect on the interaction between the fibers and the matrix material by displacing space that would normally be filled with matrix. Use of water also slowed the specimen preparation since it seemed reasonable to wait for the water to evaporate from the fibers as much as possible before pouring the resin for the tabs.

The lubricant parameters were discussed with the fiber expert at Kelmar Industries. The recommendation was that a solvent like acetone would most likely work well, but that a dimethyl fluid with higher viscosity could be tried with the caveat that a dimethyl fluid could inhibit matrix bonding to the fibers. Two samples were shipped from Kelmar Industries, SWS 101-20 polydimethyl siloxane and SWS 101-50 polydimethyl siloxane, the latter having the higher viscosity. The polydimethyl siloxane fluids were clear and had oily characteristics similar to mineral oil. They were not miscible with water or acetone. Both were tested with 0.584mm (0.023”) and 0.533mm (0.021”) orifices. The polydimethyl siloxane fluids exhibited no effect on the sizing, but did leave an oily coating on the fiber bundle that could potentially affect matrix bonding. There were no signs of tab bonding failure due to the oily coating during these tests.

There were no striking improvements or detriments to the results, which were similar to those obtained with water or acetone. Some sized-fiber bundles were pulled through an orifice using no lube at all, but the bundle appeared the same after the orifice. It is suspected that collimation of the sized-fiber bundles was not achieved. An unsized-fiber bundle was also pulled through an orifice without lube. The result was that the orifice "peeled" back much of the outer fiber layer and quickly clogged the orifice.

Acetone seemed to offer the most benefits as an orifice lubricant. It provided enough lubrication to keep the fibers from being damaged, left no undesirable film on the fibers, and dissipated rapidly. The fact that it solvated the sizing was more likely beneficial than detrimental since the sizing actually holds the fibers together. This means that if the fibers slipped against each other as they were collimated, sizing could inhibit the slippage. The result would be unequal lengths of fibers, which is one of the conditions that have already been determined to be undesirable. For these reasons, acetone was chosen as the orifice lubricant for this research.

Test Fixture Development and Design

The test fixture was developed in several stages. Initially, the idea of the test fixture was to mold tabs onto the ends of fiber bundles. An example mold was acquired from the testing laboratory at Hexcel®. The Hexcel® mold was used for molding tabs onto the ends of impregnated fiber bundles and served as an example of basic design requirements. These requirements included tab well dimensions and fiber groove parameters. The tab wells are recessed areas in the molds into which resin or other tab material is poured to form the tabs around the ends of the fiber bundles. The original

intention was to use the same basic design modified for a specimen gage length of 254mm (10”). In order to reduce handling of the fibers, the molds were to be placed end to end on a long table and the fiber bundles were to be drawn through an orifice and laid directly into the molds. However, problems arise once the fiber specimens are removed from the molds to be tested. There are no reasonable methods to remove the specimens from the molds without bending or to keep the specimens properly aligned as they are placed into the testing equipment. The bending could cause specimen damage, potentially affecting results, and misalignment causes erroneous test results. Another problem with removing the specimens from the molds for testing is that the molded tabs have an irregular tab face on the side where the tab material is poured into the mold’s tab well. This irregular tab face could also cause misalignment when clamped into the test equipment. Simply molding tabs into place and testing presented enough possibilities for error that alternatives had to be explored.

It became clear during the preliminary design period that it would be ideal if the specimen could be tested without removing it from the mold. This would require a mold

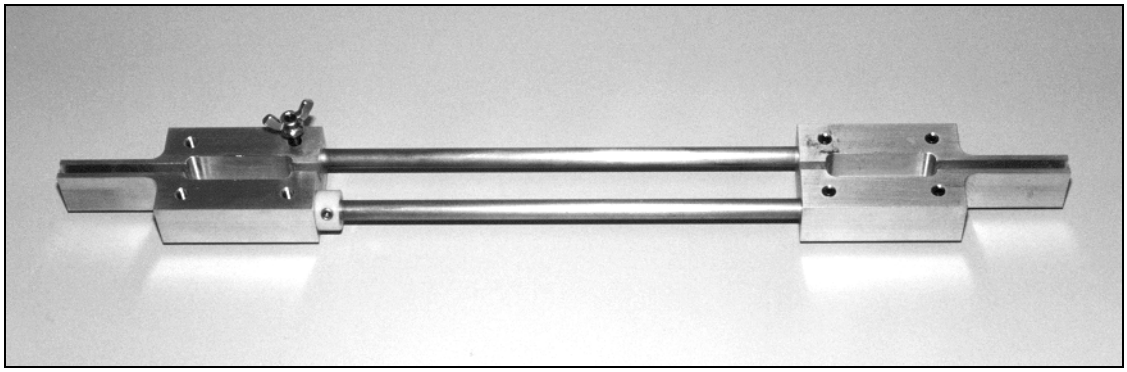

Figure 3.3. Photo of first design produced as a test fixture

that was also a testing fixture that could be clamped into an Instron test machine. The testing fixture would require a method for maintaining alignment and the determined specimen gage length. Provisions would also be necessary to allow the change in length that occurs during tensile tests. The design was narrowed to one having separate fixture ends connected by rods that would allow sliding during tests. The separate fixture ends each required tab wells and fiber grooves to be machined into them. A final parameter was that the Instron grips could clamp a maximum thickness of 11.43mm (0.45”). This dimension dictated the maximum thickness of the fixture ends. The resulting test fixture is shown in Figure 3.3.

The alignment rods were held stationary in one end of the fixtures by set screws and were allowed to slide in the other end. The gage length was set by adjusting shaft collars on the alignment rods so that the fixture ends could be set back to the preset position after each test. It was necessary to hold the sliding end of the fixture in place between specimen preparation and final testing. For this, special set screws were assembled to avoid the usual damage caused by set screws to the surfaces they are screwed against. In this case, the set screws were set against the metal alignment rods in the section that was required to slide freely through the sliding end of the test fixtures. Damage to the alignment rods could cause excess drag or binding between the rods and the sliding ends of the fixtures, resulting in inaccurate test results. The set screws were assembled by starting with standard 1” x 1/4”- NC socket set screws. Appropriately sized pieces of nylon cut from a shaft bushing were then driven into the hexagonal socket ends of the set screws leaving about three millimeters of nylon extended beyond the end of the set screws. On the opposite ends, standard hexagonal jam nuts were screwed onto

the set screws, followed by standard wing nuts that were screwed on until the ends of the set screws were flush with the upper end of the threads. The standard hexagonal jam nuts were then tightened against the bottom side of the wing nuts, holding them into place. This produced wing bolts with non-marring nylon ends that could be turned with

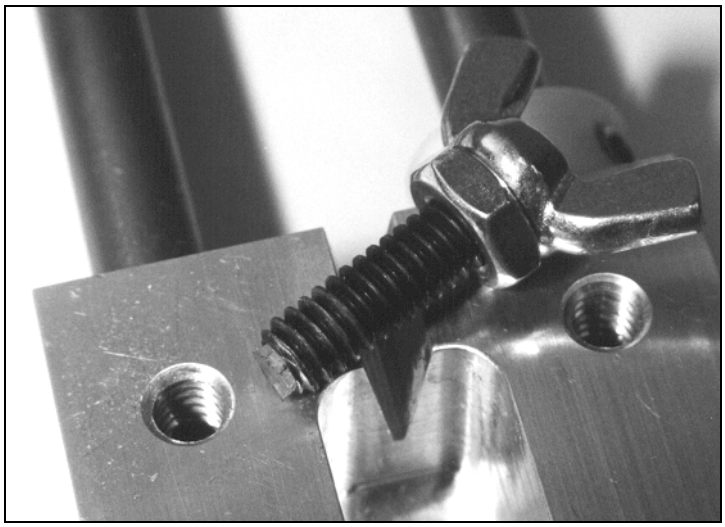

Figure 3.4. Photo of non-marring locking wing bolt

sufficient torque by hand to lock or unlock the position of the sliding ends of the fixtures. The locking wing bolt is shown in Figure 3.4. Six of these test fixtures were produced and were used for the development portion of the dry-bundle tests.

It became apparent during test development that this test fixture design had two disadvantages. The first disadvantage was an overall length of 483mm (19”) and the second was possible effects from the alignment rods during tests. The 483mm (19”) length was mostly an inconvenience, which caused the upper grip height to be high enough to make average height operators stretch to reach the grip. This was bothersome because the upper grip had to be tightened and loosened by hand for each test. The

length also required that the Instron cross head be raised to nearly maximum height to accommodate the test fixture and the 2224 N (500 lbf) load cell. This made tightening and loosening the cross head more difficult and presented a possible safety risk. This was an issue since the Instron to be used for these tests also had to be used for other projects between test runs, requiring numerous cross head adjustments.

The possible effects from the alignment rods during tests were of more concern. Under ideal test conditions, the increased load, caused by frictional drag between the alignment rods and the sliding end of the test fixture, would be negligible. However, slight misalignment of the grips or misalignment due to foreign material between the grip jaws and the test fixture could cause increased frictional drag. The initial dry-bundle tests conducted on various fibers had maximum loads between 53 N (12 lbf) and 178 N (40 lbf). With loads this small, frictional drag could induce considerable error in the results and there was enough variation in the test results that it was preferable to alleviate the possibility of any influence the alignment rods could introduce during tests. Since the rods maintained the specimen alignment while the fixture was clamped into the Instron grips, the alignment rods would have to be removed or disconnected between the two ends of the test fixture after the fixture was clamped into the grips.

After 58 groups of six specimens were tested with the original design of test fixture, the fixtures were reevaluated since there were at least 1200 specimens to be tested for this research. Using only six fixtures, 200 groups of tests would have to be conducted and there was the possibility of 12 to 24 hours turn around per group to allow for resin to cure. It was evident that more fixtures would be needed to complete the tests in a reasonable time period. More fixtures would also give a better statistical

representation of results since variations within a test group would be reduced. It was determined that if more test fixtures were going to be produced, the design should be improved to address the disadvantages of the original design as well as simplify the production of the fixtures.

The first parameter that was considered was the necessity to remove the alignment rods or disconnect the two ends of the test fixtures in some manner. Joints in the alignment rods would be required to disconnect the two ends. In order to alleviate the possibility of slack in a joint between halves of the alignment rods, this scenario was rejected in favor of removal of the alignment rods once the fixtures were clamped into the Instron grips. The possibility of modifying the original design so that the alignment rods could be removed was considered, but the design required a significant amount of machine work and did not address the length problem.

The length could be reduced if the tab mold well area of the test fixtures could be clamped directly between the grip jaws. This would differ from the original design fixture, which had clamped above the upper tab well and below the lower tab well as the fixture was placed vertically in the Instron grips. Originally, it was thought that a 13mm x 13mm x 52mm (1/2” x 1/2” x 2”) resin block was needed as a tab on the ends of the fibers. During the tests with the original fixtures, it was discovered that a tab 6mm x 13mm x 52mm (1/4” x 1/2” x 2”) was sufficient. A shallower tab well area and an efficient design would allow the tab mold area to be clamped between the grip jaws, reducing the overall length of the test fixture. This new design could be machined from a standard thickness of 9.5mm (3/8”) or 11mm (7/16”) aluminum, which would fit between the Instron grip jaws. The problem of incorporating the removable alignment rods had to

be addressed next. Although other geometries were considered for the alignment rods, round rods offered the most advantages. V-grooves could be machined longitudinally into the side edges of the test fixture ends and the round rods would maintain alignment while they were held into place. Another constraint for the design was that the rods would have to be removed from the sides of the fixtures and within the prescribed maximum grip jaw opening. To facilitate this, the original 9.5mm (3/8") rod size was reduced to 8mm (5/16"), which was considered the minimum size that would offer enough rigidity over the required span. Several options were considered for holding the

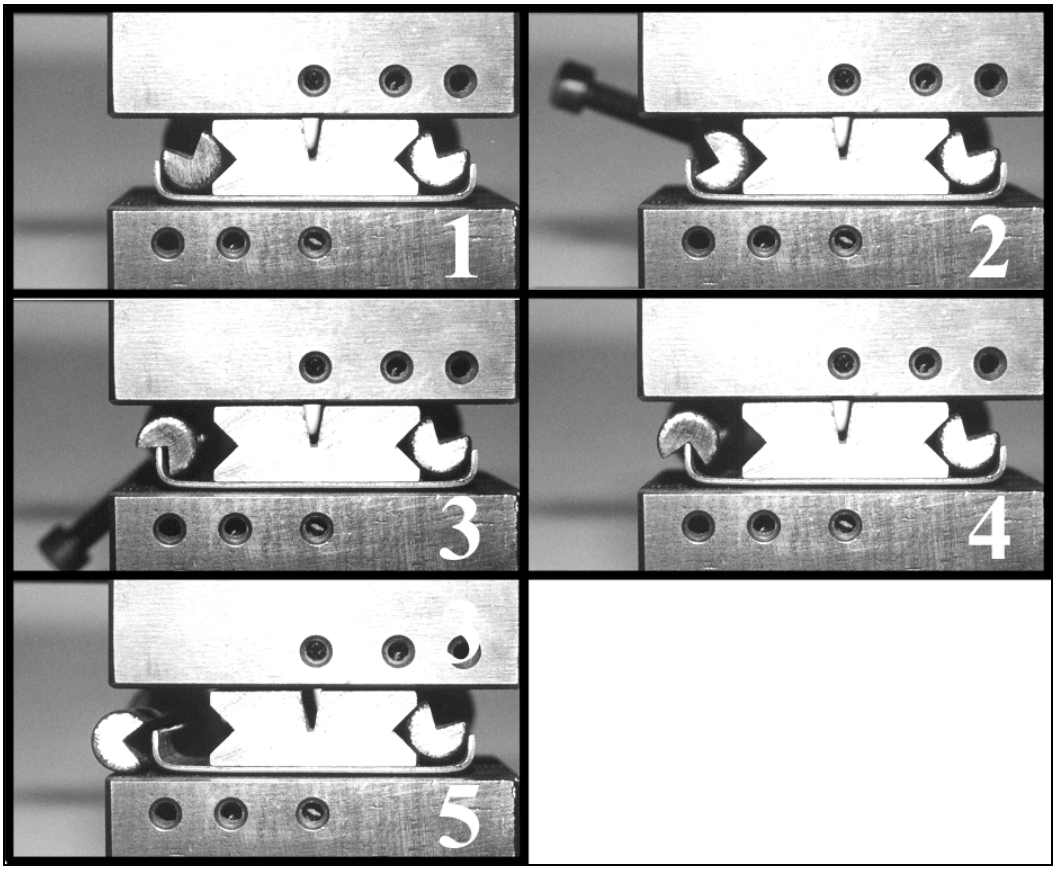

Figure 3.5. Photos of the sequence as the alignment rod is removed from the new test fixture

alignment rods into the V-grooves, including screws, magnets, springs, and spring plates. Each had their attributes, but the final spring plate design that was chosen offered some machining benefits as well as the ability to quickly remove the rods during testing and easily reassemble the fixtures.

The fixture end is shown between the grip jaws with the alignment rods in place Figure 3.5. The sequence of events as an alignment rod of the new fixture is rotated to release it is shown in the five frames of Figure 3.5. The rod is held into the v-groove by the spring plate as shown in frame 1. The alignment rod is rotated to release it from the v-groove as shown in frame 2. Further rotation of the rod allows the groove in the rod to start moving past the spring plate as shown in frame 3. The v-groove in the rod straddles the spring plate as the rod moves further away from the fixture end in frame 4. The alignment rod has cleared the fixture end in frame 5 and can be taken away.

The new fixture design is shown in Figure 3.6 and is shown along side the original fixture in Figure 3.7. The general reduction of the size of the new test fixture relative to the first design can be seen in Figure 3.7. The new design was both shorter

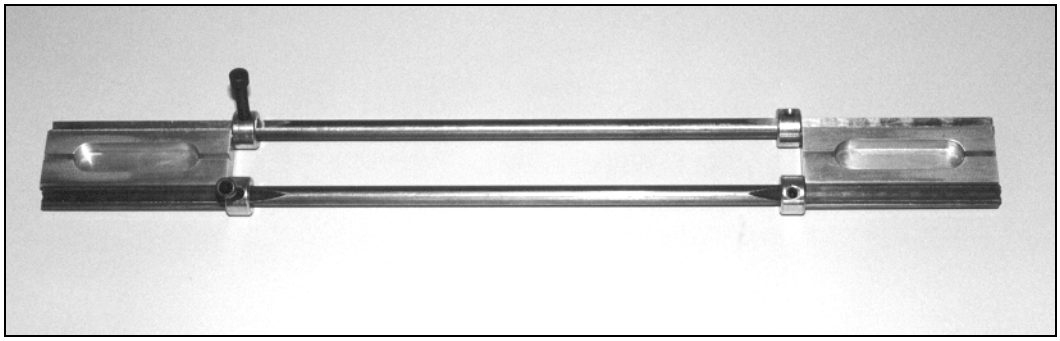

Figure 3.6. Photo of test fixture produced with new design

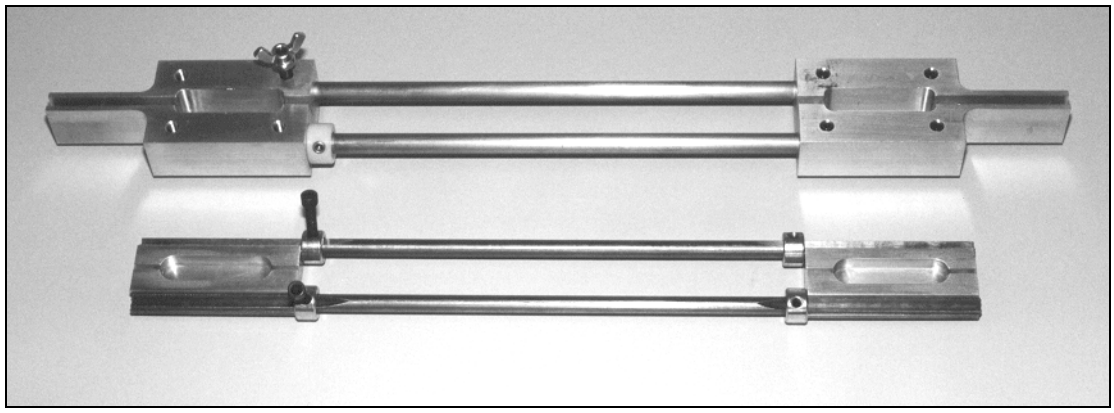

Figure 3.7. Photo of old design and new design test fixtures

and considerably less bulky than the original design. Thirty of the improved test fixtures were produced and used for the subsequent tests.

Development of Specimen Preparation Procedure

Specimen preparation consists of the steps required to get the fiber bundle from the spool, collimate it, place it into the test fixtures, and have it ready to test. It was decided in the initial stages of this research that the fiber bundles should be drawn through an orifice and into a series of test fixtures which were lined end-to-end. Handling of the specimens would be reduced by pulling the specimens into the lined up fixtures rather than into individual fixtures. This method would necessitate some provision for managing the fiber before the orifice to minimize harmful effects of handling, as well as to minimize issues with different fiber length in the specimens. There were two possible methods for pre-orifice handling of the fiber bundles. The first was to roll the fiber bundles off from the spools as the bundles were drawn through the orifice. The second method was to roll the needed length of fiber bundles from the

spools onto a smooth working surface, cut them to length, then draw the length of fibers through the orifice. The second method was chosen because of its simplicity. The former method of rolling the fibers directly off from the spools then through the orifice would have required a mechanism to maintain slack as they would be pulled through the orifice. The slack would be necessary because the fibers have an abrasive effect against the roll of fibers if the bundles are pulled from the rolls while maintaining tension. This is because the fiber bundles are wound with a steep lead angle across the spools at the manufacturers. This abrasive effect would cause damage to both the fiber bundle pulled from the roll and the fiber bundles exposed on the surface of the roll. The possibilities of fiber damage were greatly reduced by first rolling the fiber bundle onto a smooth work surface and cutting it to length before pulling it through the orifice.

The next consideration for specimen preparation was that the fibers would need to be kept reasonably taut after they were placed into the test fixtures. The tension would have to be maintained while the tabs were molded onto the ends of the fiber bundles. The easiest method for this was to clamp the fiber bundle at one end of the line of test fixtures and attach a weight to the leading end of the fiber bundle, which would be hung over the end of the workbench. Initially, the leading end of each fiber bundle was tied into a knot through which a paper clip was hooked. The weight consisted of a light-duty c-clamp with a mass of about 335 grams and was attached to the paper clip via string. The end of the string had a loop that was hooked onto the paper clip at the leading end of the fiber bundle, which could be pulled through the orifice and placed into the test fixtures. The weight had to be placed on the end of the workbench while the other end of the fiber bundle was clamped. Once the trailing end of the fiber bundle was clamped, the weight

was allowed to hang over the edge of the workbench. It worked best to keep the first test fixture about 100mm (4”) from the end of the workbench and line the other fixtures from the end of the first one. Later in the course of this research, standard black cast 3/4 inch 90 degree pipe elbows, which weighed about 200 grams each, were used as weights because they were compact and inexpensive. The c-clamps were large enough to contact the neighboring fiber bundles or c-clamps and although no problems were caused, the more compact pipe elbows replaced the c-clamps.

After the first four developmental test groups of fiber bundles had been prepared and tested, the need for a better method of fastening the weight to the leading end of the fiber bundle was apparent. Although a knot in the fiber bundle may have introduced slight problems due to the sharp bending of the fiber bundle in the knotted area, it worked adequately with sized fibers. However, unsized fibers were extremely difficult to tie into a knot. This was because of all of the loose-fine fibers at the leading end of the bundle and a method with far less manipulation of the end of the bundle was needed. The possibility of gluing the fiber bundle end to the string attached to the weight was considered, but was rejected since holding the string and the fiber bundle in alignment while the glue sets would be difficult. Since super-glue works well on rubber products, an attempt was made to glue part of a latex laboratory glove to the end of a fiber bundle; the result was a strong bond. It was discovered that the finger portion of a latex glove could be quite successfully bonded by saturating the first 15mm (5/8”) of the bundle end with super-glue, placing the precut finger portion of a glove over the fiber end, and squeezing the bonded area between one’s fingers for about ten seconds. Then, a paper clip hooked through the loop in the end of the weight string could be bent to make a hook

that could pierce the bonded latex and be hooked through it. This created a dependable and efficient method of fastening a weight to the end of a fiber bundle while the desired constant length of individual fibers was maintained. A fiber bundle is shown in Figure 3.8 with the bonded finger portion and the paperclip hook used as described above.

Several items were tried as clamps for the trailing ends of the fiber bundles. Hemostats worked satisfactorily, but had to be supported in some manner to keep them

Figure 3.8. Fiber bundle end glued into glove fingertip with weight attached

upright until the tension could be applied with the weight. If the hemostats were allowed to lay over, which was the natural tendency, the fiber bundles were bent severely, compromising the collimation of the fibers. The hemostats could be kept upright by appropriately clamping other hemostats to the handle portion or by supporting the hemostat with a piece of modeling clay pressed onto the handle to create a small base.

Small needle nose Vise-Grips®, 100mm (4”) and 150mm (6”), were also used as clamps. The sharp edges of the jaws caused fiber damage, sometimes completely severing the bundle. This could be remedied by placing a short section of polyethylene tubing over the fiber bundle before clamping the Vise-Grip® in place. The Vise-Grips® were usable, but their mass was too high and the requirement of using the protective tubing over the fibers deemed them undesirable for this application. The item that was finally chosen to

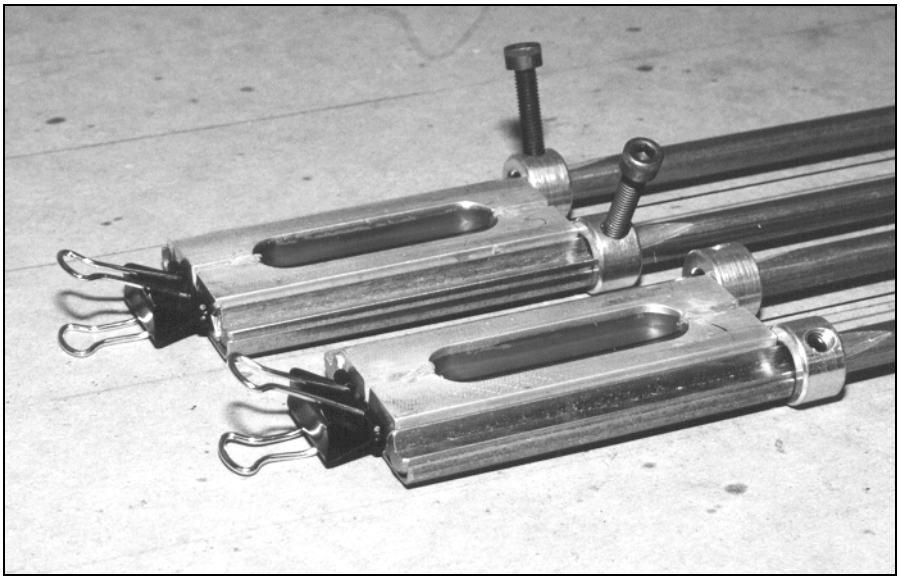

Figure 3.9. End of fiber bundle held at test fixture end with ACCO® binder clip

clamp the trailing end of the fiber bundles was the small size ACCO® binder clip. Shown in use in Figure 3.9, it clamped tight, was smooth and rounded where it contacted the fibers, was small, and had low enough mass that it was not injurious to the fiber bundles.

The use of the orifice and orifice lubrication method evolved moderately during the development of the specimen preparation procedure. Initially, the orifice was held by

a c-clamp which was placed in a 225mm (9”) square foil pan. The foil pan was to catch the excess lubricating fluid, primarily acetone. The acetone was dispensed with a one-liter laboratory wash bottle as the fiber bundle was pulled through the orifice. This was possible only because short lines of the original six fixtures allowed one to pull the fibers with one hand while dispensing the acetone with the other. Once longer lines of test fixtures were used, a 50-ml pipette supported on a laboratory ring stand was used to dispense the lubricating fluid. The ring stand was also a convenient place to clamp the orifice.

Once the fiber bundles were in place in the line of test fixtures, and were kept taut with the weight connected to the leading end, tabs needed to be molded onto the fiber bundle at both ends of each of the test fixtures. Polyester resin was chosen as the tab material for the dry-bundle tests. Therefore, the fiber grooves in the fixtures had to be blocked in a temporary manner to keep the resin from flowing out of the tab well areas

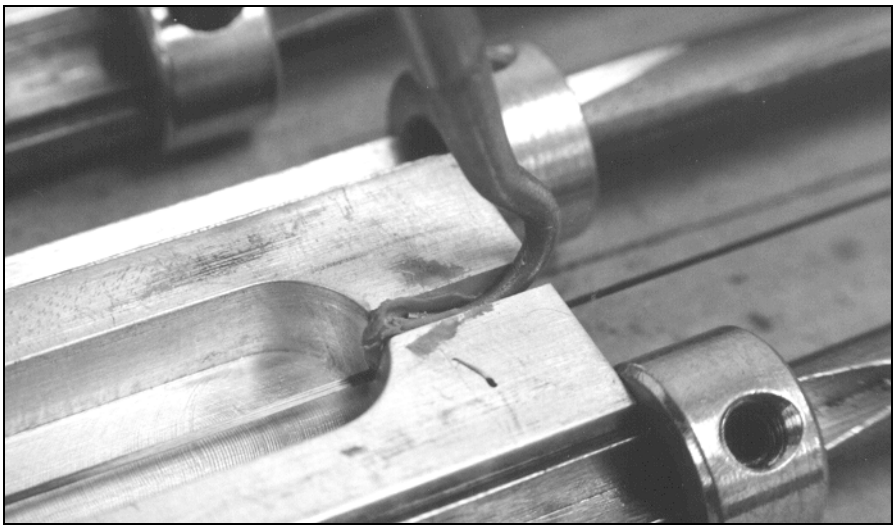

Figure 3.10. O-ring pick used to press clay into fixture groove to block resin flow

through the fiber grooves. Some sort of rubber plug was considered, but would have to be specially manufactured. Modeling clay was chosen because of availability and its ability to conform around the fiber bundle with a minimum effect on it. The clay was carefully pressed into place with the hooked end of an O-ring pick as shown in Figure 3.10. The resin could then be poured into the tab well areas.

One area of concern that was taken into account during test development, as well as during the testing was the possibility of stress concentrations at the fiber-tab interface area. Tabs molded onto the ends of the fiber bundles by using a resin that impregnates the bundle in the tab area seem to offer the least possibility of stress concentrations at the fiber-tab interface. This method essentially creates a composite in the tab areas from which the dry-fiber bundle protrudes. The fibers are continuous from the tab areas into the gage section of the dry-fiber bundles. This method should cause minimal influence on the fiber bundle, since the tab resin flows into and around the fiber bundle without the need for any external influences to force the resin into the bundle. Once the resin flows into place, it cures and bonds to the fibers with no bias createds that could cause a stress concentration. Clamping onto the bundles would cause definite stress concentrations. The textile industry tests fiber bundles by wrapping each end of the bundles around fixed spools that are clamped into the test machine grips. Friction between the fiber bundles and the spools is sufficient to hold the bundles for testing. This method would not meet the established criterion that the fibers all be the same length within the bundles. Clamping and the use of fixed spools for testing were both rejected as possible methods to hold the fiber-bundle ends because of the negative influences of each of these methods.

During the dry-bundle tests, the appearance of a frayed out section in the fiber bundle usually occurred when fibers failed. This frayed out section was usually in the center region of the gage section as shown in Figure 3.11. The frayed fibers are fibers that have retracted after failures. Due to entanglements with other fibers, the broken fibers retract and fray out in close proximity to the area of the failure. This is a good

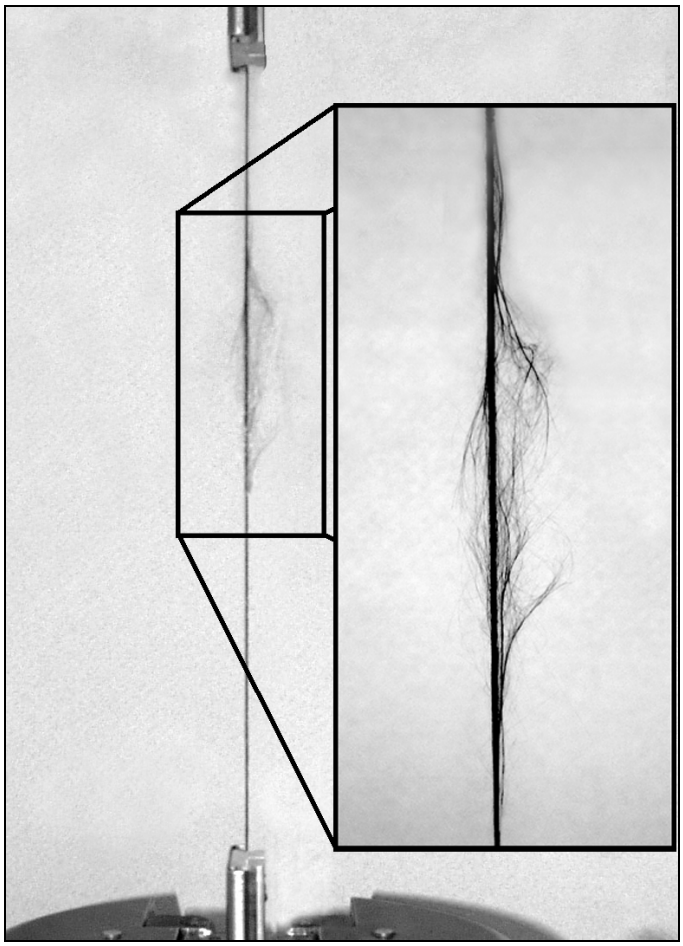

Figure 3.11. Photo with inset close-up of frayed fibers in the gage section

indication that the failures occurred within the gage sections of the fiber bundles and were not promoted by stress concentrations at the fiber-tab interfaces. Some dry-unsized

bundles were pulled in the test machine until the remaining bundle ends separated. The fibers that remained attached to each tab were checked to see how many, if any, remained that extended the length of the gage section. Only a few fibers that remained attached to the tabs were the length of the gage section. The majority of the broken fibers indicated that the fibers usually failed in the center region of the gage section. It is expected that some fibers would fail near the fiber-tab interface, due to the inherent distribution of flaws along the fibers in a bundle.

Another indication that there were no stress concentrations caused at the fiber-tab interfaces was test data collected for precursor-fiber bundles during early developmental testing. Hexcel® had supplied some spools of precursor-fiber bundles from their production facility for testing. The tests of the precursor fibers employed the same test methods used for this research. Schimpf [15] compared these test results to dry tow tenacity test results he had compiled for Hexcel®. Schimpf stated that the test results from this test method matched the results that he had collected. If stress concentrations were present, the results from this test method would have yielded lower load values.

Polyester resin was the first resin tried for molding the tabs onto the fiber ends. Originally, it appeared that about 24 hours would be required for the resin to cure enough before testing the fiber bundle. This restricted the test rate to 30 specimens per day. It was desirable to test more specimens per day so some other tab materials were tested. Automotive body putty, quickset epoxy, and hot-melt glue were tried as tab materials.

The issues of concern for a tab material were cure time period, ability to release from the fixtures, and bonding ability with the fiber bundle. Body putty cured within four hours, an acceptable time period, and released well from the fixtures. However, the

putty had a consistency that was too viscous to flow into the dry-fiber bundles and bond with all of the fibers. This was unacceptable because only the outer fibers would form an interface with the body putty tab. The consequence would be erroneous test results due to the inner fibers carrying only the load imposed upon them by friction from their neighboring fibers. The body putty used polyester resin as a base material and would surely have bonded well to a fiber bundle impregnated with polyester resin. The quickset epoxy cured within 20 to 30 minutes, but was also too viscous to flow into a fiber bundle to bond with all of the fibers. The worst problem with the quickset epoxy however, was that it did not release from the test fixture. It formed a remarkable bond with the aluminum test fixture, even with a release coating, creating a problem of cleaning the fixture for the next test. This method was therefore eliminated. The hot melt glue that was tried was Macromelt® 6300 obtained from Henkel Adhesives. Again, the hot glue was too viscous to flow into the fiber bundle, but it was usably cured within minutes and it released well from the test fixtures. It is noted that this hot melt glue is the industry standard for impregnated bundle tests.

Since polyester resin seemed to be the best material for tabs, in an attempt to increase the test rate it was decided to find the minimum cure time required for reliable test results. Originally, it was believed that 24 hours would be required between tests because the resin tabs were checked for one test group after about seven hours. It was found that the resin was curing, but still had a firm-gelled quality that would not allow testing. Another test group was checked after about eight hours to find that the resin was cured and solid enough for testing. This meant that two groups of 30 specimens could be tested each day. A first group could be tested early in the morning, a second group could

be prepared. Later in the afternoon or early evening, the second group could be tested and another group prepared for the next morning. The curing of the resin tabs was checked for the second group of specimens at earlier intervals and it was discovered that sometimes the tabs were solid after less than five hours. The difference seemed to be the temperature of the room. On one day that the room was noticeably cool, the resin tabs were still only firmly gelled after six hours. It was important to make sure the tabs were cured solid before testing the group of specimens. It was noticed that a sticky surface on top of the polyester was usually encountered with the shorter cure times, but as long as the resin was solid under the sticky surface, there was no problem with proceeding with the tests.

Synopsis of the Dry-Bundle Test Specimen Preparation Procedure

The following synopsis is to provide a brief overview of the steps required to prepare dry-fiber bundle test specimens prior to testing. This is a summary for easy implementation in a production environment. Extensive development was required as discussed above in this chapter, but the final procedure is simple and pragmatic. Although this procedure appears complicated, with a little practice it is practical for a production environment. This procedure requires a workbench area about 7m (23') long to prepare lines of eight test fixtures.

1.) Assemble test fixtures and place them end-to-end in a straight line, beginning about 100mm (4") from one end of the workbench. To allow separation of the test fixtures without disturbing the specimens, place a spacer between the contacting ends of the

test fixtures. A piece of 6mm (1/4”) polyethylene tubing about 13mm (1/2”) works well and allows the fiber bundles to be cut between fixtures after the tabs are cured.

2.) Carefully roll the carbon-fiber bundle onto a smooth table in reasonable alignment with the test fixtures.

3.) Use super glue to bond a finger portion of a latex laboratory glove onto the leading end of the fiber bundle.

4.) Wind the leading end of the fiber bundle through the pigtail orifice.

5.) Attach the tension weight to the bonded latex finger tip on the leading end of the fiber bundle.

6.) Start the flow of the orifice lubricating fluid and slowly pull the fiber bundle through the orifice and into the line of test fixtures. Stop the flow of the lubricating fluid.

7.) Clamp the trailing end of the fiber bundle and hang the weight over the end of the workbench to keep the bundle taut.

8.) Carefully press modeling clay into the fiber grooves at each end of the tab resin wells to block the flow of resin out of the tab wells.

9.) Pour resin into each tab well, but fill each tab well to only 1~2mm (0.080~0.160”) from the surface of the test fixture. Allow the resin to cure.

10.) Remove weight from the leading end of fiber bundle and carefully cut the bundle connecting each test fixture.

11.) The specimens are now ready for the test procedure.

CHAPTER 4

IMPREGNATED-BUNDLE TEST DEVELOPMENT

The general concepts and motivation of impregnated-bundle testing were understood before this stage of the research was approached. The specific needs to conduct impregnated-bundle tests were established. Extensive impregnated-bundle testing is conducted regularly by industry [eg. Hexcel® data], but this is usually with low viscosity resins. Typical structural resins for composites are more viscous and impregnating bundles can be difficult. Hence, a method of successfully impregnating carbon fiber bundles in a laboratory setting was considered to be the first task. Impregnation methods were explored within the parameters of the facilities available. A heated-pneumatic plate press was chosen as the most viable option for impregnating the fiber bundles. Discussion of the design considerations and construction of the plate press follows in this chapter. It was necessary to modify the plate press after initial construction, so that vacuum could be applied, in order to achieve the desired specimen quality. Finally, procedures were developed for proper impregnated-bundle specimen preparation and curing to insure that tests of the specimens could yield the best results. A synopsis of the procedures for impregnated-bundle specimen preparation are presented at the end of this chapter.

Impregnated-Bundle Test Method

The motivation of the impregnated-bundle tests was to explore the composite performance of the same carbon fibers that underwent dry-bundle tests when used in conjunction with matrix materials. The impregnated-bundle portion of this research was conducted using two different epoxies as matrix materials. One epoxy, Hexcel® 3501-6, is a brittle matrix material, while the other, Hexcel® 8552, allows more yielding and strain to failure. These matrix materials were used in conjunction with the same production lots of carbon fibers that were used for all of the dry-bundle tests. The maximum loads were expected to be higher than the dry-fiber bundles because of load sharing, as was discussed in chapter 2.

Impregnating the fiber bundles with the epoxies presented a significant challenge. This was due to the high viscosities of the epoxies. Both 8552 and 3501-6 have a consistency at room temperature similar to that of stiff chewing gum. The 3501-6 is slightly less viscous than the 8552, but neither one will readily flow into a fiber bundle by low pressure and capillary action like polyester resin. In industry, the epoxies are spread onto release sheets as a film. Then the fiber bundles are placed between two of these epoxy films and rolled through rollers to press the epoxy into the fiber bundles. Complexity and cost would not allow this method to be used in the laboratory. A roller method was initially considered wherein the fiber bundles would be bathed in heated epoxy, then rolled between two rollers to press the epoxy into the fibers and squeegee away excess epoxy. After working with the dry-fiber bundles it was apparent that the sticky nature of the epoxy on the rollers would have a tendency to pull the fiber bundles

apart as they exited the rollers; the method would simply be too abusive to the fibers. A method was considered in which epoxy would be heated and applied to two flat rubber-faced platen surfaces, between which the fiber bundles would be placed. The platen/fiber sandwich would then be placed into a press where pressure would be applied for an adequate time period. Availability to the necessary press, as well as the necessity of heated platens deterred the use of this method. Both cylindrical vacuum and pressure chambers were considered, but there was no realistic solution to getting specimens into and out of the chamber without considerable time, mess, and possible damage to the fiber bundles. The method that was finally chosen was to use a plate press that consisted of two heavy plates. One of the plates would have a rubber diaphragm attached so that air pressure could be applied between the plate and the diaphragm. It was determined that it would be best to attach the diaphragm to the upper plate to allow the lower plate to function as a base plate where the specimens could be prepared for impregnation. Heated epoxy would be spread onto the lower plate and onto an upper surface. The fiber bundles would be placed between the epoxied lower plate and upper surface. Then the upper plate would be clamped to the lower plate so that the diaphragm would press the epoxy into the fiber bundles when air pressure was applied. The plate opposing the diaphragm plate would require a heating element of some sort to keep the epoxy fluid enough to flow into the fibers of the bundles.

Plate Press Construction

The first consideration for the construction of the plate press was the physical size that was required. The constraining factors for the size of the plate press were the

specimen length and number of specimens to be prepared each time. Since the test fixtures were 381mm (15”) long, the working surface had to be at least 406mm (16”) in one dimension to produce specimens long enough and to allow some working room at the ends of the specimens. It was preferable to prepare at least 30 specimens at a time, since that was the number of test fixtures. Allowing about 13mm (1/2”) between specimens on the plate would produce at least 30 specimens in 406mm (16”). This meant that an area 406mm (16”) square would be needed for the working surface. An additional 25.4mm (1”) perimeter around the working area was also necessary to allow for fastening the diaphragm to one of the plates. Therefore, the plates needed to be 457mm (18”) square. It was anticipated that about 689 kPa (100 psi) would be required to press the epoxy into the fiber bundles. The plates needed to be thick enough to resist flexing since the force

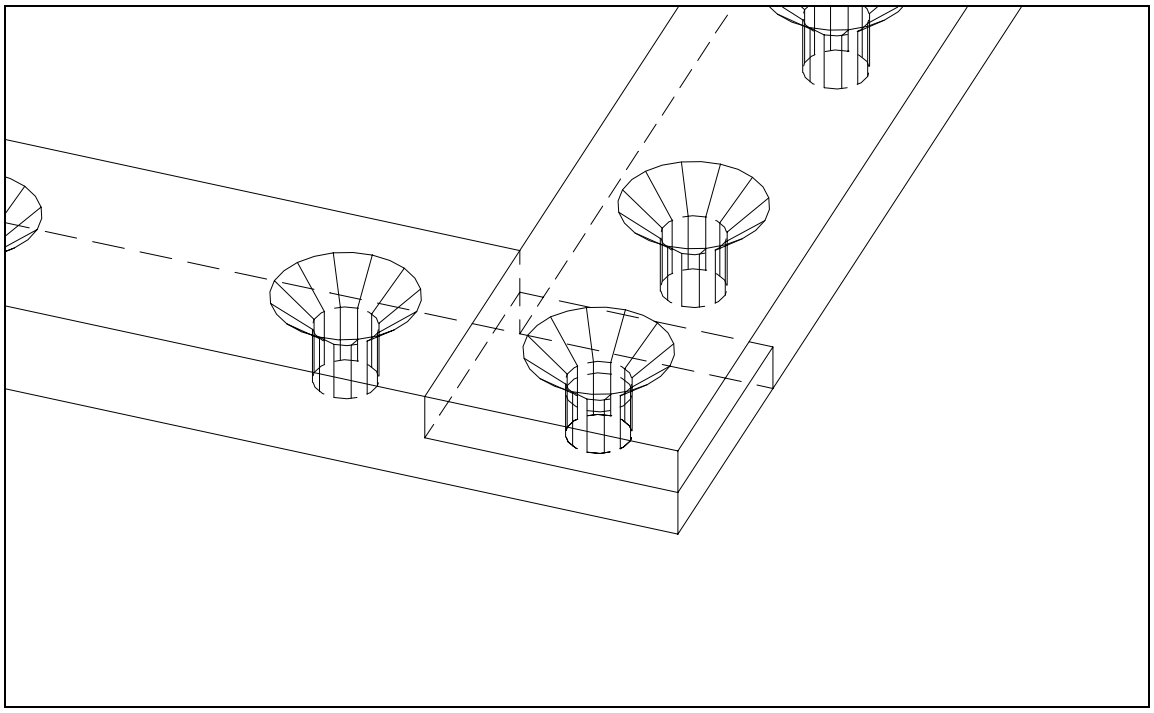

Figure 4.1. Overlapping corners of first design of diaphragm retainer sections

created by 689 kPa (100 psi) over the 406mm (16”) square surface would be about 114 kN (25600 lbf). Two 6061 aluminum plates which were 25.4mm (1”) thick and 457mm (18”) square were chosen as the basis of the plate press. Aluminum was chosen as the plate material to facilitate the machine work required and because its thermal conductivity is such that the heating of the plate would be reasonably even throughout. Buna N (nitrile) rubber in a thickness of 3.2mm (1/8”) was chosen as the diaphragm material due to its ability to withstand working temperatures up to 149°C (300°F) and its availability. A perimeter of 9.5mm x 25.4mm (3/8” x 1”) 6061 aluminum was used to hold the diaphragm in place. This was accomplished by using four individual pieces 457mm (18”) long and machining the ends so that they overlapped in the corners as shown in Figure 4.1. One common screw was used through the overlapped

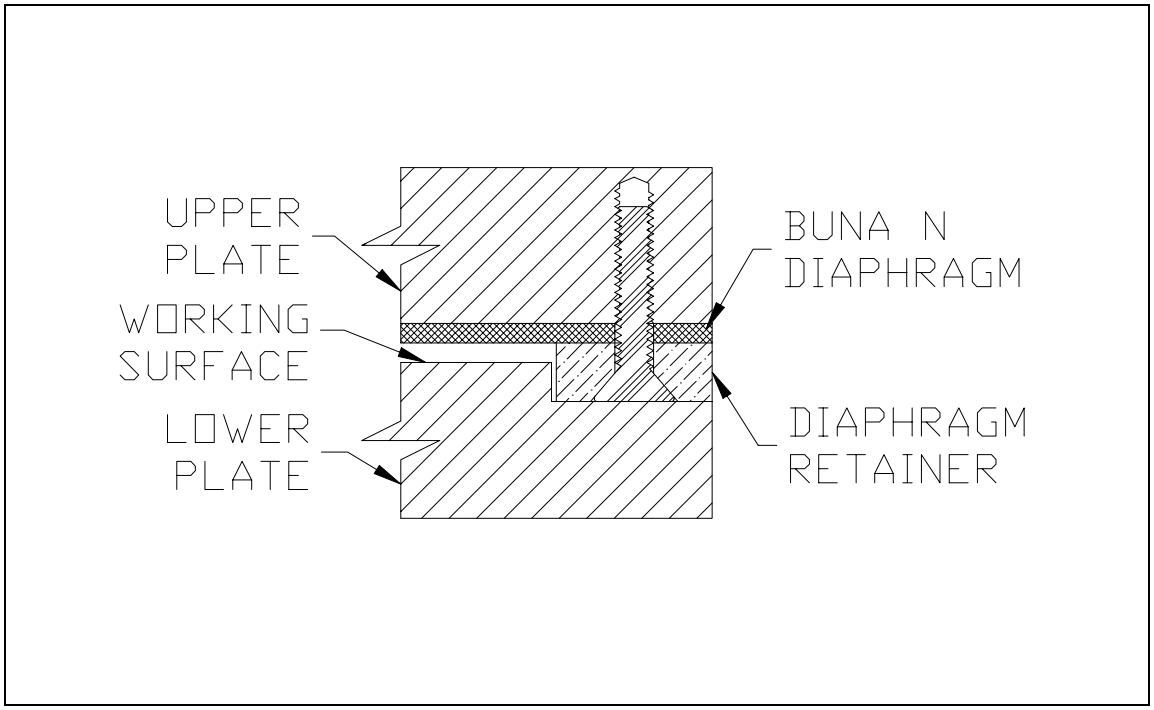

Figure 4.2. Cross-sectional view of first design of the edge of the plate press

diaphragm retainer pieces at each corner. The next screw away from each corner screw was spaced 25.4mm (1”) measuring from center to center of the screws. The rest of the screws were spaced on 38.1mm (1.5”) centers.

Space was required between the diaphragm and the working surface on the opposing plate to allow room for the epoxy, fiber bundles, and the necessary sheets of release material. Machining a void behind the diaphragm into its mounting plate could have provided this space. However, this method was not used, due to the additional machine work needed and since it was undesirable to reduce the thickness of the plate by 3.2mm (1/8”), the space considered necessary to provide enough room for the epoxy, fiber bundles, and release sheets. The method chosen to provide working space was to machine around the perimeter of the base plate where the diaphragm retainer clamped against the base plate when the plate press was closed. The diaphragm retainer acted as a limiting spacer against the flat base plate to provide 9.5mm (3/8”) of space between the working surface and the diaphragm. Machining the base plate down 6mm (1/4”) where the diaphragm retainer mated, reduced the space between the diaphragm and the working surface to the desired 3.2mm (1/8”). A cross section of the edge of the plate press is shown in figure 4.2. The diaphragm retainer was held in place by 1/4” x 1-1/4” NC grade eight flat head socket screws that were countersunk into the retainer to allow it to fit flat against the base plate.

The two press plates were clamped together by eight 1/2” x 5”-NC grade five bolts that fit through steel loops that were bolted to the aluminum plates in appropriate places to provide even support around the plate press. Calculations showed that only two of these bolts would be sufficient to withstand the forces of the plates pushing away from

each other, but two bolts certainly would not have held the plates together without flexing along the edges. Eight bolts also increased the safety of using the plate press. Hinges at the rear of the plate press allowed the top to be properly aligned when it was hinged down into place. Four legs constructed from 25.4mm (1") square tubing, held the base plate 100mm (4") above the workbench.

The last item needed for the base of the completed plate press was a heating element to keep the base plate warm enough to reduce the viscosity of the epoxy. It was important to control the temperature, since too high a temperature could cause the epoxy to start to cure in the plate press, as well as damage the diaphragm. Individual strip heating elements were available, but they required far more space than was available to

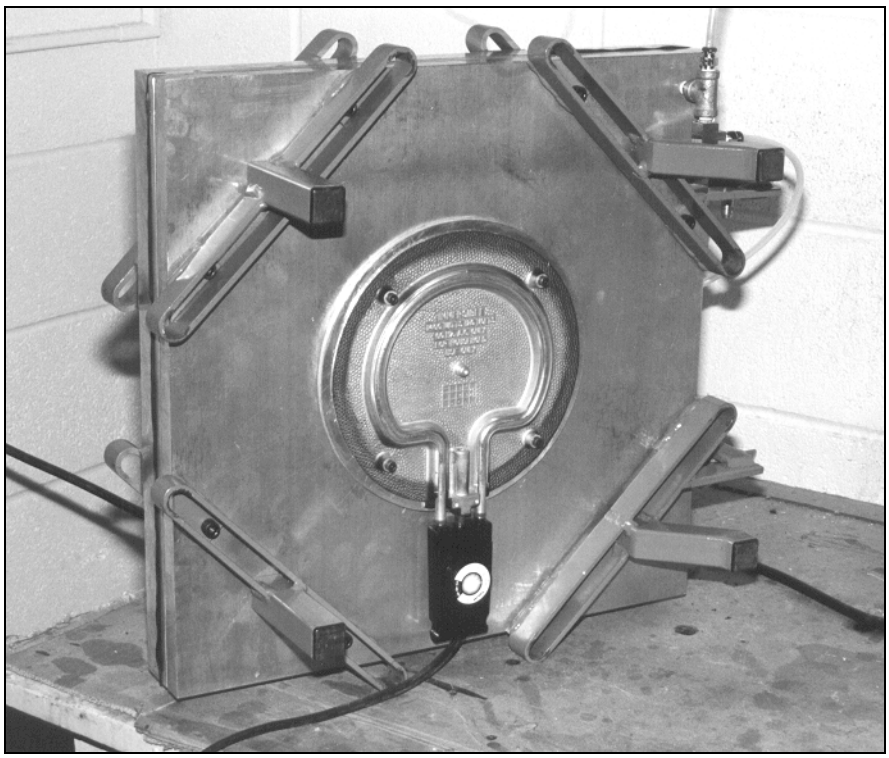

Figure 4.3. Bottom view of completed plate press with heating element in place

supply enough energy to heat the plate in a reasonable amount of time. In addition, these heating elements had no temperature control. Electrically heated household appliances were first considered as a source for heat because of their simple heat controllers and their availability at reasonable costs. Upon researching these appliances, it was found that electric fry pans, griddles, and deep fryers had heating elements capable of between 1000 watts and 1500 watts that were compact enough to fit easily into the required space. A deep fryer with a 1400-watt element was chosen. It was necessary to cut away the upper portion of the cooking pot with a band saw, leaving only the flat-round bottom with the heating element attached. The heating element was fastened to the base plate by four bolts, which fit into drilled and tapped holes. A 6mm (1/4") spacer plate was required to allow the temperature control unit enough clearance from the base plate. The spacer plate was an aluminum disk, since the thermal properties of aluminum would allow rapid conduction of the heat into the base plate. The bottom of the completed plate press with

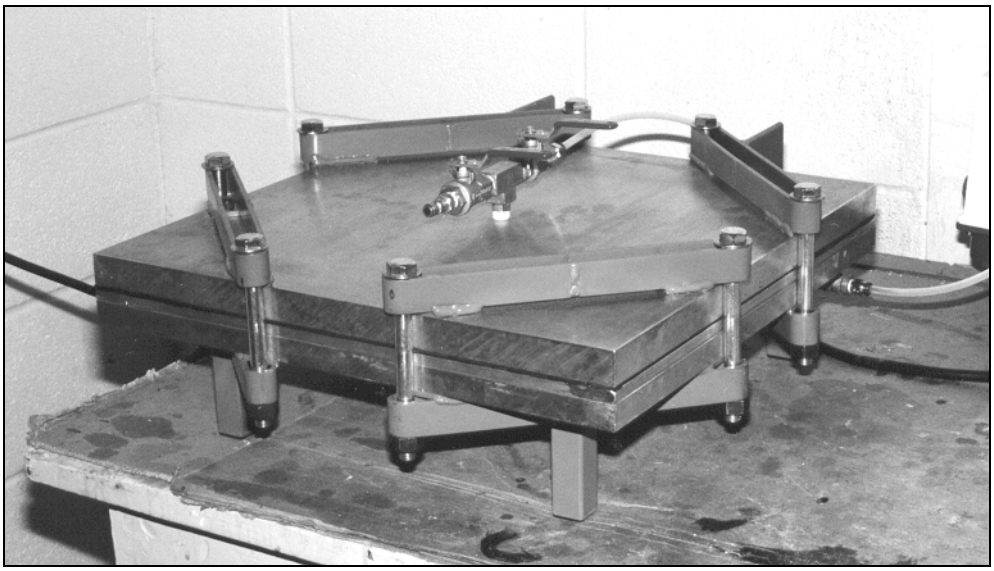

Figure 4.4. Completed plate press with clamp bolts in place

the heating element attached is shown in Figure 4.3. This completed the plate press, which is shown with the clamp bolts in place in Figure 4.4.

The plate press was safety tested before use by installing the clamp bolts and applying air pressure behind the diaphragm starting with 138 kPa (20 psi) and increasing the air pressure in 34.5 kPa (5 psi) increments to 689 kPa (100 psi). The test was successful. It was observed that the plates exhibited less than one millimeter flex in the center of the square plates at 689 kPa (100 psi).

The plate press was tested by impregnating the fiber bundles with Hexcel® 8552 epoxy. Different methods and warmer temperatures were tried, but porosity in the impregnated fiber bundles remained a problem. The ability to evacuate the space containing the fiber bundles was considered as a possible solution. This meant sealing the working area so that vacuum could be applied on the lower side of the diaphragm while air pressure was applied above the diaphragm.

Plate Press Phase Two

Two methods were considered for sealing the working area. One was to machine the working surface down, leaving a ridge around the perimeter, which could seal against the outer edges of the diaphragm to the inside of the diaphragm retainer. This would also require additional machining of the base plate perimeter where the diaphragm retainer mates against it to allow the plates to fit closer together. The second method was to machine an O-ring groove into the base plate where it could seal against the diaphragm retainer. The second method was chosen because it maintained a flat working surface, whereas method one would leave the raised sealing ridge around the perimeter of the

working surface. Also, the second method preserved the full thickness of the aluminum base plate, which was preferable. The cross-sectional view shown in Figure 4.5 illustrates the location of the O-ring in the modified base plate. The O-ring groove followed a 4.8mm (3/16”) radius at each corner of the base plate, insuring smooth directional changes of the O-ring in these areas.

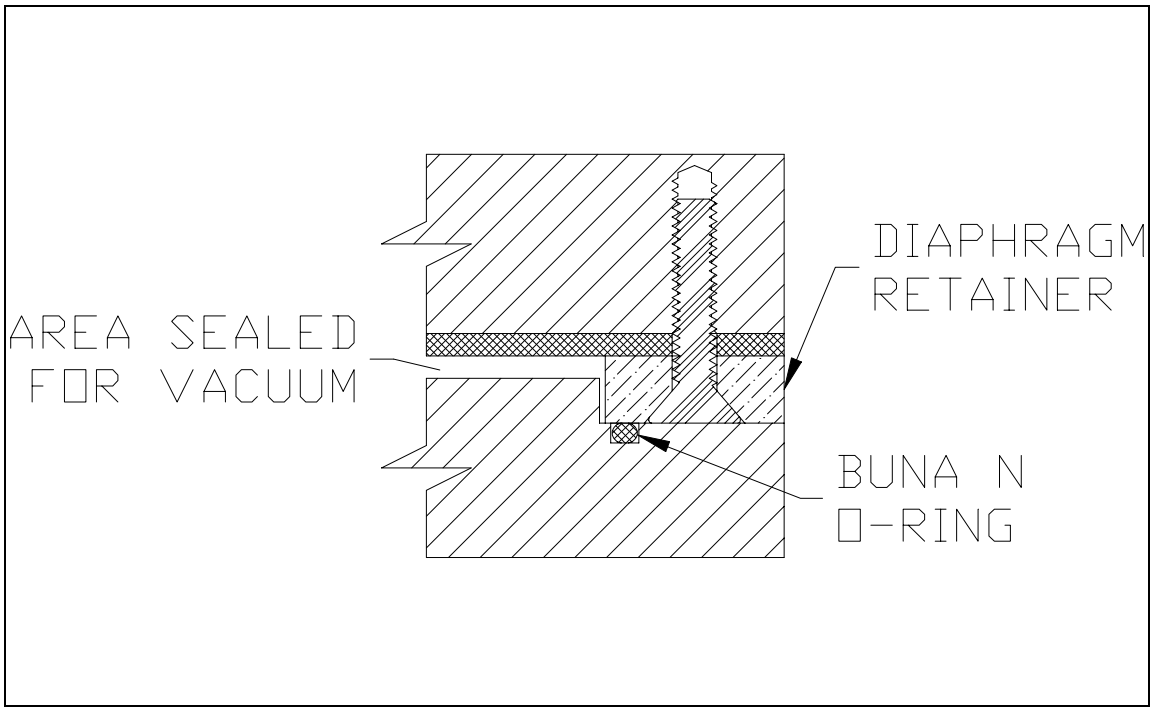

Figure 4.5. Cross-sectional view of second design of the plate press edge with O-ring to seal work area

Sealing against the diaphragm retainer required that the overlapped corner areas of the retainer be sealed. Due to the many surfaces in the overlapped corners and their orientations, the most reliable method to seal against leaks was to weld the corner areas. This required a TIG welder since the retainer was aluminum and the welded corner areas required machining to provide a surface smooth enough to seal against the O-ring. The

modified corner of the diaphragm retainer is shown in Figure 4.6. If the necessity to seal the plate press in this manner could have been anticipated, the resultant one-piece diaphragm retainer would have been considerably easier to construct from one plate

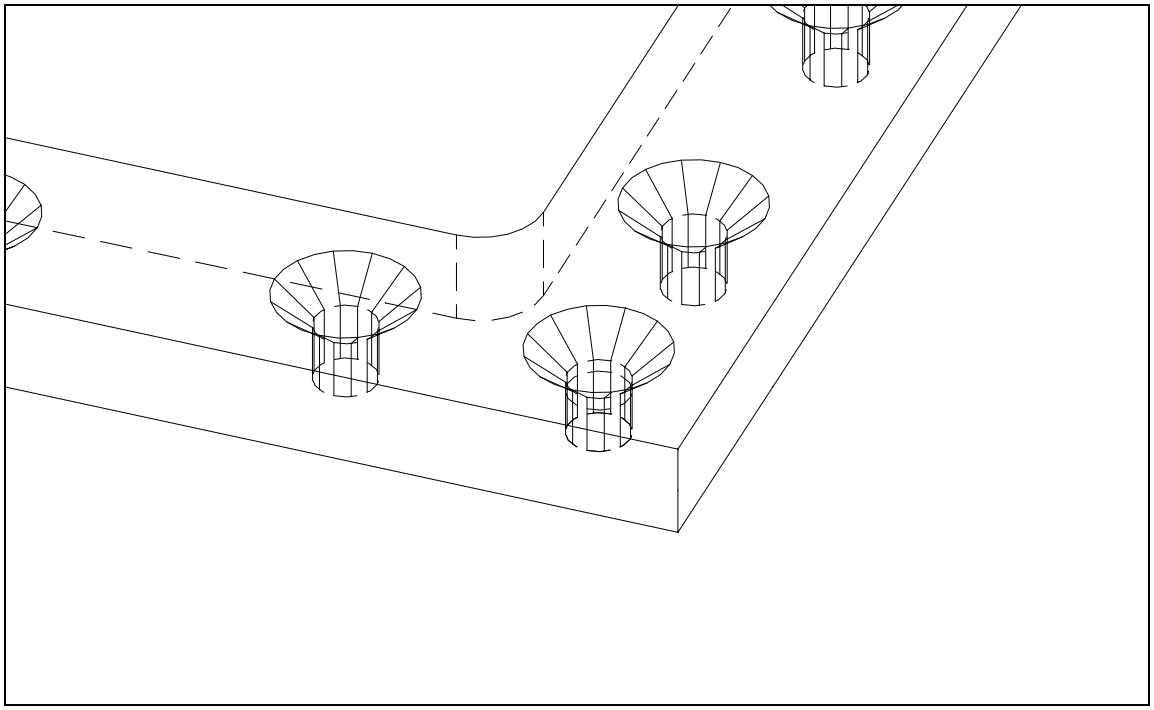

Figure 4.6. Corner of modified diaphragm retainer for second plate press design

9.5mm (3/8”) thick rather than welding together the individual pieces at the corners. In this case, however, the choice was made to weld and machine the corner areas since all of the screw holes were already properly located, drilled, and countersunk. The modifications that allowed the use of vacuum with the plate press proved fruitful, virtually eliminating porosity in the impregnated specimens.

Development of the Impregnated Bundle Specimen Preparation Procedure

As stated previously, impregnating the fiber bundles with the viscous epoxies turned out to be a nontrivial matter. Unlike the dry-bundle tests, each test specimen would have to be prepared individually in a length appropriate for the test fixtures. Each specimen would have to be cut to length, impregnated with epoxy, cured in an oven, and prepared in the test fixture before the final test. For over 600 test specimens, this meant a great number of steps, since each specimen would require handling many times before being ready for testing. It was extremely important to produce high quality impregnated specimens that would have characteristics representative of the high quality composite materials that are used in the aerospace and aircraft industry. This meant porosity would have to be virtually eliminated and that high fiber volumes would have to be maintained in the specimens. The goal of using the plate press was to force the epoxies into the fiber bundles to produce these high-quality specimens.

The 8552 and 3501-6 epoxies used for this research were provided by Hexcel®. Both of these epoxies were in 3.6-kg (8 lb.) quantities, which were packaged in plastic bags and shipped in dry ice. The large blocks of epoxy contained in the plastic bags, were broken into smaller pieces with a hammer and placed into plastic freezer containers so that only small quantities of the epoxy would have to be removed from the freezer during specimen preparation. These epoxies were stored in a freezer until use because they are pre-catalyzed. This means that no added catalyst is required to promote the epoxies to cure; they must only be heated to 176° C (350° F) for about two hours. In their frozen forms, the 8552 was hard and brittle, while the 3501-6 was more crumbly

when broken with the hammer. At room temperature, 8552 has the consistency of chewing gum or taffy, while 3501-6 is slightly less viscous, but has similar characteristics. When heated to about 60° C (140° F), the viscosity difference became more apparent, with the 3501-6 being like thick honey and the 8552 being like a soft caramel. The 8552 would achieve a honey-like consistency when heated to over 93° C (200° F).

Once the plate press had been constructed, the immediate challenge was develop a procedure that would dependably produce the desired specimens. Initially, only air pressure was used in development of the procedure. The use of vacuum was incorporated later. The original intention was to apply a thin layer of epoxy, 0.5mm to 1mm (0.020”-0.040”) thick onto two sheets of release material. The fiber bundles would be placed into the epoxy on one of the release sheets and the other epoxy coated release sheet would be placed on top of the first, sandwiching the fiber bundles between the epoxy layers. The epoxy/fiber sandwich would then be placed onto the base plate of the plate press and covered with a plastic sheet to keep the epoxy from contacting the diaphragm. It was decided to use the surface of the heated plate press to heat the epoxy so that it could be spread onto the release sheets. This was achieved by laying the two release sheets side by side on the heated base plate. The pieces of frozen epoxy were then placed onto the release sheets. When the epoxy was sufficiently heated, it could be spread evenly with a laboratory spatula and the fibers were placed into the epoxy. Then, the second epoxy-coated release sheet would be folded over onto the first one, encasing the fibers in epoxy. The materials on the base plate had to be covered by a plastic sheet to separate the diaphragm from the epoxy coated materials. A sheet of thin Teflon® was used during

actual specimen preparation. It was desirable to keep the epoxy away from the diaphragm because of possible damage to the diaphragm that could be caused by repeated cleaning. The Teflon® sheet also provided a release surface, which allowed the plate press to be opened after use. Otherwise, the diaphragm would be bonded to the opposing surface after use, causing difficulty in opening the plate press, as well as possible damage to the specimens or the press diaphragm.

The plate press was closed and bolted together securely once the fibers and epoxy were in place. Then, an air hose was connected to the fitting on the plate press. It was best to turn the air regulator to zero before connecting the air hose, then raise the pressure to the desired pressure. The specimens were subjected to the heat and pressure for 30 to 60 minutes. At this time, the heating element was unplugged and the air regulator was turned back to zero pressure. The bolts were then removed from the perimeter of the plate press and it was opened. The release sheets and plastic remained on the base plate. The Teflon® sheet was removed from the upper release sheet and the release sheets were removed with the fibers and epoxy between them.

The specimens to test for porosity were made using 8552 epoxy because it offered the greatest challenge due to its higher viscosity. The initial specimens were made in groups of four to six, in lengths of about 150mm (6”) and were cured in a standard kitchen oven at 176° C (350° F). Once the plate press was opened after impregnating the fiber bundle specimens, the release sheets were separated and the impregnated fiber bundles were peeled away from their attached release sheet. Initially, the fiber bundles were peeled away from the release sheet while the epoxy was still warm. This caused strings of the gooey epoxy to pull away along with the fiber bundle. These specimens

were placed between plastic sheets to be taken to the oven for curing. The small sized ACCO® binder clips were used to clamp onto the ends of the specimens. The loops of the binder clips were hooked on paper clips that had been appropriately bent to allow the binder clips and fibers to hang straight down. Then, another binder clip was clipped onto the bottom of each suspended fiber bundle to maintain straight specimens. The specimens were cured for two hours at the desired temperature. Then, the binder clips were removed, leaving cured-impregnated fiber bundle specimens.

The specimens were checked for porosity by cutting them into lengths of about 15mm (5/8”), mounting them in plastic, and polishing the end of the plastic block in which the specimen sections were mounted. The specimens were cut to the proper length using an abrasive cut-off wheel to avoid the damage that could be caused by a hacksaw or by wire cutters. The specimen lengths were placed so that the polished end of the mounting block would expose a cross section of the impregnated fiber. The polished specimens were examined using a microscope.

Development of Non-Porous High Fiber Volume Specimens

For clarity, a system designating the layers of materials used for each of the tests will be introduced here. This system is quite similar to the designation commonly used to show the layup of composite materials. The abbreviations for the materials are separated by forward slashes and the group of layers is enclosed by left and right square brackets. The material list designates the materials from the bottom to the top layer as it goes from left to right between the brackets. For example, [R/E/F/E/R/T] designates the bottom layer being R, followed in order by layers E, F, E, R, and the top layer of T.

The abbreviations for each of the materials used, as well as information about the suppliers and the materials, are listed as follows:

A = Absorbent material

From: Richmond Aircraft Products
310-404-2440

This material was supplied on a roll 1.22m (4') wide and appeared to be cotton. It was in a thickness of about 6mm (1/4") and was unwoven. Its fibers were loosely packed, similar to a cotton ball, but were formed into flat material.

E = Epoxy

From: Hexcel Corporation
5794 West Las Positas Blvd.
Pleasanton, CA 94588-8781
925-847-9500 Fax 925-734-9042

This material is described in detail above in the text.

F = Fiber bundles

AS-4

From: Hexcel Corporation
5794 West Las Positas Blvd.
Pleasanton, CA 94588-8781
925-847-9500 Fax 925-734-9042

T300

From: Amoco Polymers, Inc.
P.O. Box 849
Greenville, SC 29602-0849
864-277-5720

R = Release material: Release Ease-234 P TFP

From: Airtech Advanced Materials Group
Airtech International Inc.
5700 Skylab Road
Huntington Beach, CA 92647
714-899-8100 Fax 714-899-8179

This material was a woven Teflon material that was supplied on rolls 0.91m (3') wide. It was available in both porous and nonporous forms, but the porous type was the only type used in this research.

T = Teflon sheet: WL 4900.B.0005. lot # 793635-6
From: Airtech Advanced Materials Group
Airtech International Inc.
5700 Skylab Road
Huntington Beach, CA 92647
714-899-8100 Fax 714-899-8179
This material was a thin sheet of Teflon that was supplied on a roll 1.37m (54") wide.

The various material layups and process conditions used while developing the fiber bundle impregnating procedure are shown in Table 4.1. It can be seen that nine

Table 4.1. Impregnation Conditions and Results for Procedure Development

Test	**Materials**	**Temperature**	**Pressure**	**Results**
1	[R/E/F/E/R/T]	60°C (140° F)	345 kPa (50 psi)	Macroscopic voids
2	[R/E/F/E/R/T]	60°C (140° F)	689 kPa (100 psi)	Macroscopic voids Smaller than test 1
3	[T/E/F/E/T]	60°C (140° F)	689 kPa (100 psi)	Macroscopic voids Smaller than test 1
4	[R/E/F/E/R/T/ruler]	60°C (140° F)	689 kPa (100 psi)	Macroscopic voids Smaller than test 1
5	[R/E/F/E/R/T]	93°C (200° F)	689 kPa (100 psi)	Macroscopic voids Slight improvement
6	[R/E/F/E/R/A/T]	93°C (200° F)	689 kPa (100 psi)	Some minute macroscopic voids Some microscopic voids Marked improvement
7	[R/E/F/E/R/A/T]	99°C (210° F)	689 kPa (100 psi) w/vacuum	Some microscopic voids Porosity virtually eliminated
8	[R/E/F//R/A/T]	99°C (210° F)	689 kPa (100 psi) w/vacuum	Some microscopic voids Porosity virtually eliminated
9	[R/E/F//R/A/T] Plate press cooled w/press. & vac.	93°C (200° F)	689 kPa (100 psi)	Some microscopic voids Porosity virtually eliminated

procedures were tried before the quality objectives, minimum porosity and high fiber content, were achieved. Some of these nine were repeated to verify results.

The first test was conducted using less severe conditions. It had been anticipated that a pressure of 689 kPa (100 psi) would be necessary to impregnate the fiber bundles. However, the lower pressure was used first to see if there was a possibility of obtaining acceptable results. The cured specimens obtained had excess matrix material surrounding the fiber bundles. This was apparent because of the non-uniform diameter along the length of the specimens. Also, some of the fiber bundles had been impregnated with the less viscous polyester resin in earlier stages of this research, the result being an impregnated bundle with a uniform diameter of about 0.5mm (0.020”). The polyester-impregnated fiber bundles gave an example of the approximate size of an impregnated bundle with no excess matrix material. The epoxy-impregnated fiber bundles had obviously excessive amounts of epoxy stuck to the outside of the fiber bundles before curing. However, it was thought that at the higher temperatures of curing could possibly cause excess matrix to become less viscous and flow off from the specimen before curing. This was not the case, however, and the resultant specimens had diameters two or more times the diameter of the polyester-impregnated fiber bundles. The specimens were cut, mounted, polished, and examined for porosity. There were many macroscopic voids that rendered the quality of these specimens unacceptable.

Tests 2, 3, and 4 were all set up in the plate press at the same time. Some different material layups were used along with the higher air pressure of 689 kPa (100 psi). All of the layups essentially sandwiched the fiber bundles in epoxy between other materials. A thin stainless steel ruler was placed on top of the specimens of test 4. It was

thought that a reasonably ridged surface applying even pressure might have a tendency to squeeze out more excess epoxy than the compliant surface where only the diaphragm applied pressure. It was apparent from the results of all three of these tests, that the higher pressure generally reduced the size of the voids, but not necessarily the number of voids. The diameters of the specimens were still large and non-uniform.

Test 5 was conducted using a higher temperature to further reduce the viscosity of the epoxy to allow it to flow easier among the fine fibers of a bundle. There was a slight improvement, indicating that lower viscosity was beneficial. The diameter of the specimens remained large and non-uniform.

The material layup was changed slightly to include a layer of absorbent material for test 6. The absorbent material was placed just below the top layer of Teflon®. It was considered that the epoxy encasing the fiber bundles was trapping air voids within the bundles. Once pressure was applied, the bundle would be subjected to the same forces from all sides if the epoxy would not flow away from the fiber bundles. The idea was that the layer of absorbent material should allow the epoxy to flow through the porous release material into the absorbent layer, which would in turn allow the epoxy to flow through and away from the fiber bundles. The high temperature and pressure were used again, since they gave beneficial results in the prior tests. The results of adding the absorbent layer were marked improvements with respect to porosity, as well as uniform specimen diameters that were similar to the polyester-impregnated specimens. The macroscopic voids were nearly eliminated and microscopic voids were sparse. These were the first specimens made that had little excess epoxy on them, yielding fiber volumes high enough to be considered close to those desired. At this point, it appeared

that benefits from further increases in temperature and pressure would be limited, since much higher temperatures and pressures could exceed the safe operating limits of the plate press. Vacuum applied to the work area between the diaphragm and the base plate was the only remaining reasonable possibility of further improving the specimen quality using this method of impregnation.

Tests 7 and 8 were set up in the plate press together after the press was modified for use with vacuum. Both material layups were similar and included the absorbent layer that improved previous results. The only difference in the material layups was that test 8 only had a layer of epoxy below the fiber bundles. This required that the epoxy flow through the bundles to get to the absorbent layer. The resultant specimens from these tests were essentially identical.

Test 9 was set up with the same layup as test 8, but was prepared with slightly lower temperature. Essentially the only difference was that the plate press was allowed to cool to room temperature with pressure and vacuum applied. The resultant specimens exhibited virtually identical characteristics as those from tests 8 and 9. However, removing the cooled specimens from the release sheet resulted in none of the strings of epoxy exhibited with warm specimen removal. The vacuum used in tests 7, 8, and 9 virtually eliminated porosity in the specimens and the fiber volumes remained high enough to continue with further tests. The incorporation of vacuum completed the evolution of the fiber-bundle impregnation procedure enabling full-length specimens to be produced for preliminary tests.

Curing Impregnated Specimens: Before full-length specimens could be produced, it was necessary to improvise a method of hanging the specimens in an oven while they cured. It was foreseeable that there was a possibility of needing to cure two groups of impregnated fibers at a time. This meant that space for at least 60 fiber bundles would be required and a wire grid was considered the best type of area from which the fibers could hang. An enclosure was constructed from square sections that make up quick interlocking shelves for household use. The sections were 356mm (14") square and formed a wire gridwork of nine squares along each side. Some of the square sections were cut in half and welded to full-sized pieces so that the final enclosure measured

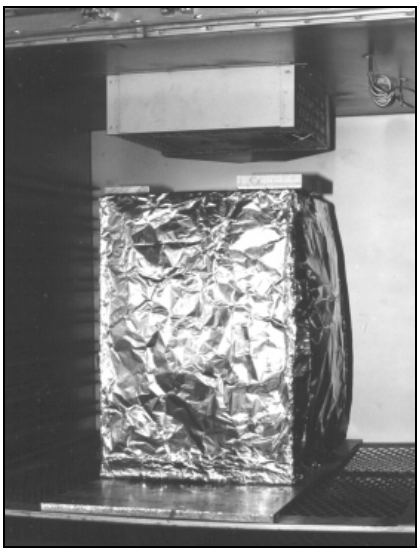

Figure 4.7. Curing enclosure inside oven

356mm (14") square and was 533mm (21") high. It was necessary to wrap the enclosure with aluminum foil because the only oven available that would accept the enclosure was a large convection oven. The impregnated specimens would have been blown about,

most likely sticking them together without the aluminum foil to protect them from the forced-moving air within the oven. The enclosure is shown inside the convection oven in Figure 4.7. Hooks for hanging the fibers from the binder clips were made from paper clips and were hooked over the gridwork of wires in the top of the enclosure. Again, once the fiber bundles were hung from the binder clips, small binder clips were attached to the bottom of the fiber bundles to provide weight to keep the specimens straight as they cured. The hanging-impregnated fiber bundles are shown in Figure 4.8. The left frame shows a view of the top of the enclosure where the fiber bundles were hung from the wire gridwork. The right frame shows the bottom of the impregnated fiber bundles with the small binder clips attached for weight. The impregnated fiber bundles are shown before they were placed in the oven for the epoxy to cure.

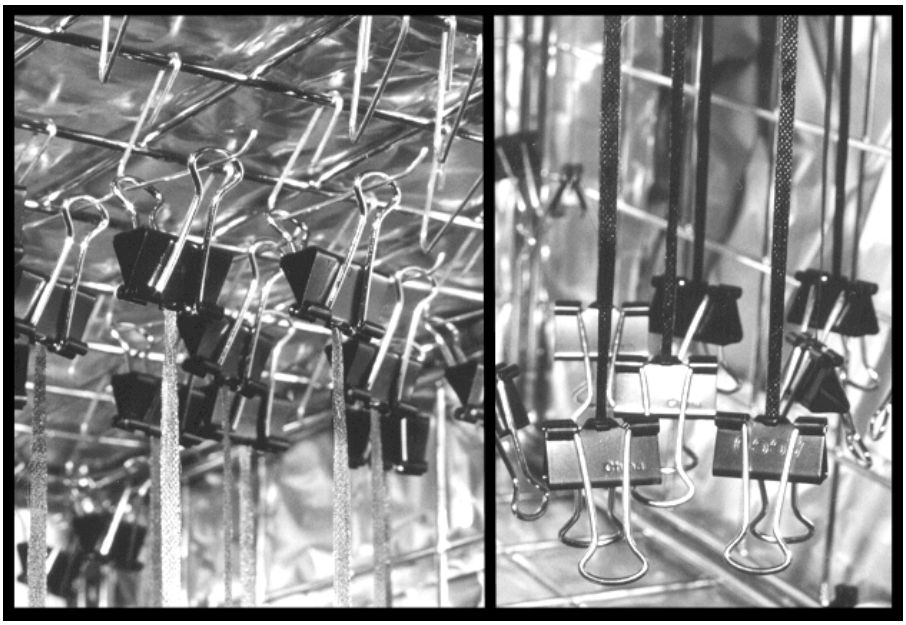

Figure 4.8. Impregnated specimens hung from binder clips inside curing enclosure with binder clips attached as weights

Verification of Specimen Quality: Six full-length specimens were impregnated and cured for initial ultimate load tensile tests. The specimens were placed into the test fixtures and polyester resin was used to mold tabs onto the specimen ends. After the polyester was cured for about 16 hours, an attempt was made to test the specimens. The first two slipped in the polyester tabs so the others were allowed to cure for another 48 hours. The result was that the tabs still slipped. One specimen was pulled until the larger ends of the specimen stopped at the tabs and it failed. The displacement data was of no use, but the maximum tensile strength indicated that the tensile strengths of the specimens were on target. Another group of 24 impregnated specimens was prepared. Another six specimens were placed in fixtures and tabbed with polyester. However, this time each of the ends of the specimens were sanded with 320 grit sandpaper in an attempt to increase the grip that the polyester could get on the specimens. Even with three days cure time for the polyester, the tabs all slipped, although at generally higher loads. Clearly, polyester, which has a reputation of poor bonding characteristics, could not be used for the tabs for the impregnated bundle tests.

Since it was known that Hexcel® used Henkel Adhesives' Macromelt® 6300 hot melt glue as tab material for some of their tests, further investigation was warranted. Macromelt® 6300 was tried earlier in this research as possible tab material with a polyester impregnated carbon fiber bundle. The hot melt glue exhibited two undesirable traits, shrinkage upon cooling and a tendency to bow the specimen in the length of the tab. The shrinkage was mostly an annoyance that would require more care during tensile tests and it was discovered that Macromelt® 6300 had less tendency to bow the epoxy-impregnated specimens than it had with the polyester impregnated bundle. The reason

for the difference in bowing was not pursued. It was speculated, however, that the high temperature of the hot melt glue, about 240° C (464° F), had more of a tendency to soften the cured polyester than it did the cured epoxy, which had already been exposed to 177° C (350° F) during curing. Two nice attributes of Macromelt® 6300 were that it released well from the fixtures and set rapidly, enabling testing soon after specimen preparation. Six specimens were prepared and tested with Macromelt® 6300 as tab material. Another favorable attribute of Macromelt® 6300 was discovered as these six specimens were tested, in that it bonded well to the specimens and did not slip when used as tab material. Macromelt® 6300 was tried as a tab material with polyester-impregnated carbon-fiber bundles early in this research. The Macromelt® 6300 tended to cause an undesirable bend in the tab section of the specimens. This behavior was not present when the Macromelt® 6300 was used with epoxy-impregnated carbon-fiber bundles. It is suspected that the bending was due to the heat softening the polyester resin along with different cooling rates on the tops and bottoms of the tabs. The epoxy-impregnated specimens exhibited no bending in the tab sections because they were stiffer and better able to withstand the temperature of the hot-melt glue.

Stress was calculated for the specimens using the data that was collected from the six successful tests, along with density data obtained from Hexcel®. Hexcel® provided density and mass per unit length data for each of the production lots of fibers that they furnished. The stress was calculated by using the Hexcel® data with the maximum load obtained from a tensile test as shown in the following formula.

$$\text{Stress} = \frac{\text{Load}_{max}}{\left(\frac{\text{Mass}_{fiber}}{\text{Length}}\right)} = \frac{\text{Load}_{max}}{\text{Area}_{fiber}} \qquad (23)$$

The stresses were calculated in this manner for the maximum and minimum loads obtained from the six tests. The stresses obtained proved that the specimens produced were of high quality and were representative of the high-quality composite materials of interest.

Since the process for producing specimens was refined, it was necessary to choose which material layup would be used for producing all of the specimens. The decision was made to use the layup, [R/E/F//R/A/T], that was used for tests 8 and 9 because it produced high-quality specimens without the film of epoxy on both sides. It was preferable to use only one epoxy film layer if the desired specimen quality could be achieved, since the films of epoxy on the release sheets were difficult to produce. The procedure for impregnation of fiber bundles with epoxy was established at this point.

The sequence of steps involved with the procedure is shown in Figure 4.9. The closed plate press at the beginning of the procedure is shown in frame 1. In frame 2, the heating element of the plate press has been plugged in and the bottom release sheet has been placed onto the base plate. The pieces of frozen epoxy that have been placed onto the release sheet are shown in Frame 3. As the base plate heats up, the pieces of epoxy begin to soften enough to be spread with a laboratory spatula as shown in frame 4. The epoxy must be repeatedly spread back and forth across the release sheet in differing directions to obtain a reasonably even and thin layer of epoxy as shown in frame 5. A

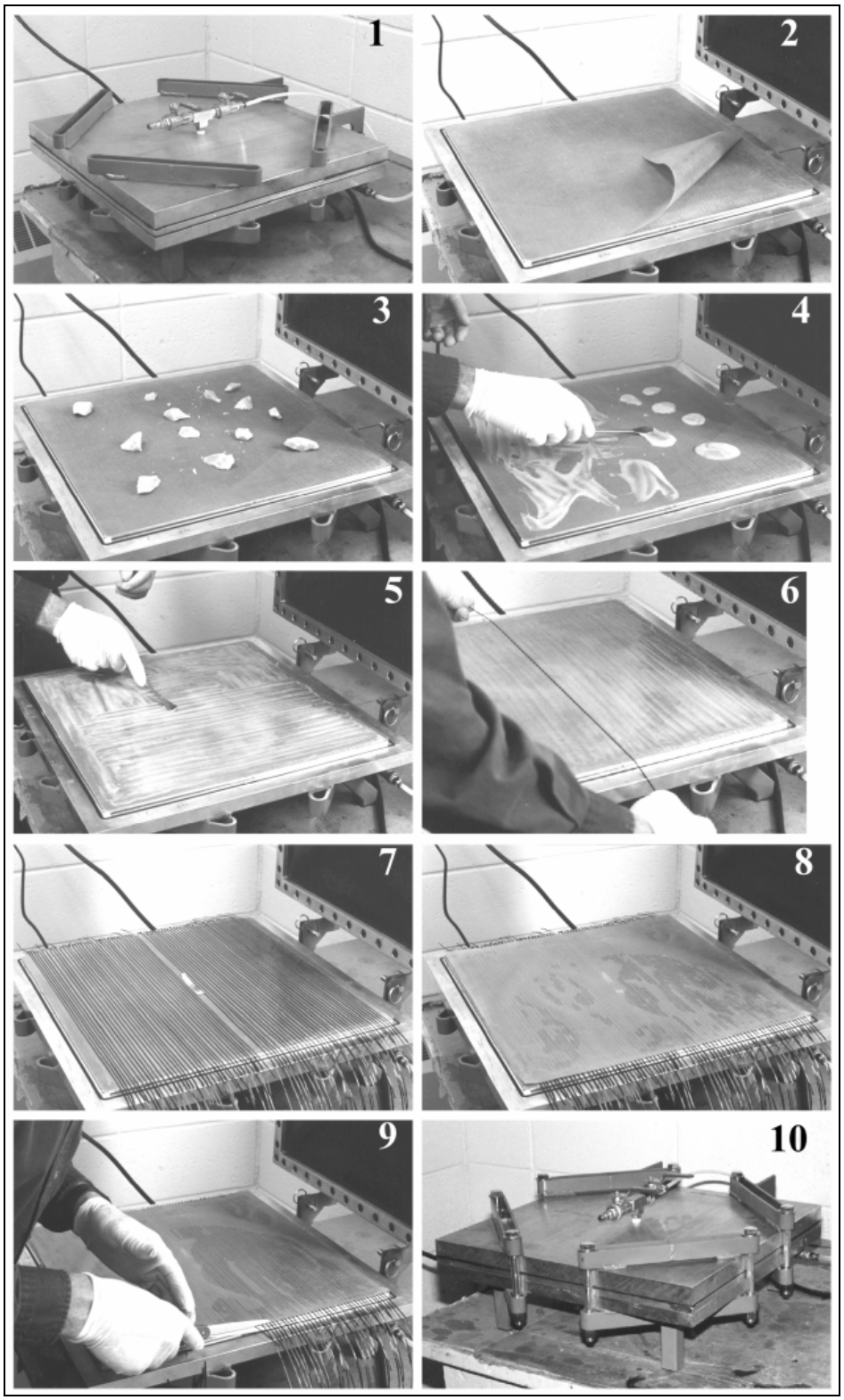

Figure 4.9. Sequence of steps for epoxy impregnation of carbon fiber bundles

wider spreading tool would have been beneficial, but the epoxy had a tendency to cool and build up on the small spatula. A larger tool would require a heat source to keep the epoxy from cooling on the end of the tool to an undesirable consistency. Spreading the epoxy entailed about 20 minutes of the procedure. Therefore, a larger heated tool to spread the epoxy could be warranted if a larger number of impregnated specimens were needed. Once the epoxy film was prepared, the fiber bundles were laid into the epoxy film as shown in frame 6. Initially, the bundles were drawn through an orifice without lubricant in an attempt to keep the fibers as collimated as possible. Acetone was used as a lubricant with the dry bundles of carbon fibers and has been used as a solvent to make the epoxies less viscous. However, acetone changes the properties of the cured epoxies, so no lubricant was used on the fiber bundles before they were placed into the epoxy matrix. The orifice was not used after the first two groups of fibers were impregnated. The sized fibers rolled together to fit through the orifice, but essentially returned to their previous state before they were laid into the epoxy. The orifice was disastrous when used without lubricant with unsized fibers. The outer fibers of the bundle peeled back and built up at the orifice as the bundle was drawn through, causing too much damage to the bundle to deem any tests of it valid. The best method for sized fibers was determined to be one in which the end of the fiber bundle was held in one gloved hand while the fibers were rolled from the roll, which was supported by a horizontal spindle. The leading end of the fiber bundle was held above the roll height so that the fiber bundle was hanging vertically after it was cut from the roll. The fiber bundles come off from the roll as a flat ribbon, especially the sized fibers. It was important to make sure that no twists occurred in the ribbon before it was laid into the epoxy, because the twist would remain in the

cured specimen. This was achieved on the sized bundles, by gently pulling the fiber bundle between the index finger and thumb of a gloved hand, only applying enough pressure to keep the bundle untwisted along its length. This method could not be used with unsized fibers, however. Too much fiber damage occurred as the bundle was drawn through the gloved fingers. The best method for the unsized fibers was to first tightly hold the leading end of the fiber bundle and unroll it as before. Once the bundle was cut and held vertically, the trailing end of the bundle could be taken about 150mm (6") up from the end by the other hand. It was important to leave plenty of extra working length with the unsized fibers because the outer fibers had a tendency to fray loosely from the bundle at the ends. This was the reason for grabbing the bundle up from the end, so that all of the fibers would be held. Once the length of fiber bundle was held between one's hands, it was important to keep it taut enough that air movement would not blow the individual fibers about. Then, the bundle could be laid into the epoxy.

The plate press with all of the fiber bundles laid in place is shown in Frame 7 of Figure 4.9. The fiber bundles shown in this picture are sized. It was possible to fit as many as 80 specimens of sized bundles in the plate press at a time, because they could be carefully placed with a small space between them. The sizing kept the fiber bundles narrow and uniform. The unsized bundles were naturally wider and required slightly more space between them, only allowing about 40 specimens to be impregnated at a time. It was necessary to be time efficient when preparing a group of specimens. The epoxies had a cohesive nature that caused them to slowly pull towards the center of the release sheet once the epoxy layer was spread out. This tendency was more prevalent at the edges, but also caused holes to form in the epoxy film in areas where it was thinner. It

was necessary to watch the epoxy layer while the fiber bundles were being laid in place, so that epoxy could be spread across the holes with a laboratory spatula before fiber bundles were laid in the areas. The holes would sometimes reappear between fiber bundles, but the epoxy along the fiber bundles remained continuous. It was also necessary to keep spreading the epoxy along the edges towards the outer edges of the release sheet, since the epoxy had a tendency to migrate toward the center. During preparation of one of the early groups of impregnated fibers, the movement of the epoxy caused the middle sections of the outer three or four specimens to move together and touch, ruining the specimens. The ends of the fiber bundles maintained spaces between them. The best technique for laying the fiber bundles into the epoxy was to start in the center and work outward. This enabled the outer edge of the epoxy to be spread thin again before fibers were laid in place. It was also best to allow more space between the bundles near the edges and not to place the fiber bundles all the way to the edge of the epoxy film, allowing the epoxy some room to move before it would start to carry a fiber bundle with it. Since two different lots of fiber bundles were usually impregnated at once, the first lot would start in the center and work toward the edge. Then, the second lot would again start at the center and work toward the opposite edge. A label, indicating placement of the two lots was placed between them and can be seen in the center of frame 7.

Once the fiber bundles were laid in place, the second release sheet was placed next, as shown in Frame 8. It was important to make sure that the second release sheet was aligned properly as it was laid down. A small amount of angular misalignment could turn out to be a large overhang from the work surface. Too much overhang could

interfere with the vacuum seal O-ring. Once the second release sheet was started into place, it could not be adjusted. This is because moving the release sheet would have a smearing effect on all of the fiber bundles. Fortunately, no major misalignments occurred during specimen production, but overhanging release sheet material could have been trimmed with scissors. A group of specimens would have to be discarded if a wrinkle occurred while the second release sheet was laid in place.

The excess lengths of the fiber bundles were trimmed as shown in Frame 9. This was easier after the second release sheet was laid in place because it held the fiber bundles more securely in place. Initially, the sections of fiber bundles were cut to the length required for the finished specimens, but it was impossible to place the shorter bundles into the epoxy without getting epoxy on the fingertips of the gloves. The epoxy on the gloves caused the next fiber section to stick to the fingertips, making it difficult to precisely place the fiber bundles. Once the excess fibers were trimmed, a layer of the absorbent material was placed next. It was found to be beneficial with the 8552 epoxy if another layer of the absorbent material about 32mm (1-1/4”) wide was placed around the perimeter of the working surface. This was to insure that any excess epoxy would be absorbed before it flowed past the edge of the working surface, avoiding the cleaning that would be necessary of the sealing surface and O-ring if epoxy flowed to the sealing area. It was necessary to use a double layer of the absorbent material with the 3501-6 epoxy. Using the previously described absorbent arrangement that was used with the 8552, excess epoxy flowed beyond the edge of the working surface, along nearly the entire length of the seal area during preparation of the first group of 3501-6 specimens. Over one hour was required to clean up the epoxy that flowed beyond the working surface,

hence, it was important to make sure that the excess epoxy would was absorbed. The double absorbent layer successfully averted further problems with the excess epoxy.

The final layer of the fiber impregnation layup was a thin sheet of Teflon® material. The Teflon® sheet offered a non-stick surface between the diaphragm and the epoxy-saturated absorbent layer after fiber bundle impregnation. Once the Teflon® layer was in place, the plate press was closed and the bolts were installed to hold it tightly together as shown in frame 10 of Figure 4.9. After the plate press was clamped together, vacuum was first applied to both sides of the diaphragm to allow as much air as possible to be removed before applying pressure on the fiber-epoxy layup with the diaphragm. After the vacuum was applied for about two minutes, air pressure was slowly applied to the upper side of the diaphragm until 689 kPa (100 psi) was attained. The vacuum, air pressure, and heat were maintained for about 30 minutes. Then, the heating element was unplugged and the vacuum pump was switched off. The ball valve that controls airflow to the diaphragm was closed with pressure still applied, and the air hose was disconnected. The vacuum would bleed down after the pump was switched off, with the rate being dependent on how well the perimeter sealed. Sometimes carbon fibers or fibers from the absorbent material inadvertently got on the sealing area, causing a slow leak. The diaphragm held air pressure for as long as desired, which allowed pressure to be maintained in the plate press until it was cool and the specimens were ready for removal.

The plate press required about three hours to cool to room temperature, once heated. The pressure was released and the plate press was opened as shown in frame 1 of Figure 4.10. In this particular case, the Teflon® sheet was stuck onto the diaphragm

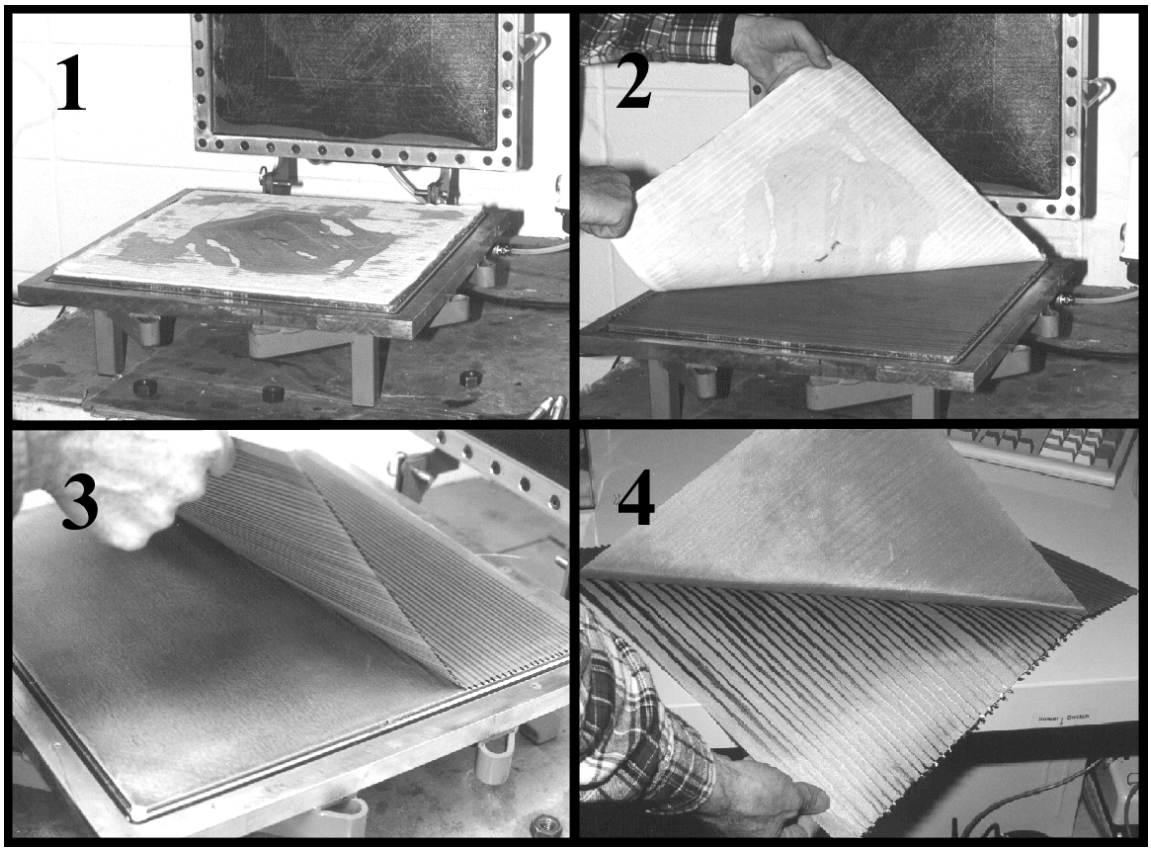

Figure 4.10. Sequence of steps after epoxy has been pressed into fiber bundles

when the plate press was opened. Sometimes it remained on the epoxy-soaked absorbent layer. The Teflon® sheet could be easily peeled from either surface. The absorbent layer, which has excess epoxy in it, as it was peeled away from the release sheet beneath it can be seen in Frame 2 of Figure 4.10. Both release sheets were removed simultaneously with the impregnated fiber bundles between them, as shown if frame 3 of Figure 4.10. The release sheets were separated from the base plate so that the bend of the release sheets was in the same direction as the fibers were laid. This was to reduce possible damage that could be caused by excessive longitudinal bending of the impregnated fiber bundles. The upper release sheet was peeled away, leaving the

impregnated bundles stuck to the bottom release sheet as shown in Frame 4 of Figure 4.10. The individual fiber bundles could then be removed and hung in the enclosure for curing, as previously described. Caution was required while pulling the impregnated fiber bundle from the release sheet. Some longitudinal bending was unavoidable, but bending could be reduced by avoiding a steep angle between the bundle and the release sheet as the fiber bundle was pulled away. Occasionally, even with delicate handling, an edge in the middle of an impregnated fiber bundle would separate away and remain stuck to the release sheet. In these cases, the damaged specimens were discarded. Extra specimens were always made in case specimens were damaged during preparation procedures.

Synopsis of the Impregnated-Bundle Test Specimen Preparation Procedure

The following synopsis is to provide a brief overview of the steps required to prepare impregnated-fiber bundle test specimens prior to testing. This is only a brief overview and does not address many details that are included in the preceding narrative. This procedure requires a workbench area about 2m (6.5') long to accommodate the plate press and provide general working area. Access to a compressed air supply and a vacuum pump are also necessities.

1.) Precut the necessary pieces of release material, absorbent, and Teflon® sheets. It worked best to allow about 6mm (1/4") of space around the perimeter of the working area of the base plate of the plate press.

2.) Plug in the plate press heating element and set the temperature to about 82°C (180°F).

3.) Start with a clean base plate surface and place the first layer of release sheet material on the base plate. It was found to be beneficial if several small chips of epoxy were allowed to melt between the base plate and the first release sheet. This keeps the release sheet from sliding around as the epoxy was spread out.

4.) Place the frozen chunks of epoxy on the release sheet. It works best to place the epoxy chunks in a spread out manner because it requires less work with a spatula later to spread the melted epoxy around. Allow the epoxy to melt.

5.) Spread the epoxy into an even layer with a laboratory spatula. Remove excess epoxy at this point if it appears that too much has been placed on the release sheet. Excess epoxy can be scraped from the release sheet with the laboratory spatula. It is best to scrape in a criss-cross grid and respread the epoxy to evenly remove heavy excess from the epoxy film layer.

6.) Use gloved hands to unroll lengths of carbon-fiber bundles from the roll. These lengths should exceed the width of the base plate by at least 50.8mm (2”). It is better to have more. Make sure the length of bundle is not twisted and lay it into the epoxy film. Repeat step 6 for the desired number of specimens. It is best to start at the center and work outwards.

7.) Place the second release sheet over the specimens that have been laid into the epoxy film. Make sure alignment is correct before allowing the release sheet to contact the epoxy film. It works best to start at a corner, align the edge, and gently lay the release sheet into place.

8.) Use scissors to trim the excess length of fiber bundles along the edges of the base plate. Make sure to clean fiber remnants from the O-ring seal.

9.) Lay the necessary absorbent layers into place followed by the Teflon® layer.

10.) Close the plate press, install the perimeter bolts, and tighten them evenly in a criss-cross manner.

11.) Increase the temperature setting of the heater control to about 93°C (200°F).

12.) Close the appropriate valves, start the vacuum pump, and evacuate the working area within the plate press.

13.) Connect the compressed air hose to the plate press and slowly apply air pressure up to 689kPa (100psi).

14.) Allow the temperature, vacuum, and pressure to be applied for 30 minutes minimum. This seems to be sufficient. Periods of time up to 75 minutes were tried and yielded no benefits or detriments.

15.) Unplug the heating element, switch off the vacuum pump, close the air valve, and disconnect the air hose. Leave the air pressure in the plate press. Allow the plate press to cool.

16.) Release the air pressure from the plate press. Loosen and remove the perimeter bolts. Open the plate press. On occasion, the halves of the press are stuck together by epoxy. In these cases, air pressure can be carefully applied to the diaphragm of the plate press and used to force it open. Only low air pressures were ever required to aid the opening of the plate press.

17.) Remove the Teflon® layer. If this is done carefully, it can be reused. Remove the absorbent layers and discard. Carefully remove both release sheet layers together.

18.) Carefully separate the release sheets. The specimens had a tendency to stay on the bottom release sheet.

19.) Remove the individual specimens and hang them in the curing enclosure. Attach a small binder clamp to the bottom of each specimen to keep it straight.

20.) Place curing enclosure in the oven. Care must be taken when moving the enclosure with the uncured specimens. Rapid movements can cause the specimens to sway into each other, causing them to stick together. They could usually be separated without damage.

21.) Cure specimens at 177°C (350°F) for 2 hours.

22.) Remove enclosure from the oven and remove the specimens from the enclosure.

23.) Place specimens in assembled test fixtures.

24.) Pour Macromelt® 6300 hot melt glue into each tab well, but fill each tab well to only 1~2mm (0.080~0.160”) from the surface of the test fixture. Allow the Macromelt® 6300 hot melt glue to cool.

25.) The specimens are now ready for the test procedure.

As discussed throughout this chapter, extensive development was required for this procedure. Although these procedures appear complex, they can be efficiently used in a production environment. It was found that by coordinating specimen curing and specimen impregnation times, two batches of impregnated specimens could be produced daily. More practice and refined techniques could increase production of the impregnated specimens. Testing and data analysis can be done during curing times and plate press cooling periods. This procedure could easily be implemented by existing industry test facilities.

CHAPTER 5

DATA COLLECTION

This chapter entails discussion of the equipment used for testing and the test setup for the tensile tests of both dry and impregnated bundles. Test procedures were first developed for the dry-bundle specimens and then were extended for use with the impregnated-bundle specimens. Modifications were implemented where necessary to test the higher strength impregnated bundles. Finally, test data collection methods are discussed at the end of this chapter.

Equipment

All of the tensile tests for this research were conducted using an Instron® universal screw drive servo-electric test machine. This Instron® machine is located in Montana State University's composite materials test laboratory. The Instron® machine was fitted with an Eaton-Lebow® 2.22 kN (500 lbf) load cell and was interfaced with a computer that used Instron® digital control software. The specific equipment information is as follows:

Instron® Corporation universal screw drive servo-electric test machine
Model: 8562 A1477-1004 Serial number: H0706

Eaton-Lebow® 2.22 kN (500 lbf) load cell

Model: 3132 Serial number: 8786

Instron® Corporation digital control software

Series 9
Series IV Automated Materials Testing System – Version 5.25
Copyright 1985-92

The standard hydraulically operated grip was used to clamp onto the lower end of the test fixtures. The upper part of the test fixtures was gripped with a manually operated screw

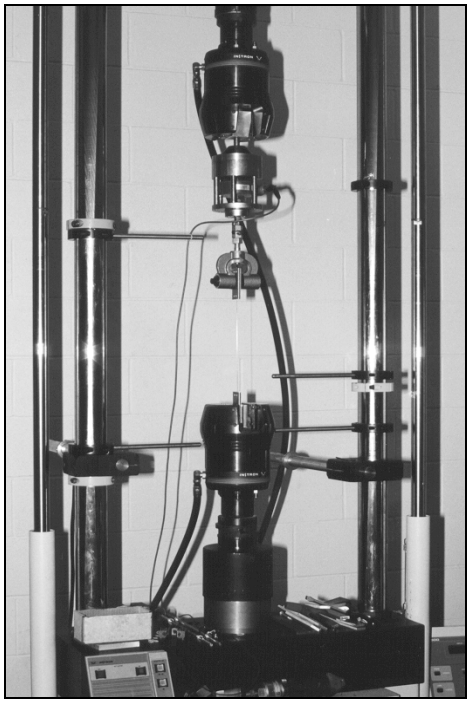

Figure 5.1. Eaton-Lebow 2.22 kN load cell clamped into upper Instron® grip

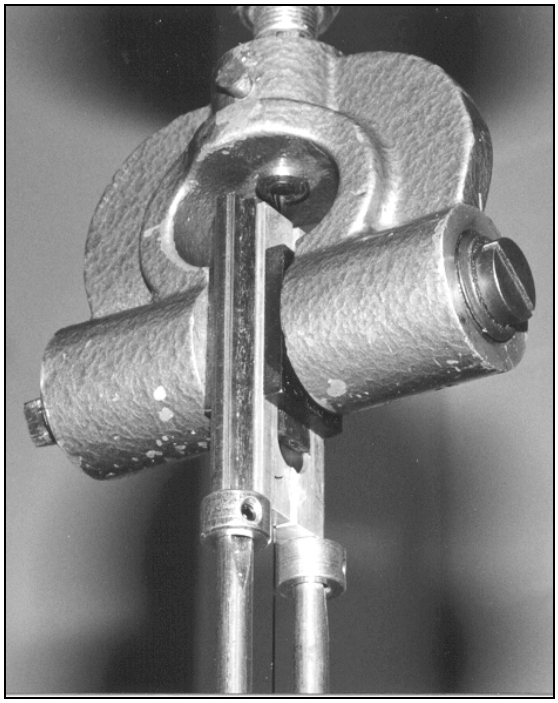

Figure 5.2. Upper clamp with test fixture in place

clamp, which was connected to the load cell above. In Figure 5.1 the Eaton-Lebow 2.22 kN (500 lbf) load cell is shown clamped into the Instron® test machine's upper grip with

the manual screw clamp mounted to the bottom of the load cell. A close view of the upper end of a test fixture clamped into the manually operated upper grip is shown in Figure 5.2.

Test Setup

The tensile tests were basic in principle. The specimens were subjected to increasing tensile loads while the corresponding loads and displacements were recorded until the specimen failed. The parameters for the tensile tests were entered into the Instron® Series 9 digital control program. Displacement control was used to provide a constant extension rate of the specimens during the tests. A test rate of 0.254 mm (0.010 in.) per second was used for preliminary dry-bundle tests. This rate proved to be too fast, requiring less than 20 seconds per test. Since the test extension rate can affect test results, this rate was slowed to 0.127 mm (0.005 in.) per second, half of the original. This rate generally required less than a minute for the dry-bundle tests and less than 1.5 minutes for the impregnated-bundle tests. The data-sampling rate was set to four samples per second. This sampling rate generally produced from 90 data points for some brief dry-bundle tests to 360 data points for some of the longer impregnated-bundle tests.

Development of Dry-Bundle Test Procedure

The dry-bundle test procedure evolved some over the course of this research. As previously stated, the tensile tests were reasonably basic, however an anomaly that presented its self during preliminary tests was a small zigzag in the lower linear portion of some of the data. The zigzag was caused by a small movement of the polyester tabs

on the ends of the specimens. Polyester resin exhibits shrinkage of about seven percent as it cures, according to *Handbook of Composites* [15]. Due to this shrinkage, the tabs would shrink away from the tab well sides around the perimeter of the tabs, but remain bonded to the aluminum test fixture on the backside of the tab. This bond would initially hold during a test, but would release when its strength was exceeded during the tests. When the bond released, the tab was allowed to move the distance that the polyester had shrunk away from the test fixture inside the tab well. The distance that the tabs moved was small, only about 0.029mm (0.0011") per tab, but it momentarily reduced the load, causing a small zigzag or offset in the data before the test continued. The actual tab shrinkage experienced was calculated from the offsets in several data sets and was found to actually be on the order of 0.1 percent. The desired information could be obtained from the test, but the data required repair to align the points above and below the zigzag. In Figure 5.3 the distinct zigzag, which was caused by a sudden release of the tab-fixture bond, is shown in the linear portion of the graphed data. An audible click or

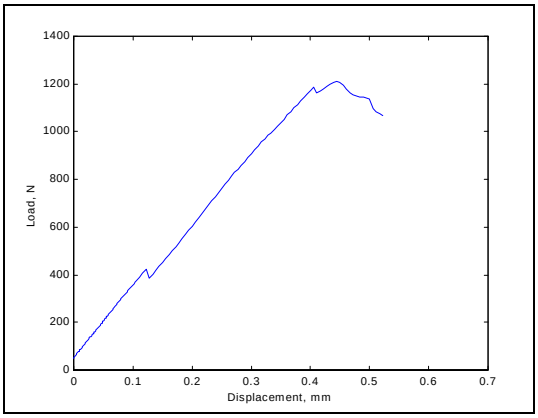

Figure 5.3. Raw data with prominent zigzag caused by tab release in test fixture

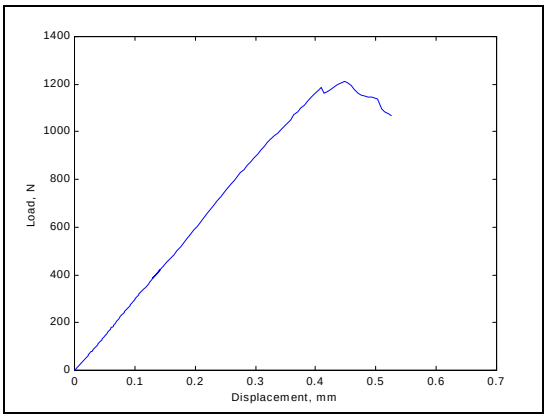

Figure 5.4. Repaired data with upper and lower data aligned and beginning at the origin

snap emanated from the tab area each time that a coinciding sharp zigzag could be seen on the data graph screen. In Figure 5.4 the same data is shown after it was repaired to lineup the respective upper and lower portions of the data with respect to the zigzag. The data was also shifted so that the linear portion of the data aligned with the origin.

The possibility was considered that if the tab could be held in place with additional force, the zigzags in the data could be eliminated. To accomplish this, pieces of rubber were inserted between the tabs and the test machine grips before they were clamped tight. The rubber pieces were thicker than the depth of the void between the top of the tab and the surface of the test fixture. The compression of the rubber applied force against the tab and increased the tab-fixture bond's ability to hold throughout the test. The rubber inserts greatly reduced the occurrence of the zigzags in the data, but did not

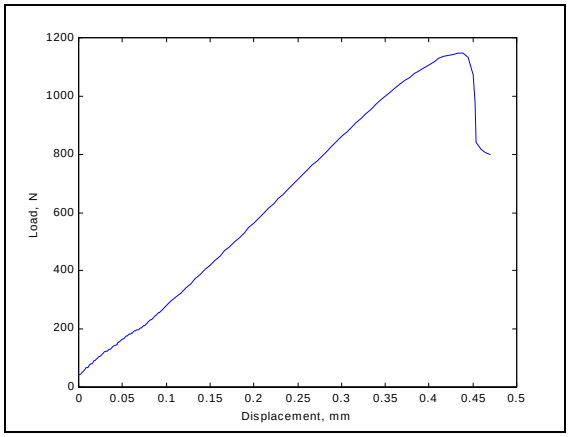

Figure 5.5. Raw data with less prominent zigzag caused by gradual tab release in test fixture

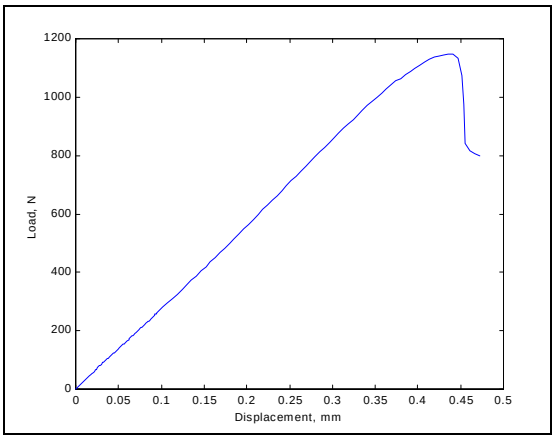

Figure 5.6. Repaired data with upper and lower data aligned and beginning at the origin

entirely eliminate them. The rubber inserts caused another type of zigzag to emerge in the linear portion of the data when the tab-fixture bond released. As shown in Figure 5.5,

this less conspicuous misalignment was more gradual than the zigzags that occurred without the rubber inserts. The more gradual nature of the zigzag was caused by the tab's movement being inhibited by the compressed rubber insert. The tabs still moved the same distance as without the insert, but over a longer period of time. Therefore, the offset in the linear portion of the data was the same in either case if the tab-fixture bond released. Again, the desired information could be obtained from the data, but only after repair to align the data above and below the zigzag in the data. Figure 5.6 shows the data from Figure 5.5 after it was repaired to correct the zigzag as before. Not all of the zigzags that occurred while using the rubber inserts were the gradual type. If the rubber was not compressed much, it would allow the tab-fixture bond to hold up to a higher load and then release quickly, causing the misalignment to be the more distinct type shown in Figure 5.3. The rubber inserts contributed to a significant reduction of misalignments in the data and the tests proceeded to completion.

Development of Impregnated-Bundle Test Procedure

The polyester tabs were only used for the tests of the dry bundles of carbon fibers. The impregnated bundle tests were conducted using Macromelt® 6300 as the tab material as discussed in chapter 4. The Macromelt® 6300 also exhibited shrinkage as it cooled, but to a slightly greater extent than the polyester. The knowledge acquired during the dry-bundle tests was useful for the impregnated bundle tests also. The Macromelt® 6300 tabs did not bond to the aluminum test fixtures, so the tabs could move about 0.5 mm (0.020") longitudinally with the specimens. The rubber inserts were also used for the impregnated bundle tests to hold the tabs tightly into the test fixtures. It was discovered

early in the impregnated-bundle tests that the upper end of the test fixtures required less care when they were clamped into the upper grip. This was because gravity kept the upper tabs of the specimens against the center-facing end of the tab well in the test fixtures. As the specimens were tested, the tabs on each end of the specimens moved toward the center-facing ends of the tab wells if there was space between the tab and the end of the tab well. Essentially, any slack between the Instron® machine's grips was taken up as the tests proceeded, similar to a loose chain being pulled from its ends. Again, gravity ensured that the slack was taken up in the upper end of the test fixtures. The lower end, however, required that the specimen end with its tab be lifted slightly so that it was tight against the center-facing upper end of the lower test fixture end. Since the impregnated fiber bundles were not as fragile as the dry bundles, the specimens could simply be gripped by one's fingers and pulled upward until the tab contacted the end of the tab well. The lower grip could then be clamped with a rubber insert in place, to hold the tab in place. Occasionally, a slight amount of slack would inadvertently remain after a specimen was clamped into the grips. Again, the data indicated the slack by the telltale zigzag in the data, which was otherwise almost perfectly linear until specimen failure. Due to the slack being taken up prior to testing, a slight bow in the specimens caused an offset in the raw data. The load remained at zero even though the extension increased until the slack was taken up in the specimens. This created an offset beginning at the bottom of the data that required that the data be shifted so that it aligned linearly with the origin.

Test Data Collection

The test data were collected on a computer, which used the Instron® digital control software. The test program interfaced with the Instron® test machine to control the test parameters. The program monitored each test and recorded corresponding load and displacement data. The data groups were converted to ASCII files to enable them to be evaluated by other computer programs and were stored on 3.5 inch floppy disks with backups.

CHAPTER 6

STATISTICAL ANALYSIS OF THE COLLECTED DATA

The statistical methods had to be determined for these types of tests once all of the data were collected from testing the specimens. The test data were examined and the relevant information that could be derived from them was determined. The term "Normalized Bundle Stiffness," or NBS, must be introduced at this point. The NBS is analogous to modulus, but is used on a load-strain basis rather than a stress-strain basis. NBS, therefore, has the units of load, N, and represents the slope of the linear portion of test results on a load-strain diagram. For the dry-bundle tests, the normalized bundle stiffness, NBS, of the linear portions of the data and the maximum loads with corresponding displacements were determined. In addition, the secant NBS slope was used for the calculation of the theoretical number of individual fibers that broke at the first major failure. The theoretical number of broken individual fibers was only calculated for each unsized fiber-bundle test. The NBS and maximum load values were obtained for the impregnated-bundle tests. The mean values and standard deviations were calculated for each result from each production lot. Then, the mean values and standard deviations were calculated combining the data from all three production lots for each type of fiber.

Reasoning of the Statistical Analysis

Before any statistical analysis could transpire, it was necessary to examine the results that had been obtained from the ongoing tests to determine what information was relevant. Dr. Doug Cairns and Dr. E. M. Wu were consulted during several meetings to examine graphed data from dry-bundle tests and consider the parameters for statistical analysis. After examining graphed test data from both sized and unsized fibers and observing some unexpected trends in the data, it was thought that entanglement of the individual fibers after breakage could be the reason for the peculiar trends. It was observed in many cases that after the first major failure occurred, the load would drop, but then the load on the fiber bundle would begin to increase again and in some cases exceed the load before the major failure occurred. There were also differences between the sized and unsized fiber bundles that indicated that the sizing was also influencing the behavior of the fiber bundles during tests.

The possibility was considered that frictional effects within the fiber bundles might cause the results to be rate dependent. Some sized and unsized dry bundles were tested to determine if the test rate was too fast. The test rate was changed from the original rate of 0.127mm (0.005") per second to 0.051mm (0.002") per minute, which required about 60 minutes to complete each test. The data from the slow tests were plotted on a graph with corresponding data from the fast tests for comparison. The slow tests exhibited behavior that, within the variability of specimens, was identical to the faster tests, proving that the faster rate was not so fast that it affected the test results. Another interesting finding resulted from the slow tests. During a slow test of a sized

fiber bundle, the load had already reached its maximum load of 184N (41.4 lbf) and the load was descending. A question occurred as to whether or not the sizing was creating a significant frictional drag between the fibers after the maximum load was achieved and fiber failure had occurred. The load had reduced to 91.2N (20.5 lbf) and the extension of the specimen was 3.884mm (0.1529") when the thought occurred to drip some acetone onto the fiber bundle in its gage section to solvate the sizing. Frictional effects caused by sizing would be reduced once the sizing was solvated. When acetone was dripped onto the fiber bundle, the load immediately dropped to zero, indicating that all of the fibers were already broken and the entire remaining load was due to frictional effects caused by the sizing on the individual fibers. One last type of slow test was performed to determine if frictional effects between fibers in a bundle were an issue. A dry unsized fiber bundle was tested with Kelmar SWS 101-20 polydimethyl siloxane, an oily compound, applied to the fiber bundle along its gage section. The intention was to lubricate the areas within the bundle where individual fibers contacted each other. These contact areas were possibly causing frictional drag. The result was that the lubricated bundle performed virtually identically to the rest up to the first major failure. Beyond that area, the lubricated-bundle test indicated that friction, probably due to fiber entanglements, was an issue. The results from the lubricated-bundle test make sense. The only frictional drag that can occur between fibers is caused by the fibers moving at different rates or in opposite directions. There should be no frictional effects within a bundle of fibers up to the first major failure. This is because all of the fibers are stretching or extending at rates that have negligible differences. This is analogous to stretching two identical rulers side-by-side. As the rulers extend, all of the marks on the rulers still line up. Frictional

effects are only an issue if the marks do not line up, indicating a difference in extension rates. The marks of the rulers are equivalent to neighboring areas on the fibers within a bundle. The lubed-bundle test did indicate lower frictional effects past the first major failure, but the overall behavior was similar to the dry test. Also, fiber entanglement after the first major failure causes subsequent data to be of little use, so reduced friction in that portion of the data is not beneficial. Plotted data are shown in Figure 6.1 from the slow tests along with representative data from fast tests, which were all performed on the same production lot of unsized fibers.

The test rate became an issue of further controversy after over 600 dry-bundle tests and over 600 impregnated-bundle tests were completed. Dr. E. M. Wu was

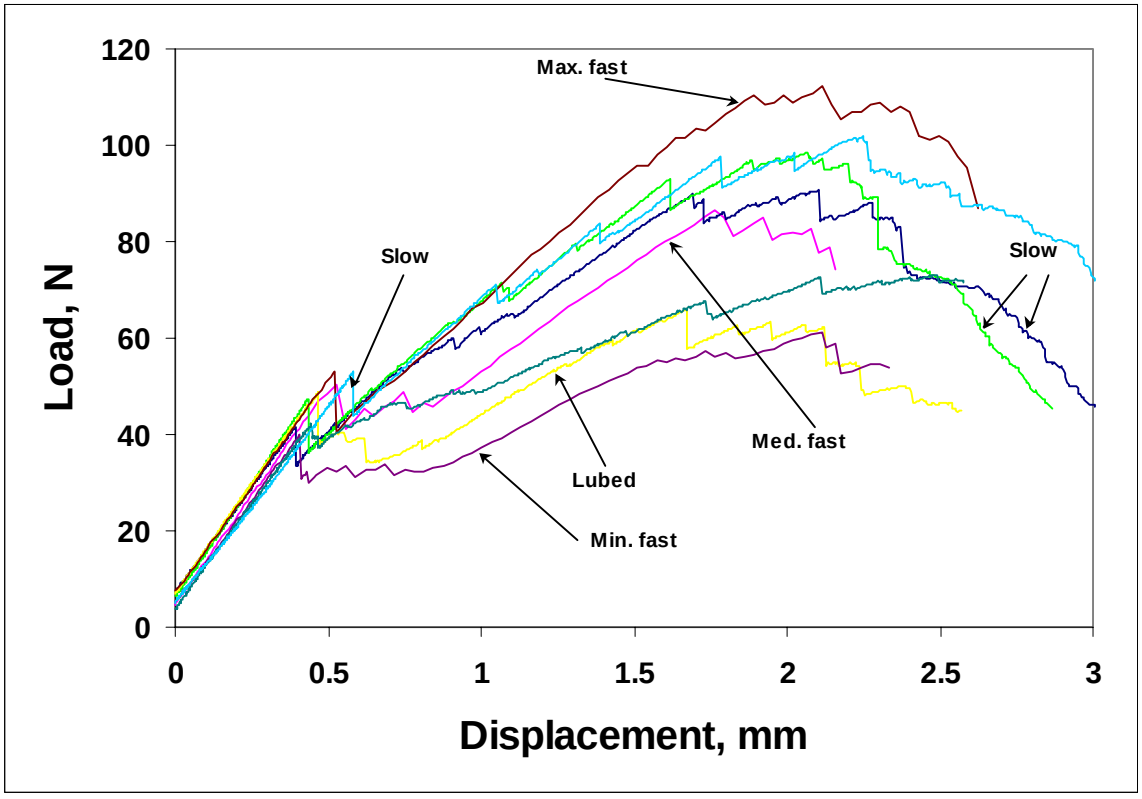

Figure 6.1. Graphed results from fast and slow dry-unsized fiber tensile tests

skeptical that the test rate of 0.127 mm (0.005 in.) per second was too fast. This test rate was used for all of these tests. Dr. Wu was concerned about rate dependent frictional effects within the fiber bundles. Frictional drag would cause the maximum load values to be erroneously high if the test rate was too fast and if frictional drag was, in fact, an issue. This concern was addressed by conducting more slow tests at the rate of 0.051mm (0.002") per minute. Results were combined with the previous slow test results for a total of 14 specimens tested at the slow rate. The maximum loads, corresponding extensions, and secant NBS slope values were entered into a statistical calculation program, SigmaStat®. The program performed a Student t-test to statistically compare the groups of fast and slow results. The t-test concluded that there was no statistically significant

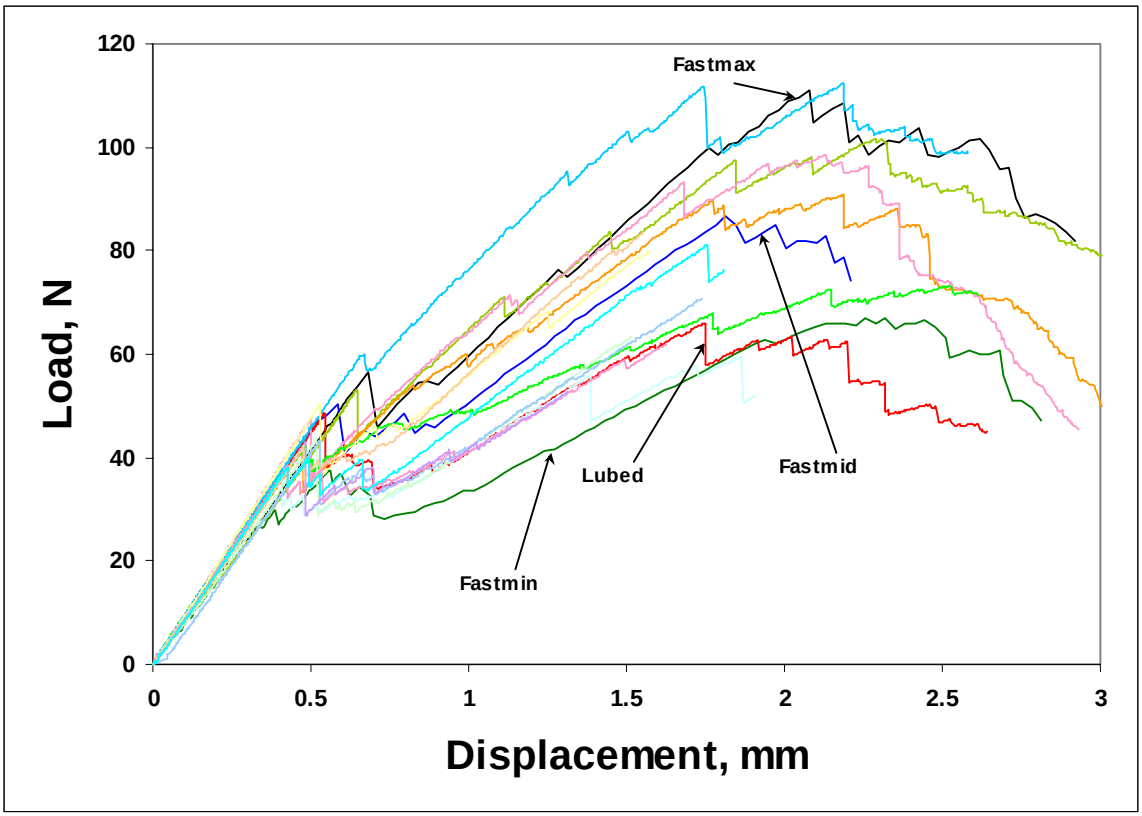

Figure 6.2. Graphed results from fast and slow dry-unsized fiber tensile tests

difference between the groups of results from the slow and fast tests. This conclusively proved that the test rate used for all of the 1200 tests was not too fast and that there was not rate dependency of the results between the fast rate and slow rate. All of the slow test data are shown in Figure 6.2 graphed along with test data from fast tests of the same production lot of fibers. The fast test data represented is for the specimens that had the maximum, minimum, and median values of the maximum loads within the group of results for the same production lot. The maximum fast, minimum fast, median fast, and lubed specimens are labeled; the remainder are all slow test results. It is clear from Figure 6.2 that all but one of the slow specimens fall within the bounds of the maximum and minimum fast test results. This reinforces the lack of rate dependence while testing these specimens.

It was determined that only the beginning and some of the middle of the data from the dry-bundle tests was useful. This was due to apparent fiber entanglement in both sized and unsized specimens, and frictional effects of sizing in sized specimens. The NBS of the initial linear portions of the data were important and could be determined. The maximum loads before the first major failure occurred could also be determined from the data just beyond the linear portion of each data set.

For the unsized fiber-bundle tests, the secant NBS slope could also be calculated from a local minimum data point just beyond the maximum load before the first major failure on each graph. A secant NBS slope is the slope between the origin and any point on a stress-strain diagram, or in this case, a load-displacement diagram or load-strain diagram. The secant NBS slope was used in the calculation of the theoretical number of individual fibers that broke at the first major failure. In this calculation, it is assumed that

all of the individual fibers within the fiber bundle are loaded equally and the combined load carrying capability yields a given overall NBS for the fiber bundle. Since the bundles contain 3000 individual fibers, each individual fiber contributes 1/3000th of the slope of the overall NBS. Therefore, when a number of fibers break, the slope of the NBS is reduced by the same relative amount. That is, if 25 percent of the fibers broke, the load should be reduced by a corresponding amount and the new slope of the NBS would be reduced by 25 percent of the original NBS. This new NBS value is the secant NBS slope of interest. The equation used for the calculation of the number of broken fibers is

$$\text{Fibers broke} = 3000\left(1 - \frac{y}{xE}\right) \tag{24}$$

where y is the load, x is the corresponding displacement, and E is the overall NBS for all 3000 fibers.

It was decided that the data contained no meaningful information from shortly after the first major failure to the end of the test. Again, this was apparently due to entanglements of the broken fibers in both the sized and unsized fiber bundles and due partially to the effects of sizing causing frictional drag in the sized fiber bundles.

The results from the impregnated-bundle tests were basic. Each test yielded a linear load versus displacement plot up to failure of the specimen. Only a limited amount of information could be obtained from such simplistic plots. The NBS, maximum load values, and dissipated strain energy for each test were the only immediately useful information that could be determined. These values were further examined as a group for the specimens from each production lot.

It was determined that the results from the tests would be in three categories, unsized fiber results, sized fiber results, and impregnated fiber results. The information to be determined from each category is as follows:

Dry-unsized fibers

1.) Overall NBS
2.) Strain at maximum load
3.) Maximum load
4.) Dissipated strain energy density
5.) Secant NBS slope after first failure
6.) Theoretical number of fibers broken at first failure
7.) Load drop at first failure
8.) Slope of the drop at first failure
9.) Theoretical number of fibers broken at 0.81% strain

Dry-sized fibers

1.) Overall NBS
2.) Strain at maximum load
3.) Maximum load
4.) Dissipated strain energy density
5.) Theoretical number of fibers broken at 0.81% strain

Impregnated fibers

1.) Overall NBS
2.) Strain at maximum load
3.) Maximum load
4.) Dissipated strain energy

Methods of Statistical Analysis

The best methods for extracting the relevant information from the data were considered after the specific needs were ascertained for each type of test group. Matlab® was chosen as the computing environment because of its versatility and because of the researcher's familiarity with Matlab®. Matlab® codes were written for each type of test data to obtain the specific information desired from each individual data set. The test results for each type of test and production lot were grouped together and saved as separate files. The results were analyzed, first as groups from specific production lots of carbon fibers, then as complete groups containing all three production lots of the specific types of carbon fibers, i.e., dry sized AS-4, dry sized T-300, and on.

It was first determined that the dry-sized fiber data, the dry-unsized fiber data, and the impregnated fiber data needed to be analyzed separately by using individualized codes. The dry-sized fiber data gave the overall NBS for the linear portion of the data and a maximum load value. Consideration had to be given to the occasional occurrence of a load value that was higher than the one that occurred at the first major failure. The higher load values occurred after the first failure and were considered to be due to broken fiber entanglement and frictional drag. The dry-unsized fiber data yielded the same information as the dry-sized fiber data with the same considerations, along with the additional information shown in the list on the previous page. The impregnated fiber data gave the listed information, however, here the highest recorded load value was always at the failure so no special considerations were necessary with respect to the maximum load.

Construction of the Matlab® Codes for Data Repair and Analysis

The first task necessary for each type of data was to determine the presence of any misalignments or zigzags that were discussed in the data collection section. If a misalignment was present in a data set, it had to be corrected by shifting the lower portion of the data to align with the upper data. Then, the entire data set had to be shifted so that the linear section of the data aligned with the origin. At this point, the corresponding maximum load and extension or strain values could be obtained and the respective information for each type of test group could be derived from the data.

Each data set was loaded into Matlab® and plotted to determine the corrections needed. Initially, it appeared that the upper and lower values of the zigzags would have to be read from the plots and entered into the program at prompts for the values. Fortunately, Matlab® offers a feature called "ginput," which stands for "graphical input." This feature enables one to simply place the cursor at a point on a graph and click the mouse button to enter the needed values into the program. This was a convenient way to visually tell where corrections were necessary and quickly enter the values. To align the data, the upper and lower values of the zigzag were entered first. The code first did a first-order polynomial fit starting at the upper point entered for the zigzag. The linear fit progressively added data points until the R^2 value fell below 0.99. Code was written to calculate R^2 values, since Matlab® had no function for this calculation. The offset of the data was calculated using the top point of the lower data, the bottom point of the upper data, and the slope of the linear fit to the upper data points. The lower data points were shifted by the amount determined to be the offset and the middle points were shifted to fit

on a line between the upper and lower sections of data. Once the data was aligned, a first order polynomial fit was again performed progressively on the combined data until the R^2 value fell outside of the specified range. This linear fit did not include all of the first data points for the set, since the initial data points were usually quite nonlinear in nature due to initial slack in the test equipment. The nonlinearity of the initial portions of the data is illustrated in Figure 6.3. Sharp rises followed by plateaus at about 2 N load can be seen in several of the graphed data sets. The identical behavior shown during each test at the same load and for the same duration indicates that the sharp rises and plateaus were due to initial slack in the test equipment or an anomaly caused by the data acquisition

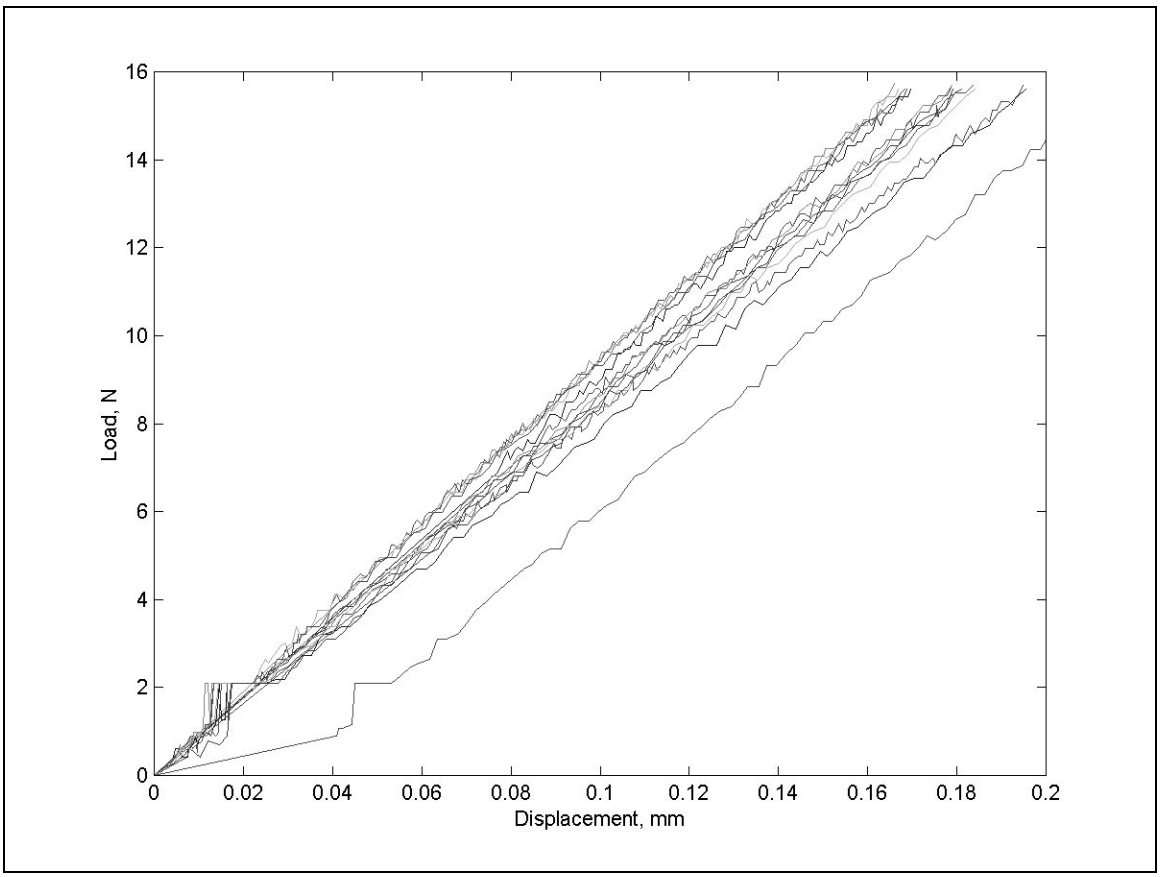

Figure 6.3. Lower portions of graphed results from slow dry-unsized fiber tensile tests

equipment. Initial slack in the equipment seems the most reasonable cause. The possibility that the sharp rises and plateaus represent actual fiber behavior must be discarded because the behavior is identical in each of the tests with a plateau. Fiber bundles always exhibit at least slight differences in behavior. The linear behavior after the plateaus is a good indication that the fibers in the bundles were collimated well. If not, the graphs would be nonlinear until all of the fibers carried their share of the load. It was important to exclude the nonlinear initial portion of the data to obtain good linear fits to the linear portion of the data. The data offset was determined from the y-axis intercept given from the linear fit and the whole data set was shifted. The points not included in the linear fit were then shifted to align with the rest of the linear portion of the data. The slope from the last linear fit was the overall NBS. This basic algorithm was used for all of the data sets before further analysis proceeded.

Both the dry-sized and dry-unsized data required consideration of the possibility of values higher than actual load as previously discussed. The only way to determine if this was the case was to plot the data and visually check the plot for the possibility. Again, the “ginput” function was used to enter into the program a point beyond which the data would not be considered for a maximum load value. Matlab® has a function, “max,” that was used to determine the maximum value in a given data set. This yielded the maximum load, which was also matched with the corresponding extension for each data set. For the dry-unsized data, the point that was entered using “ginput” was used to calculate the theoretical number of broken fibers before finding the maximum load, so it was important to locate the crosshairs precisely for the calculations. This was achieved by writing a zoom feature into the code that allowed the operator to click on the corners

of a zoom window to get a close-up view of the specific area where the first failure occurred. This allowed specific points to be chosen for the calculation of the secant NBS slope and the associated calculations.

The maximum loads for the impregnated fiber data were simply obtained using the Matlab® "max" function on each data set. The corresponding extensions were also determined for each of the maximum loads.

The results that were obtained for each group of data were saved to separate files for further analysis. A Matlab® code was written to obtain the minimum values, maximum values, mean values, and standard deviations for the results that were obtained for the respective tests. Matlab® had functions that easily gave these desired results. The coefficient of variation was also calculated for each result from the respective groups of results. These results were saved to other files for each group of data. The data from each of the first analyses were grouped into the three production lots for each type of fibers in each test and were then combined. Again, a Matlab® code was used to obtain the minimum values, maximum values, mean values, standard deviations and coefficients of variation for the overall NBS, maximum loads, and other information obtained for the respective groups of tests. These results were saved in files for each group.

Statistical Comparison of Dry and Impregnated Results

The final statistical information that needed to be obtained was a comparison between the dry-bundle results and the impregnated-bundle results. The comparison was necessary to establish whether trends could be recognized between the dry-bundle results and impregnated-bundle results from the same fiber lot numbers. It was of interest to

examine the changes in the NBS, maximum loads, and strains at the maximum loads. The increases for load and strain are self evident, based on our understanding of composite behavior as described by Rosen [2], Beyerlien and Phoenix [8], Wu and Robinson [12], and others. It was speculated that these changes would be reflected in either somewhat fixed respective constitutive property values or in values that could be recognized as percentages that were relative to the respective constitutive property values of the dry-fiber bundles. An example of the first case would be a case in which increases in values after impregnation of fiber bundles with one of the epoxy matrix materials were about 11.5 N for the NBS, about 250 N for the maximum load, and about 1.3 percent for the strain at maximum load. In this case, the same nominal increases would appear, regardless of lot numbers of the fibers. The indication would be that the matrix dominated the impregnated-fiber bundle properties. This behavior was unexpected, but the remote possibility was recognized. An example of the second case would be a case in which impregnation of the fiber bundles caused increases of about seven percent in NBS, about 143 percent in strain at maximum load, and 162 percent in maximum load. All of these would be relative to the values obtained for the dry-fiber bundles. These results would support the more likely case of the fibers dominating the characteristics of the impregnated bundles.

Examination of the results for these possibilities was accomplished by grouping the mean values of the NBS, strains at maximum load, and maximum loads for the four fiber groups. These fiber groups were sized AS-4, unsized AS-4, sized T300, and unsized T300. Within these four fiber groups, the dry-fiber results were compared to respective 3501-6 and 8552 impregnated-bundle results for the same lots of fibers. The

results were also compared for the combined results from the three lots in each fiber group.

CHAPTER 7

RESULTS AND DISCUSSION

Within this chapter, the test results that were obtained by the methods in Chapter 6 are presented and discussed. The dry-fiber bundle results are presented in two sections, one addressing the dry-sized bundle results and the other addressing the dry-unsized bundle results. The impregnated-bundle results are also presented in two sections. The first addresses the 3501-6 epoxy impregnated-fiber bundle results. The second presents the 8552 epoxy impregnated-fiber bundle results. Finally, a comparison between the dry-bundle results and the impregnated-bundle results is presented.

Fiber and Matrix Designation Nomenclature

It was necessary to develop a systematic method to name files and fiber groups during this research. The naming method allowed the relevant information about specimen groups to be identified by the name of the file. This method is used in the tables and the text of the remainder of this document. Thus, a synopsis of the nomenclature method is given at this point to aid the reader when these designations are encountered.

The following method was used to simplify sample and file names involved with this research. Dry fiber test groups used the first three characters of the sample group

name to designate pertinent information. The first four characters were used if impregnated specimens were tested. The following explanation demonstrates that the system is essentially a three-character system in both cases.

The general form of the sample names is $x_1x_2x_3$(lot number).

x_1 can be the following:

d = dry bundle
i3 = impregnated bundle using 3501-6 epoxy
i8 = impregnated bundle using 8552 epoxy

x_2 can be the following:

u = unsized
s = sized

x_3 can be the following:

a = AS-4 fiber
t = T300 fiber

The lot numbers used for this research are:

Sized Hexcel AS-4:	1788-4c, 1795-5c, 1806-5b
Unsized Hexcel AS-4:	d1439-5h, d1602-5b, 1730-5j
Sized Amoco T300:	3u0403, 3u0501, B3u0511
Unsized Amoco T300:	3u0403u, 3u0501u, B3u0511u

It should be noted that the sized and unsized Amoco fiber lot numbers differ only by the postscript “u” after the lot number of the unsized fibers. This is because the same lots of fibers were used for both groups of tests. The sizing was washed from the fibers used for the unsized tests. The postscript “u” is a precautionary redundancy when used in addition to the “u” as the x_2 character. For example, “dsa1788-4c” represents the group of dry, sized, AS-4 fiber bundles from lot number 1788-4c. Another example is, “i3ut3u0403u,” which represents the group of 3501-6 epoxy-impregnated, unsized, T300 fiber bundles from lot number 3u0403u. This simple code was used to identify all of the test groups.

Dry-Fiber Bundle Results

The dry-fiber bundle results are displayed in tables within this section and accompany additional discussion of the results where applicable. Typical graphs of test data from AS-4 and T300 dry-fiber bundle tests are shown in Figure 7.1 and Figure 7.2, respectively. Each of these data sets was chosen from within its group to exemplify the mean characteristics of the represented fiber group. The general behaviors of the fiber bundles can be seen in these two figures. It is interesting to note the differences in behaviors of the sized and unsized fiber bundles in both Figure 7.1 and Figure 7.2.

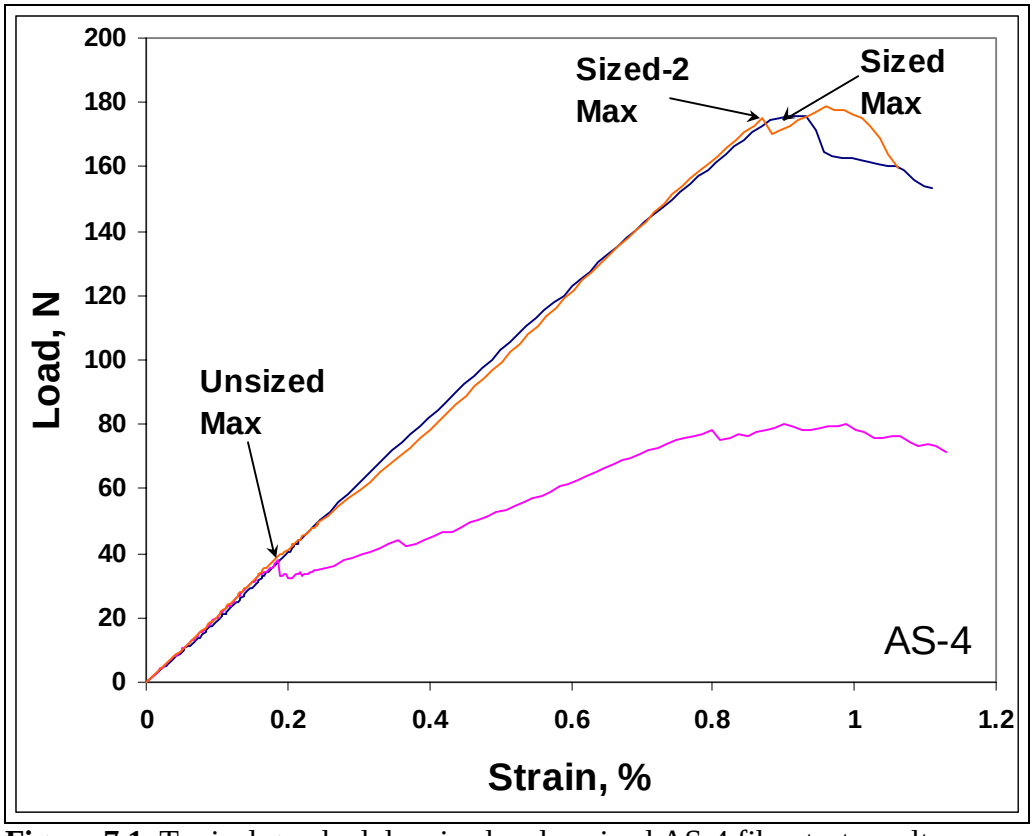

Figure 7.1. Typical graphed dry sized and unsized AS-4 fiber test results

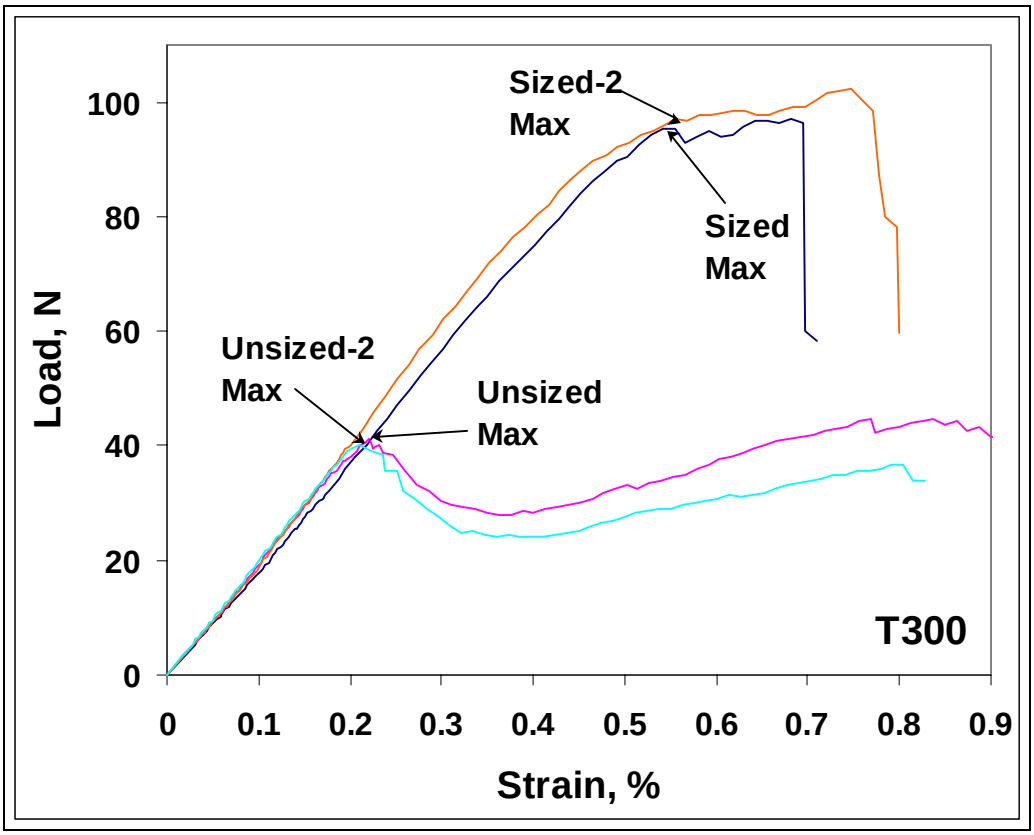

Figure 7.2. Typical graphed dry sized and unsized T300 fiber test results

Dry-Sized Fiber Bundle Test Results

The column headings for the result tables will be discussed briefly to clearly establish the meaning of the information in each column. Figure 7.3 and Figure 7.4 are provided, along with the following discussion of result table column headings, to graphically clarify the meanings of the presented results. The *NBS* refers to the normalized bundle stiffness, which is the slope of the line fit to the linear section of the graphed data on a load-strain diagram as shown in Figure 7.3. The *Strain* is the percent strain at the maximum load. *Max Load* is the maximum load achieved before the first major failure. The values in the *Strain* and *Max Load* columns may not correspond to the

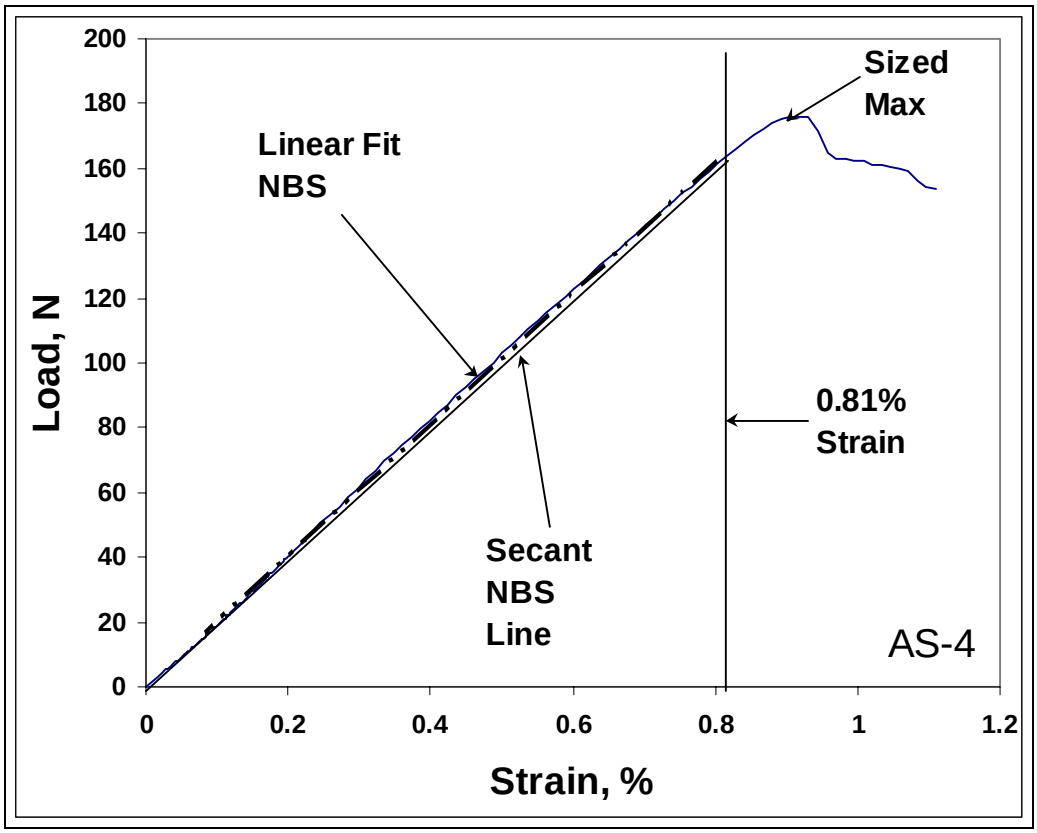

Figure 7.3. Dry-sized fiber bundle results example graph

same data sets for the *Max* and *Min* values shown. The *Energy Diff* refers to the difference in areas between the area under the graphed data up to *Max Load* and the area under a secant NBS line from the origin to the *Max Load* point on a load-displacement diagram. This area is shown in Figure 7.4. A large value for *Energy Diff* typically indicates that the graphed data exhibited substantial damage before the *Max Load* point. This behavior reduces the lower area and increases the difference in the areas. *Fibers Broke at 0.81%* is a calculation from the secant NBS value at 0.81 percent strain as shown in Figure 7.3. The tables shown in this result section do not show that some of the tests did not reach the 0.81 percent strain before the tests were stopped. In these cases, the *Fibers Broke at 0.81%* calculation used the highest strain value achieved during the

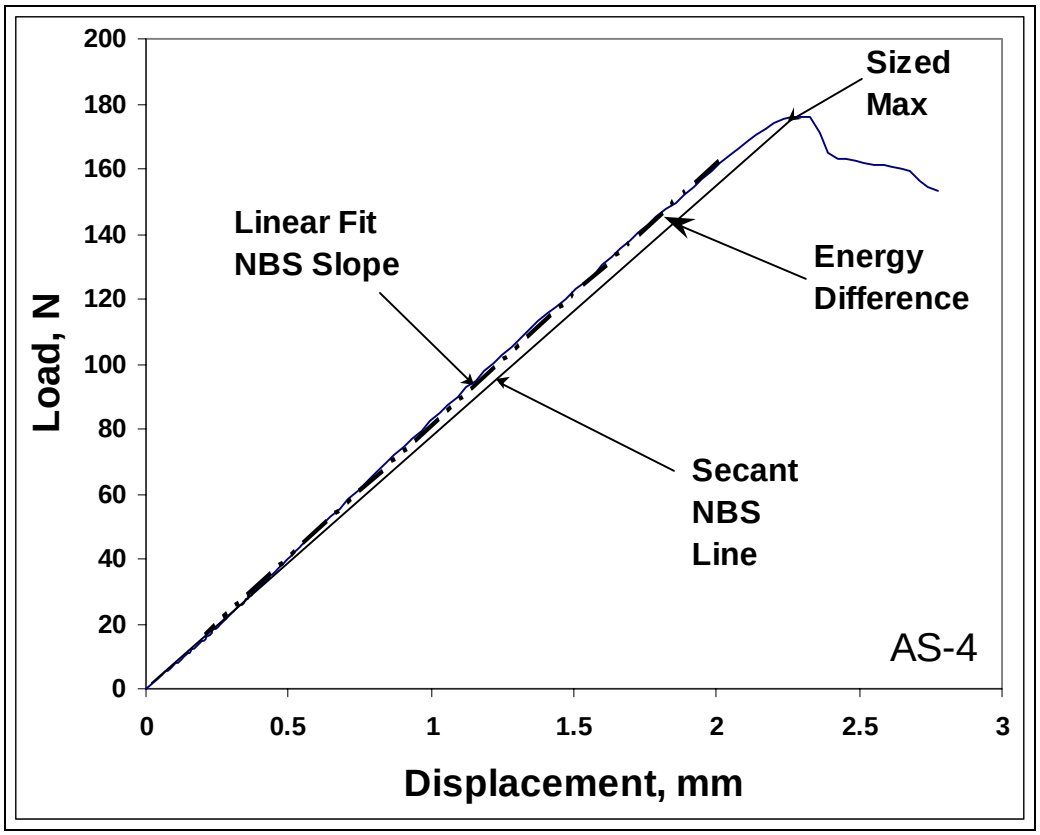

Figure 7.4. Energy difference and secant NBS example graph

test. This value was chosen as a reference point that could be used to compare fiber behaviors after the first major failures. The choice of this value was made after the testing was complete. A value was needed that was sufficiently high enough to be beyond the first major failure of even the fibers that achieved high maximum loads and strains. Unfortunately, many of the tests of lower strength fiber bundles were stopped before the strain reached 0.81 percent. Two results that were calculated for the unsized fiber results are not used for the sized fiber results. These are the *Load Drop* and *Drop Slope*. As discussed in Chapter 6, the behaviors of sized fibers are considerably different

from unsized fibers. The *Load Drop* and *Drop Slope* results for sized fibers are greatly influenced by the effects of the sizing and do not represent true fiber behavior trends.

Table 7.1. Dry-sized AS-4 statistical results

dsa1788-4c				34.0 **Specimens**	
	NBS_2 N	**Strain %**	**Max Load N**	**Energy Diff Nm**	**Fibers Broke at 0.81%**
Mean	212.6	0.99	199.5	0.01349	-17
Std. Dev.	11.7	0.07	16.5	0.00548	76
Max.	230.3	1.12	229.0	0.02656	348
Min.	191.6	0.89	171.8	0.00326	-106
COV_1, %	5.5	6.7	8.3	40.6	-434.8
dsa1795-5c				34.0 **Specimens**	
	NBS_2 N	**Strain %**	**Max Load N**	**Energy Diff Nm**	**Fibers Broke at 0.81%**
Mean	184.4	0.88	156.0	0.00825	74
Std. Dev.	10.8	0.07	16.7	0.00422	129
Max.	214.9	1.04	193.9	0.01665	504
Min.	165.2	0.71	121.2	0.00066	-49
COV_1, %	5.9	8.2	10.7	51.1	174.8
dsa1806-5b				34.0 **Specimens**	
	NBS_2 N	**Strain %**	**Max Load N**	**Energy Diff Nm**	**Fibers Broke at 0.81%**
Mean	199.8	0.85	164.1	0.00686	119
Std. Dev.	11.3	0.05	13.9	0.00511	181
Max.	225.5	0.93	193.1	0.01744	473
Min.	180.3	0.71	137.6	-0.00099	-119
COV_1, %	5.7	6.1	8.5	74.4	152.5
dsa Combined				102.0 **Specimens**	
	NBS_2 N	**Strain %**	**Max Load N**	**Energy Diff Nm**	**Fibers Broke at 0.81%**
Mean	199.0	0.91	173.0	0.00954	58
Std. Dev.	16.1	0.09	24.6	0.00569	146
Max.	230.0	1.12	229.0	0.02660	504
Min.	165.0	0.71	121.0	-0.00099	-119
COV_1, %	8.1	9.7	14.2	59.7	250.0

$_1$: COV = Coefficient Of Variation

$_2$: NBS = Normalized Bundle Stiffness

Therefore, these results were only presented for the dry-unsized fiber bundle results in the next section.

The statistical results from the dry-sized AS-4 tests are shown in Table 7.1. It can be seen that the coefficients of variation, COVs, for the NBS, strain, and maximum load were well within the 5~25 percent that Phoenix [9] stated was usually exhibited by brittle fibers. However, the *Energy Diff* and *Fibers Broke at 0.81%* COVs were considerably out of the range given by Phoenix. The high COVs associated with the *Energy Diff* values indicate that the method used to correlate the energies of the tests was not adequate. The negative mean for the *Fibers Broke at 0.81%* from the dsa1788-4c specimens indicates that there were many negative values calculated. Obviously, these results do not represent reality. The negative values indicate that the secant NBS values were greater than the respective NBS of the linear portions of the data. The other two lots of AS-4 fibers also gave some negative values as minimums for *Fibers Broke at 0.81%*. This indicates that all of these lots of sized fibers had some specimens that loaded up further after the first major failure. This enabled some of the secant NBS values to exceed the NBS of the respective linear sections. The large COVs for the *Fibers Broke at 0.81%* indicate that there is a large disparity in the behaviors of the fiber bundles after the first major failure. The negative values for the *Fibers Broke at 0.81%* indicate that using a greater strain value where loads are reduced more might be better.

The results for the dry-sized T300 tests are shown in Table 7.2. The COVs for *Strain* and *Max Load* were considerably larger than those for the AS-4 results shown in Table 7.1. The larger COV values here indicate more variability in the strength of the T300 samples than the AS-4 samples. The NBS, strains, maximum loads, and *Energy Diff* values for the T300 samples were all generally lower than those for the AS-4 samples. The strains and maximum loads for the T300 specimens were about 60 percent

of those for AS-4 specimens. The statistics for the *Fibers Broke at 0.81%* appear to be far more reasonable for the T300 fibers. It was not shown that the majority of these test

Table 7.2. **Dry-sized T300 statistical results**

dst3u0403				34.0	**Specimens**
	NBS_2 N	**Strain %**	**Max Load N**	**Energy Diff Nm**	**Fibers Broke at 0.81%**
Mean	189.1	0.63	113.0	0.00494	1063
Std. Dev.	7.7	0.10	19.4	0.00324	602
Max.	206.8	0.99	179.6	0.01777	2427
Min.	174.9	0.51	93.6	0.00097	-17
COV_1, %	4.1	16.6	17.2	65.6	56.7
dst3u0501				34.0	**Specimens**
	NBS_2 N	**Strain %**	**Max Load N**	**Energy Diff Nm**	**Fibers Broke at 0.81%**
Mean	174.8	0.49	77.2	0.00530	1516
Std. Dev.	9.6	0.08	12.2	0.00346	268
Max.	189.9	0.65	104.9	0.01614	2083
Min.	150.5	0.34	53.9	0.00042	981
COV_1, %	5.5	16.8	15.8	65.2	17.7
dstB3u0511				34.0	**Specimens**
	NBS_2 N	**Strain %**	**Max Load N**	**Energy Diff Nm**	**Fibers Broke at 0.81%**
Mean	191.6	0.59	101.4	0.00771	1345
Std. Dev.	9.6	0.10	20.3	0.00350	454
Max.	207.4	0.83	147.5	0.01999	1982
Min.	165.7	0.41	62.5	0.00310	192
COV_1, %	5.0	16.3	20.0	45.3	33.7
dst Combined				102.0	**Specimens**
	NBS_2 N	**Strain %**	**Max Load N**	**Energy Diff Nm**	**Fibers Broke at 0.81%**
Mean	185.0	0.57	97.2	0.00598	1310
Std. Dev.	11.6	0.11	23.0	0.00359	494
Max.	207.0	0.99	180.0	0.02000	2430
Min.	150.0	0.34	53.9	0.00042	-17
COV_1, %	6.3	19.2	23.7	59.9	37.8

$_1$: COV = Coefficient Of Variation

$_2$: NBS = Normalized Bundle Stiffness

were stopped before 0.81 percent strain was achieved. This means that the number of fibers broken would actually increase as a consequence of further reduced loads at the

higher strain. The mean values of fibers broken and the associated COVs were more realistic for these dry-sized T300 tests than for the dry-sized AS-4 tests. Parkins [17] shows cross-sectional areas for each of the individual lots of sized fibers. The mean cross-sectional areas of the sized fiber bundles were 1.1716E-7 m^2 and 1.1168E-7 m^2 for AS-4 and T300, respectively. There was about five percent difference between these values. On a normalized basis, the relative results remain similar to the load results.

Dry-Unsized Fiber Bundle Test Results

It is again necessary to explain each column heading for the tables in this section to aid the reader in understanding these results. Graphed test data from a typical dry-

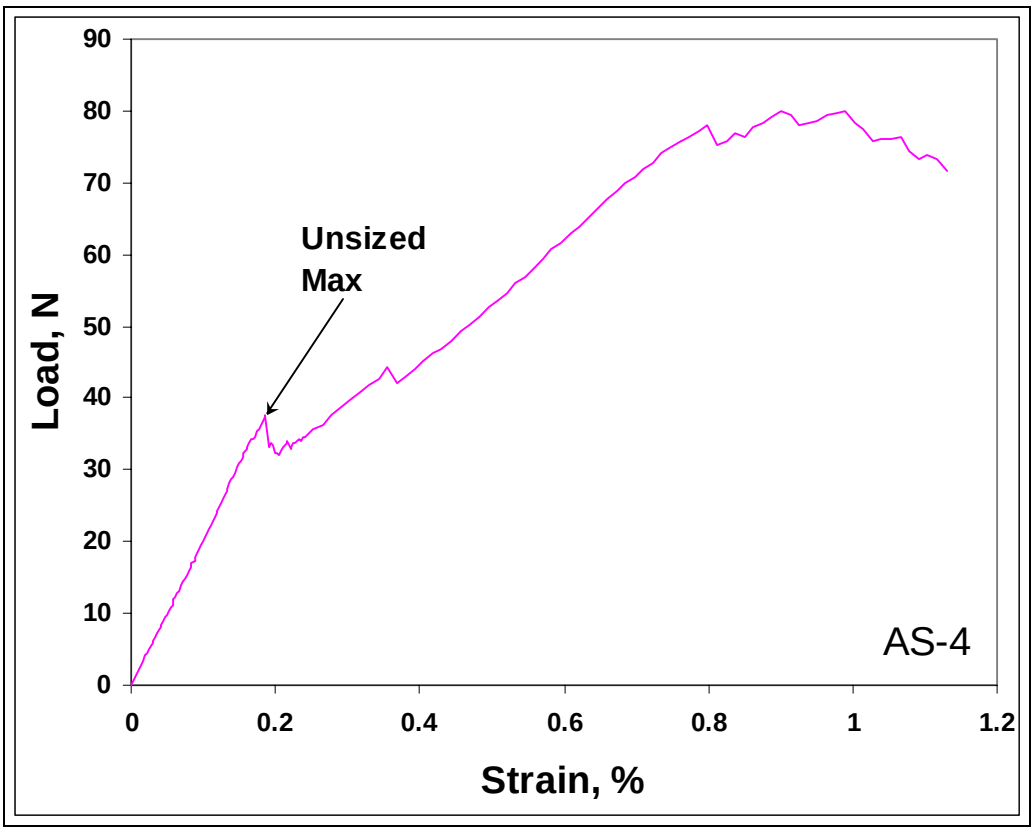

Figure 7.5. Typical graphed dry-unsized fiber bundle test data

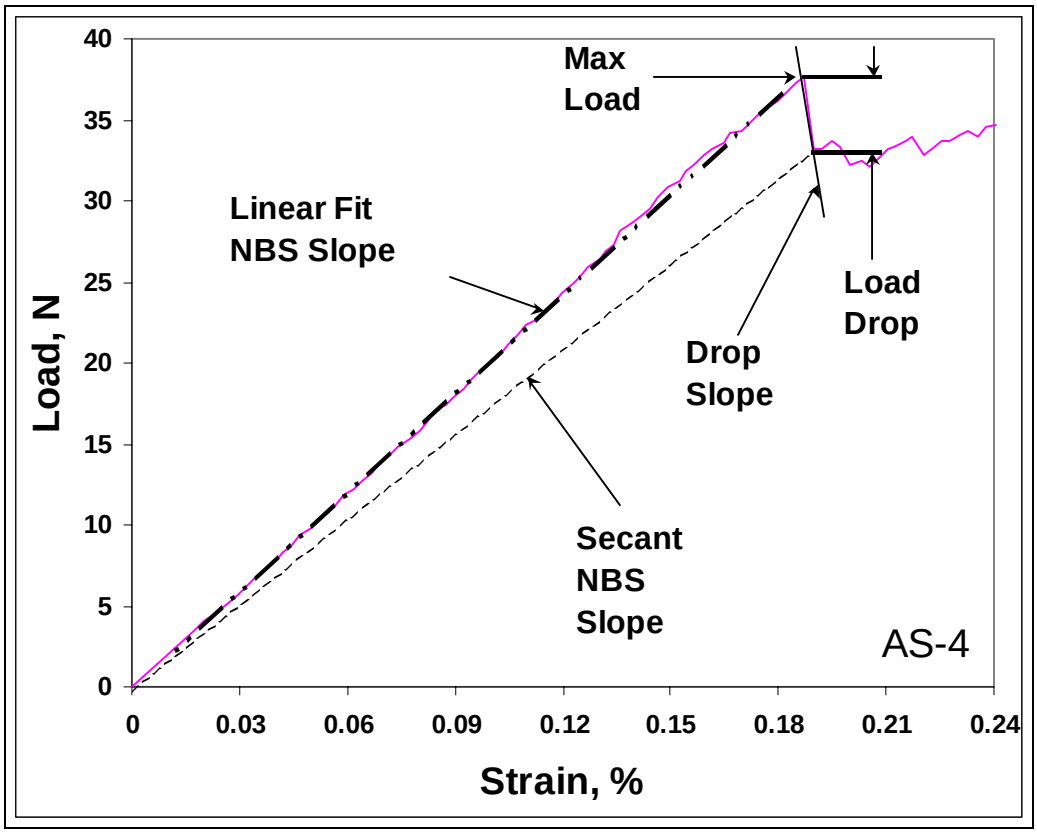

Figure 7.6. Detailed load-strain close-up graphical view to define test results

unsized fiber bundle test are shown in Figure 7.5. This data was from a test of AS-4 fibers, but is representative of the general behavior exhibited by the T300 unsized fibers. The *NBS*, *Strain*, *Max Load*, and *Fibers Broke at 0.81%* are representative of the same respective information as the tables in the previous section. The *Secant NBS* is calculated from the point where the load drop has stopped after the first major failure. This point is usually the bottom point of a V-shaped section of the plotted data, where the load has dropped before starting to build up again due to fiber entanglements. This point was sometimes chosen as a point before the load flattened off and then dropped further. The NBS slope, maximum load, and secant NBS slope are shown relative to the plotted data in Figure 7.6. The *Fibers Broke of 3000* is the theoretical number of fibers broke and is

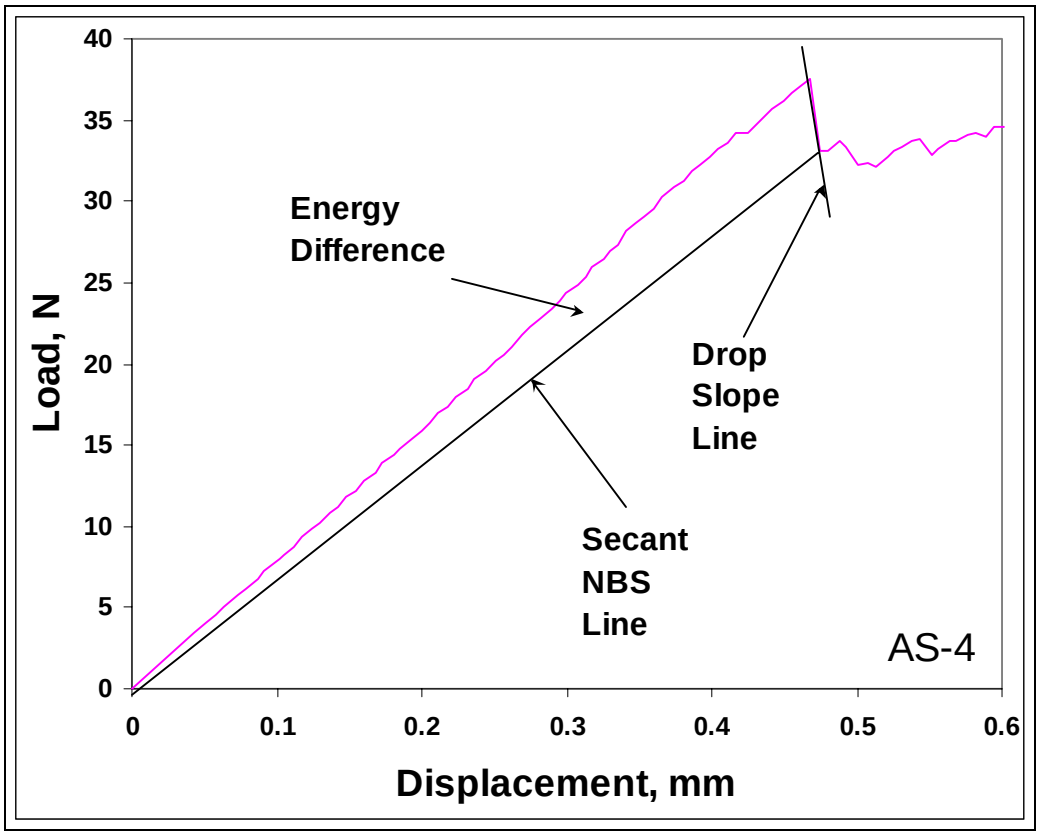

Figure 7.7. Detailed load-displacement close-up graphical view to define test results

directly based on the respective secant NBS for each test as explained in chapter 6. The *Load Drop* is simply the load drop that occurred after the first major failure. This value is the difference between the maximum load value and the load at the secant NBS point for each test. The *Drop Slope* is the slope of a line from the maximum load point to the secant NBS point for each test. This slope is an indicator of the fiber bundle behavior after the first major failure. The load drop and drop slope are shown in Figure 7.6 relative to the plotted test data. The *Energy Diff* for the unsized-fiber bundles refers to the difference in areas between the area under the graphed data up to the secant NBS point and the area under a line from the origin to the secant NBS point on a load-

displacement diagram. The area that indicates the energy difference, or dissipated strain energy density, is indicated in Figure 7.7. A large value for *Energy Diff* usually indicates large load drop at the first major failure. This behavior reduces the lower area and increases the difference in the areas.

The statistical results for the three lots of unsized AS-4 fiber samples that were tested are shown in Table 7.3, Table 7.4, and Table 7.5. The statistical results for the combined data from the three lots are shown in Table 7.6. The first two observations that were obvious after viewing theses tables were that the maximum loads and strains were much less than the sized AS-4 and that the COVs associated with these values were higher. The COVs were still within the 5~25 percent given by Phoenix, but were notably higher than the sized specimens. The NBS obtained for the unsized AS-4 fibers were in the same value range as the sized AS-4. The mean NBS of the combined unsized fibers was actually higher than the mean NBS of the combined sized AS-4 fibers. This

Table 7.3. Dry-unsized AS-4, lot # 1439-5h statistical results

duad1439-5h				67.0 **Specimens**	
	NBS_2 N	**Strain %**	**Max Load N**	**Secant NBS_2, N**	**Fibers Broke of 3000**
Mean	199.2	0.18	35.3	177.2	327
Std. Dev.	18.2	0.03	5.1	20.5	227
Max.	224.7	0.32	48.1	210.4	1269
Min.	124.3	0.12	20.6	121.7	-87
COV_1, %	9.1	16.06	14.5	11.6	69
	Load Drop N	**Drop Slope N**	**Energy Diff Nm**	**Fibers Broke at 0.81%**	
Mean	2.32	-379.7	0.00095	1686	
Std. Dev.	2.24	377.0	0.00067	248	
Max.	8.53	-15.0	0.00276	2100	
Min.	0.09	-1477.6	0.00019	1027	
COV_1, %	96.76	-99.3	70.41	15	

$_1$: COV = Coefficient Of Variation

$_2$: NBS = Normalized Bundle Stiffness

indicates that the fibers dominate the NBS of the sized fibers and that sizing does not cause an increase in the NBS of a fiber bundle. The low COVs of the secant NBS indicate similar behavior between the fibers in each lot. The low COV of the secant NBS

Table 7.4. Dry- unsized AS-4, lot # 1602-5b statistical results

duad1602-5b				67.0 Specimens	
	NBS_2 N	Strain %	Max Load N	Secant NBS_2, N	Fibers Broke of 3000
Mean	203.7	0.16	33.3	176.8	399
Std. Dev.	14.4	0.02	4.4	23.6	290
Max.	225.5	0.24	43.7	205.3	1308
Min.	159.9	0.12	22.9	107.3	40
COV_1, %	7.1	13.31	13.3	13.4	73
	Load Drop N	Drop Slope N	Energy Diff Nm	Fibers Broke at 0.81%	
Mean	4.01	-1106.5	0.00103	2077	
Std. Dev.	3.65	1241.8	0.00088	172	
Max.	17.06	-17.5	0.00424	2409	
Min.	0.09	-5913.4	0.00011	1611	
COV_1, %	90.98	-112.2	84.94	8	

$_1$: COV = Coefficient Of Variation

$_2$: NBS = Normalized Bundle Stiffness

Table 7.5. Dry- unsized AS-4, lot # 1730-5j statistical results

duad1730-5j				67.0 Specimens	
	NBS_2 N	Strain %	Max Load N	Secant NBS_2, N	Fibers Broke of 3000
Mean	206.0	0.21	44.4	164.9	598
Std. Dev.	10.8	0.03	5.4	19.2	248
Max.	223.6	0.30	56.5	214.9	1118
Min.	173.2	0.16	30.0	126.2	-25
COV_1, %	5.3	14.31	12.1	11.6	41
	Load Drop N	Drop Slope N	Energy Diff Nm	Fibers Broke at 0.81%	
Mean	8.48	-2481.4	0.00257	1450	
Std. Dev.	4.08	1714.7	0.00129	259	
Max.	16.40	-169.1	0.00470	2073	
Min.	0.65	-6533.2	0.00022	850	
COV_1, %	48.16	-69.1	49.99	18	

$_1$: COV = Coefficient Of Variation

$_2$: NBS = Normalized Bundle Stiffness

for the combined data indicates that the fibers in all of the lots behaved similarly. The mean values for *Fibers Broke of 3000* seem reasonable. The high COVs for *Fibers Broke of 3000* were due to this calculation's dependence on the secant NBS and NBS for each specimen, both of which have variability. The high COVs for *Load Drop*, *Drop Slope*, and *Energy Diff* indicate large differences in the behaviors of all of the fiber lots after the first major failure. The low COVs for *Fibers Broke at 0.81%* indicate reasonably consistent behavior of these fibers as the tests proceeded after the first major failure.

Table 7.6. Dry- unsized AS-4, Combined lots statistical results

dua Combined				201.0 **Specimens**	
	NBS_2 N	**Strain %**	**Max Load N**	**Secant NBS_2, N**	**Fibers Broke of 3000**
Mean	203.0	0.19	37.6	173.0	441
Std. Dev.	15.0	0.03	7.0	21.8	280
Max.	226.0	0.32	56.5	215.0	1310
Min.	124.0	0.12	20.6	107.0	-87
COV_1, %	7.4	18.80	18.5	12.6	63
	Load Drop N	**Drop Slope N**	**Energy Diff Nm**	**Fibers Broke at 0.81%**	
Mean	4.93	-1320.0	0.00152	1740	
Std. Dev.	4.28	1510.0	0.00123	345	
Max.	17.10	-15.0	0.00470	2410	
Min.	0.09	-6530.0	0.00011	850	
COV_1, %	86.80	-114.0	80.80	20	

$_1$: COV = Coefficient Of Variation

$_2$: NBS = Normalized Bundle Stiffness

The statistical results for the three lots of dry-unsized T300 fibers are shown in Table 7.7, Table 7.8, and Table 7.9. The statistical results for the combined data from the three lots are shown in Table 7.10. These results were interesting because the fibers used for these tests were from the same lots as those in the sized T300 fiber tests. Amoco® could not supply unsized fibers, so the sizing was washed from the sized sample fibers

Table 7.7. Dry- unsized T300, lot # 3u0403u statistical results

dut3u0403u				68.0 Specimens	
	NBS_2 N	Strain %	Max Load N	Secant NBS_2, N	Fibers Broke of 3000
Mean	200.8	0.24	45.9	172.7	422
Std. Dev.	7.4	0.03	3.5	19.1	246
Max.	214.2	0.33	56.8	206.3	1455
Min.	178.3	0.19	38.8	106.8	72
COV_1, %	3.7	11.00	7.5	11.1	58
	Load Drop N	Drop Slope N	Energy Diff Nm	Fibers Broke at 0.81%	
Mean	2.92	-374.3	0.00223	2421	
Std. Dev.	3.12	517.2	0.00139	272	
Max.	17.79	-14.1	0.00628	2769	
Min.	0.18	-2981.6	0.00030	1291	
COV_1, %	107	-138	62	11	

$_1$: COV = Coefficient Of Variation

$_2$: NBS = Normalized Bundle Stiffness

Table 7.8. Dry- unsized T300, lot # 3u0501u statistical results

dut3u0501u				70.0 Specimens	
	NBS_2 N	Strain %	Max Load N	Secant NBS_2, N	Fibers Broke of 3000
Mean	181.0	0.22	39.2	155.7	420
Std. Dev.	10.0	0.01	2.2	15.7	198
Max.	202.7	0.26	44.4	194.0	1106
Min.	154.1	0.19	32.6	108.1	-65
COV_1, %	5.5	6.17	5.7	10.1	47
	Load Drop N	Drop Slope N	Energy Diff Nm	Fibers Broke at 0.81%	
Mean	2.31	-199.4	0.00189	2294	
Std. Dev.	2.06	276.9	0.00087	139	
Max.	11.58	-14.8	0.00515	2602	
Min.	0.19	-2141.0	0.00025	1820	
COV_1, %	89	-139	46	6	

$_1$: COV = Coefficient Of Variation

$_2$: NBS = Normalized Bundle Stiffness

for the unsized tests. Again, the maximum loads for the unsized fibers were considerably less than those achieved by the sized fibers. However, the unsized T300 fiber bundles exhibited COVs for *Max Load* and *Strain* that were about half of the respective values for

the sized specimens. A point of interest was that the NBS values and the COVs for the NBS of the unsized fibers are similar to those of the sized fibers. However, as was the case with the AS-4 fibers, the unsized T300 fibers exhibited slightly higher NBS than

Table 7.9. Dry- unsized T300, lot # B3u0511u statistical results

dutB3u0511u					70.0 Specimens
	NBS_2 N	Strain %	Max Load N	Secant NBS_2, N	Fibers Broke of 3000
Mean	195.0	0.21	39.6	180.2	229
Std. Dev.	7.8	0.03	3.6	14.7	167
Max.	213.7	0.31	49.9	206.3	770
Min.	179.7	0.16	32.2	137.9	53
COV_1, %	4.0	12.18	9.1	8.2	73
	Load Drop N	Drop Slope N	Energy Diff Nm	Fibers Broke at 0.81%	
Mean	0.59	-117.2	0.00095	2046	
Std. Dev.	0.61	105.0	0.00080	260	
Max.	3.06	-18.6	0.00347	2435	
Min.	0.09	-493.9	0.00013	1261	
COV_1, %	104	-90	84	13	

$_1$: COV = Coefficient Of Variation

$_2$: NBS = Normalized Bundle Stiffness

Table 7.10. Dry- unsized T300, Combined lots statistical results

dut Combined					208.0 Specimens
	NBS_2 N	Strain %	Max Load N	Secant NBS_2, N	Fibers Broke of 3000
Mean	192.0	0.22	41.5	170.0	356
Std. Dev.	11.9	0.02	4.4	19.5	224
Max.	214.0	0.33	56.8	206.0	1450
Min.	154.0	0.16	32.2	107.0	-65
COV_1, %	6.2	11.00	10.5	11.5	63
	Load Drop N	Drop Slope N	Energy Diff Nm	Fibers Broke at 0.81%	
Mean	1.93	-229.0	0.00169	2250	
Std. Dev.	2.38	357.0	0.00118	278	
Max.	17.80	-14.1	0.00628	2770	
Min.	0.09	-2980.0	0.00013	1260	
COV_1, %	123.00	-156.0	70	12	

$_1$: COV = Coefficient Of Variation

$_2$: NBS = Normalized Bundle Stiffness

the sized T300 fibers. Comparison of the combined results in Table 7.6 and Table 7.10 reveal similarities between the unsized AS-4 and T300 for the *Secant NBS* and *Fibers Broke of 3000* columns. All of the respective values in these columns were very close. The *Load Drop* values were notably less and the *Drop Slope* values were not as steep for the unsized T300 as for the unsized AS-4 fibers. Conversely, the *Energy Diff* values and the *Fibers Broke at 0.81%* values were greater for the unsized T300 fibers than for the unsized AS-4 fibers. It is important to note that over half of the unsized T300 tests did not reach 0.81 percent strain, whereas all of the unsized AS-4 test achieved 0.81 percent strain. The greater mean of *Fibers Broke at 0.81%* for the unsized T300 indicates that the load falls off at a faster rate for the T300 than for the unsized AS-4 as the tests proceed after the first major failure. This implies that there are more lower strength fibers in this region. Parkins [17] shows cross-sectional areas for each of the individual lots of unsized AS-4 fibers. The cross-sectional areas for the sized T300 fibers may be used for the unsized T300, since the unsized T300 fibers were the same respective lots of sized fibers with the sizing washed from them. The mean cross-sectional areas of the sized fiber bundles were 1.1673E-7 m^2 and 1.1168E-7 m^2 for AS-4 and T300, respectively. There was about five percent difference between these values. On a normalized basis, the relative results remain similar to the load results.

Impregnated-Fiber Bundle Results

The impregnated-fiber test results will be addressed by first examining the results from the fibers impregnated with 3501-6 epoxy and then examining the fibers impregnated with 8552 epoxy. Again, the column headings for the result tables will be

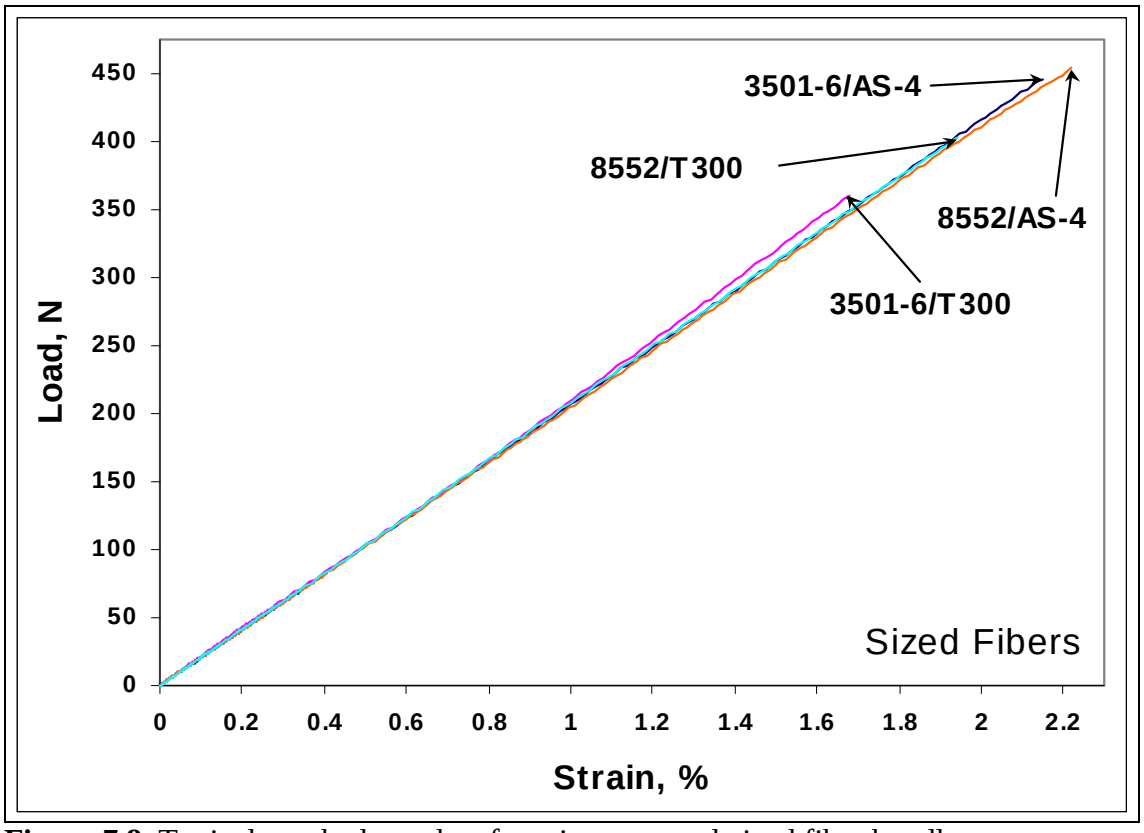

Figure 7.8. Typical graphed test data from impregnated-sized fiber bundle tests

discussed briefly to clearly establish the meaning of the information in each column. The *NBS* refers to the normalized bundle stiffness, NBS, slope of the linear section of the graphed data on a load-strain diagram. Typical plots of test data from impregnated-sized fiber bundle tests are shown in Figure 7.8. The graphed data in Figure 7.8 is representative of all of the impregnated-fiber bundle tests, which yielded plots that were very linear up to the maximum load. The *Strain* is the percent strain at the maximum load. *Max Load* is the maximum load achieved before failure. These tests were stopped upon failure because there were no possibilities of further loading the fibers after failure. The entire gage section of the specimens was usually fragmented upon failure. Rarely were there any remnants of the impregnated-fiber bundles left between the tabs. Again,

the values in the *Strain* and *Max Load* columns may not correspond to the same data sets for the *Max* and *Min* values shown. The *Energy* refers to the area under the graphed data up to *Max Load* on a load-displacement diagram. This metric was used since the energy difference was negligible compared to the dry bundle tests. That is, virtually no strain energy was dissipated up to fiber failure.

3501-6 Epoxy Impregnated-Fiber Bundle Test Results

Plotted data sets from tests of 3501-6 epoxy impregnated fiber bundles are shown in Figure 7.9. Data sets that most closely matched the mean NBS slopes and maximum

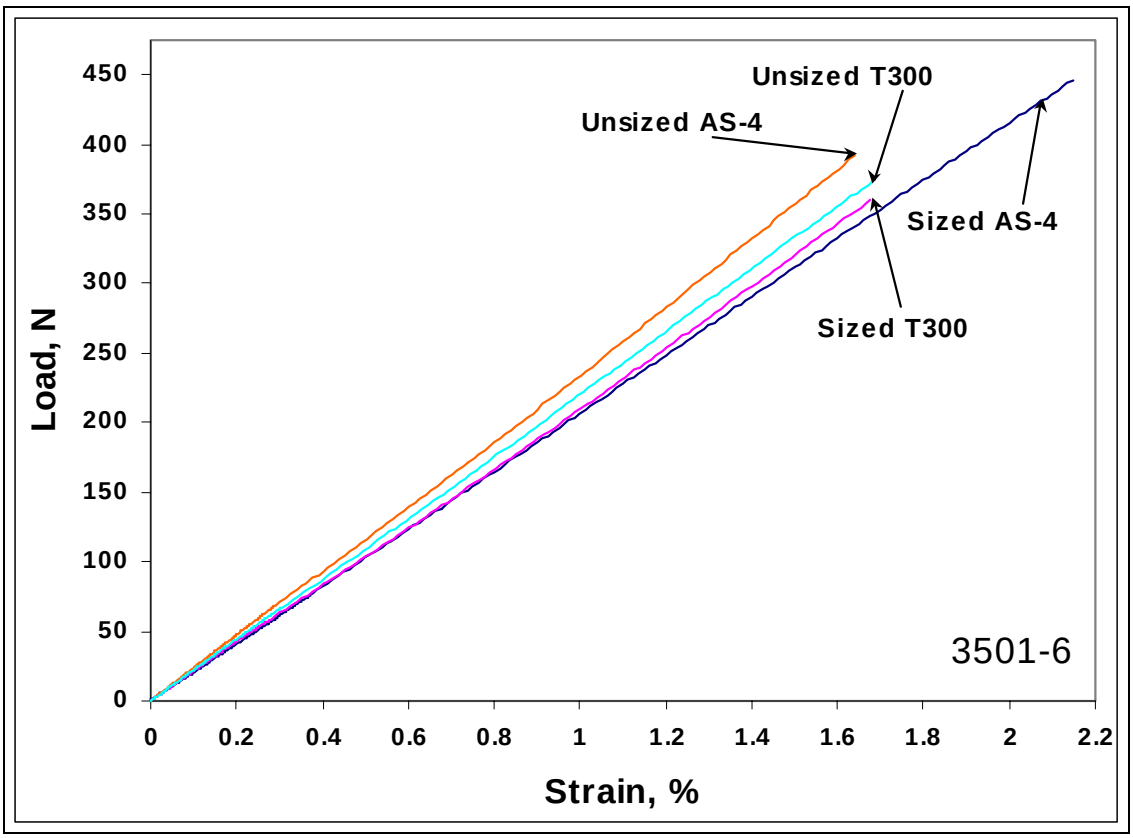

Figure 7.9. Typical graphed test data from 3501-6 impregnated-fiber bundle tests

Table 7.11. 3501-6 impregnated-sized AS-4 statistical results

i3sa1788-4c				34.0 **Specimens**
	NBS_2 N	**Strain %**	**Max Load N**	**Energy Nm**
Mean	205.0	2.30	455.4	1.34
Std. Dev.	12.9	0.25	26.7	0.22
Max.	227.5	2.87	510.2	1.84
Min.	178.8	1.70	381.6	0.82
COV_1, %	6.3	10.9	5.9	16.7
i3sa1795-5c				34.0 **Specimens**
	NBS_2 N	**Strain %**	**Max Load N**	**Energy Nm**
Mean	207.3	2.13	427.3	1.13
Std. Dev.	10.4	0.18	23.8	0.15
Max.	222.5	2.45	463.5	1.39
Min.	182.8	1.81	367.2	0.82
COV_1, %	5.0	8.3	5.6	13.3
i3sa1806-4b				33.0 **Specimens**
	NBS_2 N	**Strain %**	**Max Load N**	**Energy Nm**
Mean	212.0	2.19	452.0	1.24
Std. Dev.	8.5	0.15	26.9	0.15
Max.	230.0	2.42	488.0	1.44
Min.	193.0	1.80	373.0	0.83
COV_1, %	4.0	7.0	6.0	12.2
i3sa Combined				101.0 **Specimens**
	NBS_2 N	**Strain %**	**Max Load N**	**Energy Nm**
Mean	208.0	2.21	445.0	1.24
Std. Dev.	11.0	0.21	28.5	0.20
Max.	230.0	2.87	510.0	1.84
Min.	179.0	1.70	367.0	0.82
COV_1, %	5.3	9.5	6.4	15.9

$_1$: COV = Coefficient Of Variation

$_2$: NBS = Normalized Bundle Stiffness

loads were chosen from each group for these plots. Therefore, the plots shown are representative of the mean characteristics of each fiber group. The general characteristics of each fiber group relative to the other fiber groups can also be seen in Figure 7.9. The statistical results for the three individual lots and the combined lots of 3501-6 impregnated-sized AS-4 fibers are shown in Table 7.11. As expected, the *Strain* and *Max*

Load values were much higher than those for the dry fibers. The COVs for the *NBS*, *Strain* and *Max Load* values were similar to those for the respective values for the dry fibers. These COVs were good, considering the variabilities that can be induced by processing and the small size of the specimens. The higher COV values in the *Energy* columns were expected because the energies are nearly directly dependent on the

Table 7.12. 3501-6 impregnated-sized T300 statistical results

i3st3u0403				34.0 **Specimens**
	NBS_2 N	**Strain %**	**Max Load N**	**Energy Nm**
Mean	217.0	1.64	347.0	0.70
Std. Dev.	5.4	0.15	30.5	0.12
Max.	224.0	1.91	382.0	0.90
Min.	201.0	1.33	281.0	0.46
COV_1, %	2.5	8.8	8.8	17.3
i3st3u0501				34.0 **Specimens**
	NBS_2 N	**Strain %**	**Max Load N**	**Energy Nm**
Mean	205.0	1.80	359.0	0.79
Std. Dev.	7.0	0.16	29.6	0.13
Max.	215.0	2.05	406.0	1.00
Min.	182.0	1.47	298.0	0.53
COV_1, %	3.4	8.9	8.3	16.9
i3stB3u0511				32.0 **Specimens**
	NBS_2 N	**Strain %**	**Max Load N**	**Energy Nm**
Mean	214.0	1.91	396.0	0.94
Std. Dev.	6.3	0.15	29.1	0.13
Max.	225.0	2.08	420.0	1.07
Min.	200.0	1.33	272.0	0.43
COV_1, %	2.9	7.6	7.3	13.6
i3st Combined				100.0 **Specimens**
	NBS_2 N	**Strain %**	**Max Load N**	**Energy Nm**
Mean	212.0	1.78	367.0	0.81
Std. Dev.	8.2	0.19	36.1	0.16
Max.	225.0	2.08	420.0	1.07
Min.	182.0	1.33	272.0	0.43
COV_1, %	3.8	10.4	9.9	19.7

$_1$: COV = Coefficient Of Variation

$_2$: NBS = Normalized Bundle Stiffness

variabilities of the strains and maximum loads. In fact, the COVs for the energies were quite close to the sums of the respective COVs for strain and maximum loads.

The statistical results for the three individual lots and the combined lots of impregnated-sized T300 fibers are shown in Table 7.12. Similar to the dry-sized fiber bundle results, the 3501-6 impregnated AS-4 fibers yielded higher maximum loads and

Table 7.13. 3501-6 impregnated-unsized AS-4 statistical results

i3uad1439-5h				17.0 **Specimens**
	NBS_2 N	**Strain %**	**Max Load N**	**Energy Nm**
Mean	243.0	1.75	412.0	0.87
Std. Dev.	3.2	0.16	39.2	0.16
Max.	250.0	1.97	476.0	1.13
Min.	238.0	1.38	327.0	0.52
COV_1, %	1.3	9.2	9.5	18.5
i3uad1602-5b				17.0 **Specimens**
	NBS_2 N	**Strain %**	**Max Load N**	**Energy Nm**
Mean	235.0	1.57	348.0	0.65
Std. Dev.	7.2	0.17	44.1	0.16
Max.	246.0	1.86	422.0	0.93
Min.	220.0	1.30	264.0	0.37
COV_1, %	3.0	10.7	12.7	24.6
i3uad1730-5j				17.0 **Specimens**
	NBS_2 N	**Strain %**	**Max Load N**	**Energy Nm**
Mean	235.0	1.84	417.0	0.93
Std. Dev.	6.1	0.18	38.9	0.17
Max.	245.0	2.17	477.0	1.17
Min.	223.0	1.55	343.0	0.63
COV_1, %	2.6	9.7	9.3	18.7
i3ua Combined				51.0 **Specimens**
	NBS_2 N	**Strain %**	**Max Load N**	**Energy Nm**
Mean	238.0	1.72	392.0	0.82
Std. Dev.	6.8	0.20	51.1	0.20
Max.	250.0	2.17	477.0	1.17
Min.	220.0	1.30	264.0	0.37
COV_1, %	2.8	11.6	13.0	24.7

$_1$: COV = Coefficient Of Variation

$_2$: NBS = Normalized Bundle Stiffness

strains than the 3501-6 impregnated T300 fibers. However, the mean NBS of the combined 3501-6 impregnated T300 specimens was higher than the mean NBS of the

Table 7.14. 3501-6 impregnated-unsized T300 statistical results

i3ut3u0403u				17.0 **Specimens**
	NBS_2 N	**Strain %**	**Max Load N**	**Energy Nm**
Mean	222.0	1.66	353.0	0.70
Std. Dev.	4.1	0.11	21.4	0.09
Max.	231.0	1.86	382.0	0.88
Min.	215.0	1.50	322.0	0.59
COV_1, %	1.9	6.6	6.1	12.5
i3ut3u0501u				17.0 **Specimens**
	NBS_2 N	**Strain %**	**Max Load N**	**Energy Nm**
Mean	211.0	1.81	364.0	0.79
Std. Dev.	4.0	0.12	19.8	0.08
Max.	216.0	2.03	391.0	0.90
Min.	200.0	1.53	320.0	0.60
COV_1, %	1.9	6.7	5.4	10.3
i3utB3u0511u				16.0 **Specimens**
	NBS_2 N	**Strain %**	**Max Load N**	**Energy Nm**
Mean	222.0	1.86	402.0	0.91
Std. Dev.	5.7	0.10	19.9	0.11
Max.	228.0	2.00	426.0	1.06
Min.	209.0	1.61	346.0	0.66
COV_1, %	2.6	5.5	5.0	11.5
i3ut Combined				50.0 **Specimens**
	NBS_2 N	**Strain %**	**Max Load N**	**Energy Nm**
Mean	218.0	1.78	372.0	0.80
Std. Dev.	7.1	0.14	28.8	0.13
Max.	231.0	2.03	426.0	1.06
Min.	200.0	1.50	320.0	0.59
COV_1, %	3.2	7.9	7.7	15.7

$_1$: COV = Coefficient Of Variation

$_2$: NBS = Normalized Bundle Stiffness

i combined 3501-6 impregnated AS-4 specimens. This indicates that the 3501-6 impregnated T300 specimens were slightly stiffer, yet not as strong as the AS-4

specimens. The lower *Energy* values of the T300 specimens were indications of the lower strengths of the specimens, compared to corresponding AS-4 specimens.

The statistical results for the 3501-6 impregnated-unsized AS-4 fiber bundle tests are given in Table 7.13. The mean *Max Load* values were lower for the unsized AS-4 specimens than the sized AS-4 specimens. This was also the case for the dry-fiber bundles, which indicates that the sized AS-4 fibers were stronger fibers before sizing was applied. The *NBS* values for the impregnated-unsized AS-4 specimens were greater than those for the impregnated-sized AS-4 specimens. This was also the case for the dry-fiber bundle specimens. This indicates that the unsized AS-4 fibers were stiffer than the sized AS-4 fibers. Since the *Max Load* values were lower for the unsized AS-4 specimens than the sized AS-4 specimens, it was found to be the case as expected that the *Energy* values were lower.

The statistical results for the three individual lots and the combined lots of impregnated-unsized T300 fiber bundles are shown in Table 7.14. The COVs for this group of tests were all low compared to the respective values for the other impregnated-bundle tests. The NBS and maximum load values were greater for each of the lots of 3501-6 impregnated-unsized T300 fiber bundles than for the corresponding lots of sized T300 fibers. The respective mean *Energy* values for the unsized T300 fibers and sized T300 fibers were generally very close. The mean *Energy* values actually matched for the i3ut3u0403u and i3st3u0403 specimens as well as for the i3ut3u0501u and i3st3u0501 specimens. These results suggest that the sizing used on the T300 fiber bundles may actually be detrimental to the strength properties of composites

8552 Epoxy Impregnated-Fiber Bundle Test Results

Graphed data sets from of 8552 epoxy impregnated fiber bundle tests are shown in Figure 7.10. Again, data sets that most closely matched the mean NBS slopes and maximum loads were chosen from each group for these plots. The plots shown are representative of the mean characteristics of each fiber group relative to the other fiber groups. The first 8552 epoxy impregnated-fiber test group to be discussed is the sized-fiber AS-4 group. The statistical results for the three individual lots and the combined lots are shown in Table 7.15. The results for this group were similar to the results from the 3501-6 epoxy impregnated-fiber test group. A comparison of the i3sa combined

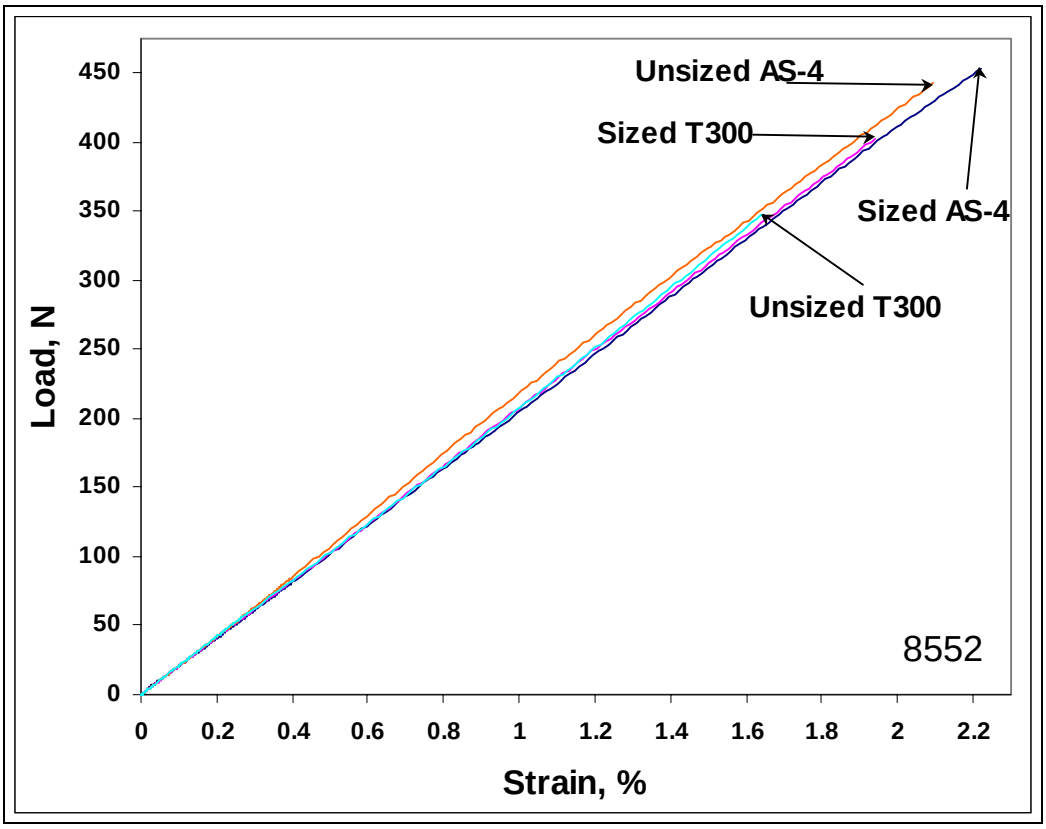

Figure 7.10. Typical graphed test data from 8552 impregnated-fiber bundle tests

Table 7.15. 8552 impregnated-sized AS-4 statistical results

i8sa1788-4c				34.0 Specimens
	NBS_2 N	Strain %	Max Load N	Energy Nm
Mean	227.0	1.99	441.0	1.09
Std. Dev.	10.2	0.12	23.2	0.12
Max.	242.0	2.23	484.0	1.30
Min.	203.0	1.77	392.0	0.85
COV_1, %	4.5	6.1	5.3	10.8
i8sa1795-5c				**34.0 Specimens**
	NBS_2 N	Strain %	Max Load N	Energy Nm
Mean	205.0	2.27	451.0	1.29
Std. Dev.	13.1	0.22	32.0	0.21
Max.	233.0	2.73	504.0	1.71
Min.	182.0	1.77	382.0	0.83
COV_1, %	6.4	9.6	7.1	15.9
i8sa1806-4b				**33.0 Specimens**
	NBS_2 N	Strain %	Max Load N	Energy Nm
Mean	207.0	2.38	470.0	1.42
Std. Dev.	18.8	0.37	45.2	0.31
Max.	230.0	3.24	535.0	2.01
Min.	149.0	1.49	326.0	0.63
COV_1, %	9.1	15.7	9.6	21.6
i8sa Combined				**101.0 Specimens**
	NBS_2 N	Strain %	Max Load N	Energy Nm
Mean	213.0	2.21	454.0	1.27
Std. Dev.	17.6	0.31	36.2	0.26
Max.	242.0	3.24	535.0	2.01
Min.	149.0	1.49	326.0	0.63
COV_1, %	8.3	13.8	8.0	20.4

$_1$: COV = Coeficient Of Variation

$_2$: NBS = Normalized Bundle Stiffness

results from Table 7.11 and the i8sa combined results from Table 7.15 showed that the mean values for the *NBS* and *Max Load* were higher for the i8sa test group. This means that the i8sa specimens were generally stronger and stiffer than the i3sa specimens. The COVs for the i8sa group were generally slightly higher than the respective values for the

i3sa group. As expected, the *Energy* values for the higher strength specimens are higher as well.

The statistical results for the 8552 impregnated-sized T300 tests are shown in Table 7.16. Comparison to the i3st results from Table 7.12 shows that the i8st specimens were again higher in strength, exhibited by the higher mean *Max Load* values for each

Table 7.16. 8552 impregnated-sized T300 statistical results

i8st3u0403				34.0 **Specimens**
	NBS_2 N	**Strain %**	**Max Load N**	**Energy Nm**
Mean	213.0	1.89	383.0	0.89
Std. Dev.	6.0	0.18	29.4	0.15
Max.	226.0	2.36	437.0	1.25
Min.	201.0	1.50	293.0	0.53
COV_1, %	2.8	9.5	7.7	17.2
i8st3u0501				34.0 **Specimens**
	NBS_2 N	**Strain %**	**Max Load N**	**Energy Nm**
Mean	195.0	2.07	395.0	1.04
Std. Dev.	9.5	0.24	41.9	0.21
Max.	212.0	2.44	447.0	1.36
Min.	174.0	1.34	253.0	0.44
COV_1, %	4.9	11.4	10.6	20.4
i8stB3u0511				32.0 **Specimens**
	NBS_2 N	**Strain %**	**Max Load N**	**Energy Nm**
Mean	209.0	2.16	434.0	1.17
Std. Dev.	7.7	0.11	14.9	0.10
Max.	220.0	2.30	465.0	1.33
Min.	196.0	1.86	405.0	0.94
COV_1, %	3.7	5.0	3.4	8.6
i8st Combined				100.0 **Specimens**
	NBS_2 N	**Strain %**	**Max Load N**	**Energy Nm**
Mean	206.0	2.04	404.0	1.03
Std. Dev.	10.8	0.22	37.6	0.20
Max.	226.0	2.44	465.0	1.36
Min.	174.0	1.34	253.0	0.44
COV_1, %	5.2	10.6	9.3	19.2

$_1$: COV = Coefficient Of Variation

$_2$: NBS = Normalized Bundle Stiffness

lot. However, the mean *NBS* values for the i8st group were all lower than the corresponding values for the i3st group. The difference in mean *Max Load* values for the i8st combined and i3st combined groups was 37 N. This is considerably greater than the 9 N difference exhibited between the same values for the i8sa combined and i3sa combined.

Table 7.17. 8552 impregnated-unsized AS-4 statistical results

i8uad1439-5h				17.0 **Specimens**
	NBS_2 N	**Strain %**	**Max Load N**	**Energy Nm**
Mean	232.0	2.02	453.0	1.14
Std. Dev.	7.9	0.13	30.5	0.14
Max.	249.0	2.20	493.0	1.34
Min.	219.0	1.73	379.0	0.82
COV_1, %	3.4	6.4	6.7	12.5
i8uad1602-5b				17.0 **Specimens**
	NBS_2 N	**Strain %**	**Max Load N**	**Energy Nm**
Mean	225.0	1.92	415.0	1.00
Std. Dev.	14.4	0.13	30.4	0.13
Max.	245.0	2.17	473.0	1.27
Min.	197.0	1.75	353.0	0.82
COV_1, %	6.4	6.8	7.3	12.8
i8uad1730-5j				17.0 **Specimens**
	NBS_2 N	**Strain %**	**Max Load N**	**Energy Nm**
Mean	221.0	2.17	462.0	1.27
Std. Dev.	10.6	0.23	31.6	0.23
Max.	235.0	2.69	520.0	1.70
Min.	189.0	1.70	376.0	0.78
COV_1, %	4.8	10.5	6.9	17.7
i8ua Combined				51.0 **Specimens**
	NBS_2 N	**Strain %**	**Max Load N**	**Energy Nm**
Mean	226.0	2.03	443.0	1.13
Std. Dev.	12.1	0.20	36.5	0.20
Max.	249.0	2.69	520.0	1.70
Min.	189.0	1.70	353.0	0.78
COV_1, %	5.4	9.6	8.2	17.8

$_1$: COV = Coefficient Of Variation

$_2$: NBS = Normalized Bundle Stiffness

The statistical results for the three individual lots and the combined lots from the 8552 impregnated-unsized AS-4 group are shown in Table 7.17. Comparison of the i8ua combined results to the i8sa combined results from Table 7.15 showed that the mean *Max Load* value for the i8sa specimens was larger. Actually, the mean *Max Load* values for the i8uad1439-5h and i8uad1730-5j lots were greater than the corresponding values for

Table 7.18. 8552 impregnated-unsized T300 statistical results

i8ut3u0403u				17.0 **Specimens**
	NBS_2 N	**Strain %**	**Max Load N**	**Energy Nm**
Mean	213.0	1.85	380.0	0.87
Std. Dev.	6.0	0.21	40.1	0.18
Max.	221.0	2.11	429.0	1.13
Min.	199.0	1.36	281.0	0.46
COV_1, %	2.8	11.1	10.6	21.0
i8ut3u0501u				17.0 **Specimens**
	NBS_2 N	**Strain %**	**Max Load N**	**Energy Nm**
Mean	199.0	1.57	301.0	0.64
Std. Dev.	6.6	0.49	96.0	0.38
Max.	210.0	2.28	428.0	1.25
Min.	186.0	0.88	162.0	0.16
COV_1, %	3.3	31.4	31.9	59.3
i8utB3u0511u				17.0 **Specimens**
	NBS_2 N	**Strain %**	**Max Load N**	**Energy Nm**
Mean	203.0	1.88	362.0	0.92
Std. Dev.	10.9	0.54	103.0	0.48
Max.	219.0	2.56	472.0	1.57
Min.	183.0	0.88	161.0	0.16
COV_1, %	5.4	28.7	28.5	52.1
i8ut Combined				51.0 **Specimens**
	NBS_2 N	**Strain %**	**Max Load N**	**Energy Nm**
Mean	205.0	1.76	348.0	0.81
Std. Dev.	9.9	0.45	89.7	0.38
Max.	221.0	2.56	472.0	1.57
Min.	183.0	0.88	161.0	0.16
COV_1, %	4.8	25.6	25.8	47.0

$_1$: COV = Coefficient Of Variation

$_2$: NBS = Normalized Bundle Stiffness

two of the three i8sa lots tested. The i8uad1602-5b lot had a mean maximum load that was 38 N lower than the nearest mean maximum load from the other two lots in the i8ua group. The COV for the *Max Load* from the i8uad1602-5b lot was reasonably low, at 7.3 percent. This indicates that the mean maximum load was low because of generally lower maximum load values rather than because of a few extremely low maximum load values adversely affecting the results. Comparison of the mean *NBS* values for the i8ua combined results and the i8sa combined results showed that the unsized i8ua group had a higher NBS than the sized i8sa group.

The statistical results for the 8552 impregnated-unsized T300 fiber bundles are shown in Table 7.18. It was immediately apparent that the COVs for *Strain*, *Max Load*, and *Energy* were comparatively high for all of the lots. However, the i8ut3u0501u and i8utB3u0511u lots showed especially high COVs. Consideration was given to the possibility that the two lots had been impregnated in the same batch. This could have caused a process-related problem that might explain the high COVs. However, upon checking the laboratory notebook, it was found that these two lots were prepared separately. The mean maximum load for the i8ut3u0501u group was 61 N less than the nearest corresponding value from the other two lots. The low maximum loads for the i8ut3u0501u group greatly affected the mean maximum load of the i8ut combined result. The i8ut combined mean maximum load was 348.0 N, which was 56 N less than the mean maximum load for the i8st group. It is interesting to note that the mean *NBS* values for each of the i8ut lots and for the combined lots were very close to the respective values for the i8st group. Also, the COVs for the *NBS* values were low for the i8ut group. This indicates little variation in the NBS within each i8ut lot.

Comparison of Dry-Bundle and Impregnated- Bundle Results

Some comparisons have already been made between some of the dry-bundle and the impregnated-bundle test results. Comparison tables have been constructed to allow comparison of the results from the dry-bundle and impregnated-bundle test for each lot of fibers tested. The combined results for each type of fiber have also been included in the tables to allow comparisons between the four types of fibers. As a graphical example, test results from dry-unsized, dry-sized, and 3501-6 impregnated-sized fiber bundles have been plotted in Figure 7.11. The relative characteristics of each group are illustrated in Figure 7.11.

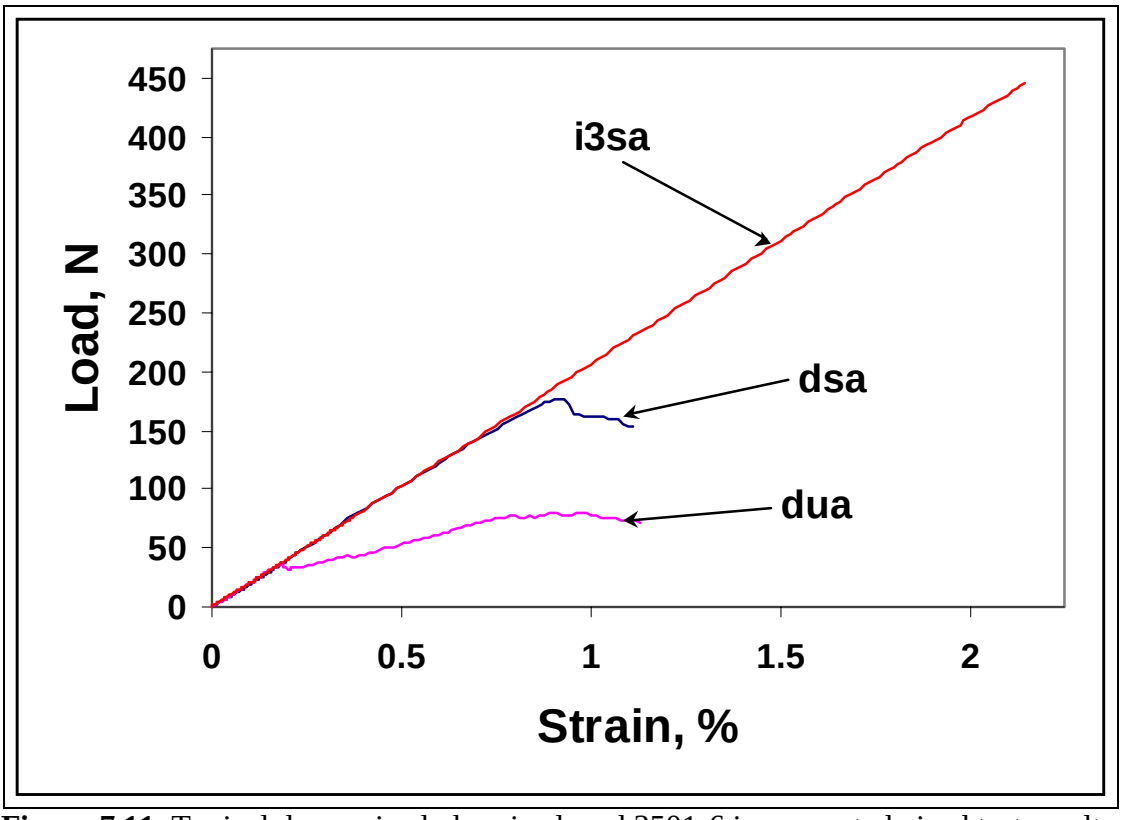

Figure 7.11. Typical dry-unsized, dry-sized, and 3501-6 impregnated-sized test results on a common graph

Four tables have been constructed, one for each of the fiber types. It is necessary to briefly discuss the table layout to aid the reader's understanding of the information presented. The table headings will also be explained to clarify the meaning of the results under each heading. The tables are grouped into three sections. The sections from top to bottom are *NBS*, *Strain*, and *Max Load*. The appropriate units are given at the top of each section. Within each section, the dry-bundle, 3501-6 impregnated-bundle, and 8552 impregnated-bundle results from each fiber lot are grouped together. These groups are followed by the grouped results for the combined fiber lots. The first table heading is *Mean Value*. These values are the mean *NBS*, *Strain*, and *Max Load* values taken directly from Table 7.1 through Table 7.18. The units for the first column are the appropriate units for the results addressed in the section. The second heading is *Change from dry*. This column gives the actual difference between the values of the respective dry-bundle results and the impregnated-bundle results. The units for the second column are the appropriate units for the results addressed in the section. The third column heading is again labeled *Change from dry*. The unit for the third column is percent. The results in this column are the percent changes represented by the differences between the dry-bundle and impregnated-bundle results. These percent changes are relative to the dry-bundle result shown for each group. The fourth and last column is labeled *Dry Fiber's Share*. The unit for this column is percent. These values are the percentage of the impregnated-bundle result that is represented by the corresponding dry-bundle result. That is, 100 percent multiplied by the quotient of the dry-bundle result divided by the impregnated-bundle result. Strain and maximum load will obviously be higher for the impregnated tests due to load sharing as discussed by Rosen [2].

The first fiber type that will be addressed is the sized AS-4. The comparison results for the sized AS-4 are shown in Table 7.19. Upon first examination, an anomaly was apparent within the 1788-4c fiber lot. This was that the mean NBS for the i3sa1788-4c group was less than the mean NBS for the dry dsa1788-4c group. The i3sa1788-4c group was the only impregnated-bundle group that had a mean NBS that was lower than its corresponding dry-bundle group. The COV of 6.3 percent for the NBS of the i3sa1788-4c specimens is shown in Table 7.11. This COV value was reasonable and indicates that the NBS were within a range similar to the other lots. Comparison of the 1788-4c lot with all other lots in Table 7.19 through Table 7.22 showed that the 1788-4c lot was the only one that showed a lower mean NBS for the 3501-6 impregnated specimens than for the 8552 impregnated specimens. The other mean values for the i3sa1788-4c group were reasonable and tend to validate the group's results. The low mean NBS value for the i3sa1788-4c group also skewed the *NBS* results for the combined lots of sized AS-4 fibers.

The *Max Load* value for the dsa1788-4c lot was the highest of the dsa lots, and was higher than all of the dst lots. Naturally, it would be expected that the 1788-4c fibers would produce strong impregnated specimens. The i3sa1788-4c fibers did produce the highest *Max Load* value of the i3sa group. In fact, as might be expected, the i3sa1788-4c fibers gave the highest *Max Load* value of all of the 3501-6 impregnated-fiber groups. However, for the i8sa group, the 1788-4c lot gave the lowest *Max Load* value. The i8sa1806-5b *Max Load* value was the highest of the i8sa group by 19 N. The dsa1806-5b *Max Load* value was the second highest of the dsa group.

Table 7.19. Sized AS-4 comparative statistical results

	Mean Value	Change from dry	Change from dry	Dry Fiber's Share
NBS_2	**N**	**N**	**%**	**%**
dsa1788-4c	212.6			
i3sa1788-4c	205.0	-7.6	-3.6	103.7
i8sa1788-4c	227.0	14.4	6.8	93.6
dsa1795-5c	184.4			
i3sa1795-5c	207.3	22.9	12.4	89.0
18sa1795-5c	205.0	20.6	11.1	90.0
dsa1806-5b	199.8			
i3sa1806-5b	212.0	12.2	6.1	94.2
i8sa1806-5b	207.0	7.2	3.6	96.5
dsa Combined	199.0			
i3sa Combined	208.0	9.0	4.5	95.7
i8sa Combined	213.0	14.0	7.0	93.4
Strain	**%**	**%**	**%**	**%**
dsa1788-4c	0.99			
i3sa1788-4c	2.30	1.3	133.0	42.9
i8sa1788-4c	1.99	1.0	101.3	49.7
dsa1795-5c	0.88			
i3sa1795-5c	2.13	1.2	141.7	41.4
18sa1795-5c	2.27	1.4	157.5	38.8
dsa1806-5b	0.85			
i3sa1806-5b	2.19	1.3	158.5	38.7
i8sa1806-5b	2.38	1.5	180.9	35.6
dsa Combined	0.91			
i3sa Combined	2.21	1.3	143.9	41.0
i8sa Combined	2.21	1.3	143.9	41.0
Max. Load	**N**	**N**	**%**	**%**
dsa1788-4c	199.5			
i3sa1788-4c	455.4	255.9	128.3	43.8
i8sa1788-4c	441.0	241.5	121.1	45.2
dsa1795-5c	156.0			
i3sa1795-5c	427.3	271.4	174.0	36.5
18sa1795-5c	451.0	295.0	189.2	34.6
dsa1806-5b	164.1			
i3sa1806-5b	452.0	287.9	175.5	36.3
i8sa1806-5b	470.0	305.9	186.5	34.9
dsa Combined	173.0			
i3sa Combined	445.0	272.0	157.2	38.9
i8sa Combined	454.0	281.0	162.4	38.1

$_2$: NBS = Normalized Bundle Stiffness

The comparison results for the sized T300 fiber group are shown in Table 7.20. The results for the individual lots in the *NBS* section showed no unusual behavior for any of the lots. Thus, the combined results for the three lots gave the general behavior. The i3st group showed a larger percentage change in NBS than the i8st group. The results in the *Strain* section also showed no unusual behavior. The i8st group did show a larger percentage change than the i3st group, unlike the results in the *NBS* section. However, the maximum loads influence these values more than the NBS. The results for the individual lots in the *Max Load* section showed that the dst3u0501 value was considerably lower than the other two dst values. However, the *Max Load* values of the i3st3u0501 and i8st3u0501 groups did not suffer because of the low *Max Load* value for the dst3u0501 group. In fact, the *Max Load* values for both of the impregnated 3u0501 groups were the second highest values of the three sized T300 lots. The percentage changes associated with the *Max Load* values of the impregnated-sized T300 fibers were considerably higher than those for the sized AS-4 fibers. Comparison of the *Max Load* values from Table 7.19 and Table 7.20 showed that even though the dst values were much lower than the dsa values, the values for the i3st and i8st groups were only moderately lower than the respective i3sa and i8sa group values. Comparison of the combined lot results from both tables determined that the *Max Load* value of the i3st group was 82 percent of the i3sa value and the i8st value was 89 percent of the i8sa value. The value for the dst group was only 56 percent of the dsa group value. The i8st group exhibited a greater percentage change in the *Max Load* value than the i3st group.

Next, the comparison results for unsized AS-4 fiber group will be examined. The results for this fiber group are shown in Table 7.21. Again, the results for the individual

Table 7.20. Sized T300 comparative statistical results

	Mean Value	Change from dry	Change from dry	Dry Fiber's Share
NBS_2	**N**	**N**	**%**	**%**
dst3u0403	189.1			
i3st3u0403	217.0	27.9	14.8	87.1
i8st3u0403	213.0	23.9	12.7	88.8
dst3u0501	174.8			
i3st3u0501	205.0	30.2	17.3	85.3
i8st3u0501	195.0	20.2	11.6	89.6
dstB3u0511	191.6			
i3stB3u0511	214.0	22.4	11.7	89.6
i8stB3u0511	209.0	17.4	9.1	91.7
dst Combined	185.0			
i3st Combined	212.0	27.0	14.6	87.3
i8st Combined	206.0	21.0	11.4	89.8
Strain	**%**	**%**	**%**	**%**
dst3u0403	0.63			
i3st3u0403	1.64	1.0	162.3	38.1
i8st3u0403	1.89	1.3	202.2	33.1
dst3u0501	0.49			
i3st3u0501	1.80	1.3	266.1	27.3
i8st3u0501	2.07	1.6	321.1	23.7
dstB3u0511	0.59			
i3stB3u0511	1.91	1.3	225.7	30.7
i8stB3u0511	2.16	1.6	268.4	27.1
dst Combined	0.57			
i3st Combined	1.78	1.2	213.4	31.9
i8st Combined	2.04	1.5	259.2	27.8
Max Load	**N**	**N**	**%**	**%**
dst3u0403	113.0			
i3st3u0403	347.0	234.0	207.2	32.6
i8st3u0403	383.0	270.0	239.0	29.5
dst3u0501	77.2			
i3st3u0501	359.0	281.8	364.9	21.5
i8st3u0501	395.0	317.8	411.5	19.6
dstB3u0511	101.4			
i3stB3u0511	396.0	294.6	290.4	25.6
i8stB3u0511	434.0	332.6	327.9	23.4
dst Combined	97.2			
i3st Combined	367.0	269.8	277.6	26.5
i8st Combined	404.0	306.8	315.6	24.1

$_2$: NBS = Normalized Bundle Stiffness

Table 7.21. Unsized AS-4 comparative statistical results

	Mean Value	Change from dry	Change from dry	Dry Fiber's Share
NBS_2	**N**	**N**	**%**	**%**
duad1439-5h	199.2			
i3uad1439-5h	243.0	43.8	22.0	82.0
i8uad1439-5h	232.0	32.8	16.5	85.9
duad1602-5b	203.7			
i3uad1602-5b	235.0	31.3	15.3	86.7
i8uad1602-5b	225.0	21.3	10.4	90.6
duad1730-5j	206.0			
i3uad1730-5j	235.0	29.0	14.1	87.6
i8uad1730-5j	221.0	15.0	7.3	93.2
dua Combined	203.0			
i3ua Combined	238.0	35.0	17.2	85.3
i8ua Combined	226.0	23.0	11.3	89.8
Strain	**%**	**%**	**%**	**%**
duad1439-5h	0.18			
i3uad1439-5h	1.75	1.6	868.7	10.3
i8uad1439-5h	2.02	1.8	1018.1	8.9
duad1602-5b	0.16			
i3uad1602-5b	1.57	1.4	868.2	10.3
i8uad1602-5b	1.92	1.8	1084.1	8.4
duad1730-5j	0.21			
i3uad1730-5j	1.84	1.6	757.6	11.7
i8uad1730-5j	2.17	2.0	911.5	9.9
dua Combined	0.19			
i3ua Combined	1.72	1.5	824.7	10.8
i8ua Combined	2.03	1.8	991.4	9.2
Max Load	**N**	**N**	**%**	**%**
duad1439-5h	35.3			
i3uad1439-5h	412.0	376.7	1068.7	8.6
i8uad1439-5h	453.0	417.7	1185.0	7.8
duad1602-5b	33.3			
i3uad1602-5b	348.0	314.7	946.3	9.6
i8uad1602-5b	415.0	381.7	1147.8	8.0
duad1730-5j	44.4			
i3uad1730-5j	417.0	372.6	839.1	10.6
i8uad1730-5j	462.0	417.6	940.5	9.6
dua Combined	37.6			
i3ua Combined	392.0	354.4	942.6	9.6
i8ua Combined	443.0	405.4	1078.2	8.5

$_2$: NBS = Normalized Bundle Stiffness

Table 7.22. Unsized T300 comparative statistical results

	Mean Value	Change from dry	Change from dry	Dry Fiber's Share
NBS_2	**N**	**N**	**%**	**%**
dut3u0403u	200.8			
i3ut3u0403u	222.0	21.2	10.5	90.5
i8ut3u0403u	213.0	12.2	6.1	94.3
dut3u0501u	181.0			
i3ut3u0501u	211.0	30.0	16.6	85.8
i8ut3u0501u	199.0	18.0	9.9	91.0
dutB3u0511u	195.0			
i3utB3u0511u	222.0	27.0	13.9	87.8
i8utB3u0511u	203.0	8.0	4.1	96.0
dut Combined	192.0			
i3ut Combined	218.0	26.0	13.5	88.1
i8ut Combined	205.0	13.0	6.8	93.7
Strain	**%**	**%**	**%**	**%**
dut3u0403u	0.24			
i3ut3u0403u	1.66	1.4	598.5	14.3
i8ut3u0403u	1.85	1.6	678.4	12.8
dut3u0501u	0.22			
i3ut3u0501u	1.81	1.6	711.1	12.3
i8ut3u0501u	1.57	1.3	603.5	14.2
dutB3u0511u	0.21			
i3utB3u0511u	1.86	1.6	775.1	11.4
i8utB3u0511u	1.88	1.7	784.5	11.3
dut Combined	0.22			
i3ut Combined	1.78	1.6	694.6	12.6
i8ut Combined	1.76	1.5	685.7	12.7
Max Load	**N**	**N**	**%**	**%**
dut3u0403u	45.9			
i3ut3u0403u	353.0	307.1	669.5	13.0
i8ut3u0403u	380.0	334.1	728.4	12.1
dut3u0501u	39.2			
i3ut3u0501u	364.0	324.8	829.3	10.8
i8ut3u0501u	301.0	261.8	668.5	13.0
dutB3u0511u	39.6			
i3utB3u0511u	402.0	362.4	914.6	9.9
i8utB3u0511u	362.0	322.4	813.7	10.9
dut Combined	41.5			
i3ut Combined	372.0	330.5	796.4	11.2
i8ut Combined	348.0	306.5	738.6	11.9

$_2$: NBS = Normalized Bundle Stiffness

lots in the *NBS* section showed no unusual behavior for any of the lots. The three dua *NBS* values were quite close to each other. Thus, the combined results for the three lots represented the general behavior. The i3st group showed a larger percentage change in NBS than the i8st group. The results in the *Strain* section showed similar behavior between the fiber lots. Each exhibited a significant percentage change for the impregnated groups. The maximum loads for the respective impregnated groups greatly influenced these values. Again, the i8st group showed a larger percentage change than the i3st group. The results for the individual dua lots in the *Max Load* section showed that the values were considerably lower than the values for the sized-fiber groups. However, the *Max Load* values of the impregnated groups increased drastically from the dry fiber groups. The *Max Load* values were generally less than those for the sized AS-4 fiber group, but were higher than the *Max Load* values for the sized T300 fiber group. The percentage changes for the i3ua and i8ua *Max Load* values were impressive. The i3ua combined and i8ua combined percentage changes were 942.6 percent and 1078.2 percent respectively. This is a good example of how the two materials of a fiber-matrix composite can compliment each other in a composite that has properties far superior to either of the constituents.

The comparison results for the unsized T300 fiber group are shown in Table 7.22. The *NBS* section results for the individual lots showed no unusual behavior for any of the lots. Again, the combined results for the three fiber lots represented the general behavior. As before, the i3st group showed a larger percentage change in NBS than the i8st group. The results in the *Strain* section showed similar behavior between the fiber lots. Similar to the unsized AS-4 group, each T300 lot exhibited a significant percentage change for

the impregnated groups. The percentage changes for the i3ut and i8ut groups were slightly less than the changes for the i3ua and i8ua groups. As before, the maximum loads for the respective impregnated groups greatly influenced these values. Again, the i8st group showed a larger percentage change than the i3st group. The results for the individual dut lots in the *Max Load* section showed that the values were considerably lower than the values for the sized-fiber groups. Overall, the *Max Load* values for the dut lots were higher than the dua lots. This is contrary to the comparison of the dsa and dst *Max Load* values, where the AS-4 values are greater than the T300 values. Similar to the unsized AS-4 fiber group results, the *Max Load* values of the impregnated T300 groups increased drastically from the dry fiber groups. The *Max Load* values were generally less than those for the unsized AS-4 fiber group. The i3ut combined *Max Load* value was greater than the i3st value by 5 N. Conversely, the i8ut combined *Max Load* value was less than the i8st value by 56 N. Again, the percentage changes for the i3ut and i8ut *Max Load* values were impressive. The i3ut combined and i8ut combined percentage changes were 796.4 percent and 738.6 percent, respectively.

It was interesting to compare the results in Table 7.20 and Table 7.22 because they represented the same production lots of fibers. A more extensive study would be necessary to make absolute conclusions about the influence of sizing on the behavior of fiber bundles. However, comparison of the two tables led to some interesting observations. First, the *NBS* values for each of the dut lots were higher that the corresponding dst lots. This was also the case for the dua combined result compared to the dsa combined result. However, the difference between the dua combined and dsa combined results could be due to variabilities in fiber properties. It is difficult to

speculate exactly why the NBS would increase once the sizing was removed from the T300 fibers. It may be due to the sizing interfering with the collimation of the fiber bundles. The sizing clearly had an influence on the *Max Load* values, which were higher for the sized fibers. It appears that the sizing acts as weak matrix material, which creates a "psuedo-composite" from the fiber bundle. This effect was discovered upon examination of some early test results. As a direct result, it was necessary to reevaluate the statistical treatment of the data, as discussed in chapter 6.

All of the data including individual load-strain diagrams are available in the Office of Naval Research Interim Progress Report for 7/1999 – 4/2000. This report, by Parkins [17], is for research conducted at Montana State University-Bozeman under MSU Contract #290055.

CHAPTER 8

CONCLUSIONS AND RECOMMENDATIONS

Conclusions

The scope of this research was very broad. Throughout the project, several developments were needed to achieve the initial objective. Again, this objective was to:

> Develop a dry-bundle test and validate it experimentally by comparison to impregnated-bundle tests.

Development of a method to impregnate the fiber bundles with epoxies or development of a method to dispense high temperature hot melt glue for tabs, for examples, both appeared to be departures from the objective. However, when one examines the compilation of the research steps and the subsequent data and results, it can be seen that each step taken during this research truly had the research objective as a focal point.

As stated in chapter 2, much research has been done that involves the theoretical behavior and modeling of carbon-fiber bundles or fiber bundles in general. However, there seems to be a major void between the theoretical aspects of fiber bundle behavior and applications of the theory for solutions to “real world” situations. Ostensibly, the data from reliable dry-fiber bundle tests has not been available to provide strength distribution functions and other information necessary for verification of the theory. Much of the theoretical work has modeled dry-fiber bundle behavior by using data from

impregnated bundle tests and incorporating assumptions to disregard or compensate for the effects of the matrix material. The data and results from this research can be used to verify the validity of the assumptions that have been used. This will confirm the validity of the models that have already been developed. Another area that could benefit from reliable dry-fiber bundle test results is research that involves single filament tests. Correlation between single filament test results and dry-fiber bundle results could eliminate the need for single filament tests. This would be beneficial because single filament testing requires much care. In addition, the high variability of single filaments requires that many specimens be tested to achieve statistically significant results.

Ultimately, new models could also be developed to correlate dry-fiber bundle test results to the properties of composites. Compilation of a database of constitutive properties of various fibers and matrix materials could lead to correlations of different combinations of fibers and matrix materials to composite material properties. This could be an important link between constitutive properties and the properties of a complete primary structure. Large structure development would be greatly benefited because production of large composite parts requires large-expensive molds. If the structural properties can only be determined from full-sized parts, changes required to improve the parts can only be achieved by building new molds or altering old ones. Many evolutionary iterations of this type are time consuming and expensive. Successful modeling of primary structures from constitutive properties would substantially reduce the developmental costs.

Development of the dry-fiber bundle test method required an idealistic approach to recognize where inconsistencies could be introduced into the results. Collimation of

the fiber bundles and maintaining the collimation and integrity of the fiber bundle specimens through preparation and testing were recognized as primary concerns for reliable fiber bundle test results. Collimation was accomplished by using "pigtail" orifices. The possibility exists that using an orifice only collimates the outer fibers of a bundle. Examination of the initial portions of the data from the slow dry-fiber bundle tests indicated that the fiber loading was even from the very beginning of the tests. It is believed that this method collimated the specimens as effectively as possible.

Maintaining the collimation and integrity of the fiber bundle specimens was achieved by drawing the fiber bundles through the orifices and directly into test fixtures. The specimens remained in the test fixtures until testing was completed. The tabs were molded onto the ends of the specimens in the fixtures and the test fixtures insured that the specimens remained straight and collimated from preparation through test completion. The first test fixture design worked well enough, but the alignment rods, which remained in place during testing, could cause error to be induced in results because of frictional drag on the alignment rods. The second test fixture design alleviated this problem by allowing the alignment rods to be removed after the fixture was clamped into the testing machine. This insured that the specimens were clamped into the test machine straight and aligned, yet suffered no ill effects from alignment rod drag during testing. After the method and fixture developments were complete, preparation and testing of the 600 dry-fiber bundle specimens were completed in 27 days.

Development of the method to impregnate the fiber bundles with the epoxy matrix materials was a major task. The plate press that was designed and constructed seemed to be the most viable method to achieve the desired quality of specimens. It required many

days of design and machine work to produce the plate press. Then several iterations of specimens were necessary to determine that further modification of the plate press was needed. More machine work was required so vacuum could be applied to the specimens to reduce porosity. More iteration of specimens proved that the plate press could be used to successfully impregnate the fiber bundles. After the specimens were impregnated and cured, some development was necessary for test preparation. This mostly involved a method of dispensing the hot melt glue that was selected as the tab material for the impregnated-bundle tests. A cast iron pan was modified with a valve in its bottom to dispense the hot melt glue in a safe and timely manner. Two months were required to produce the 600 impregnated specimens and test them after method development.

The statistical analysis of over 1200 data sets necessitated the writing of many computer codes using Matlab®. The codes were written to extract the significant results from the data sets. The obtainable results showed differences between the unsized dry-fiber bundles, the sized dry-fiber bundles, and the impregnated-fiber bundles. The results were compiled in files and tables for analysis.

In general, the NBS values for the unsized fibers were higher than those for the same type of sized fibers. This indicates that the unsized fibers tend to be slightly stiffer. This is also confirmed by using the mean cross-sectional areas given by Parkins [17] to calculate and compare moduli of the fiber bundles. The precise reason for this behavior is unclear, but this was the trend in both the AS-4 and T300 fibers. The 3501-6 epoxy increased the NBS of the specimens more than the 8552 epoxy. This behavior is reasonable because the 3501-6 epoxy is a stiff, brittle matrix, whereas the 8552 epoxy allows more yielding and strain to failure. This behavior was shown in the test results,

where the mean strains at maximum load were higher in the majority of the groups for the 8552 epoxy. For all of the fiber groups but the unsized T300, the 8552 epoxy increased the maximum loads more than the 3501-6 epoxy. The mean maximum stress values were calculated for the impregnated fiber groups. The assumption was made that the fiber volumes were comparable and the mean cross-sectional areas were used as a relative metric between fiber groups. The mean cross-sectional areas given by Parkins [17] are 1.1716E-7 m^2 and 1.1673E-7 m^2 for sized and unsized AS-4, respectively. The mean cross-sectional area of 1.1168E-7 m^2 was used for both sized and unsized T300 because both were from the same lots of fibers as previously discussed. There was about five percent difference in mean cross-sectional areas between the AS-4 and the T300. The difference was small enough that the results concurred with the maximum load results for all of the impregnated specimen results. The AS-4 fibers were generally stronger than the T300 fibers, except in the case of the dry-fiber bundles. The sized AS-4 produced stronger impregnated specimens than the unsized AS-4. The sized T300 produced stronger 8552 impregnated specimens than the unsized T300. However, this was reversed for the 3501-6 epoxy. The unsized fibers showed the highest percentage change in maximum loads when impregnated. This was due to the maximum loads of the unsized-dry fibers being lower and increasing to nearly the same strengths as the sized fibers when impregnated. Because the same lots of fibers were used for both the sized and unsized T300 tests, it was clear from the T300 results that sizing influences the maximum loads of dry-fiber bundles. The sizing was washed from the sized T300 samples for the unsized T300 tests. This means that sizing is a considerable issue in dry-fiber bundle testing.

The dry-bundle results may be summarized as follows:

- The NBS values were higher for the unsized-fiber bundles.
- AS-4 fibers were stiffer than T300 fibers.
- Sized AS-4 fibers were stronger than sized T300 fibers.
- Unsized T300 fibers were stronger than unsized AS-4 fibers.

The impregnated-bundle results may be summarized as follows:

- 3501-6 epoxy increased the NBS more than 8552.
- 8552 epoxy generally produced stronger specimens.
- AS-4 fibers produced stronger specimens than T300 fibers.
- AS-4 fibers generally produced higher NBS values than T300 fibers.
- Sized fibers generally produced stronger specimens than unsized fibers.

Overall, the development of the dry-fiber bundle test method was successful. The results that were obtained have COV values that are for the most part well within the 5~25 range discussed by Pheonix. Most of the values were toward the low end of the range. This is important because the low COV values indicate that the variabilities encountered were due to variability in the fibers rather than in the test method. Every reasonable effort was made to insure minimum introduction of variability by the test method. This test method does allow enough specimens to be efficiently tested to compile statistically significant results. Test results from a statistically significant number of specimens would cause the sample properties to dominate the results, negating the very slight amount of variability that could be introduced by the test method. Dry-fiber bundle test data using this method could be used to bridge the gap between theoretical and real fiber bundle behavior.

Recommendations

Further work as another phase of this project warrants some recommendations. Due to little control on the amount of sizing that is applied to fiber bundles during production, the influence of sizing should be further explored. It would be of interest to wash the sizing from some of the sized AS-4 fibers and compare the test results to those of the sized AS-4 to see if the results are similar to the T300 results from this research. Because most carbon-fiber bundles are sized in production, understanding the influence of sizing better would allow researchers to test the sized-fiber bundles and know how the results would correlate to results of the fibers if the sizing was washed from them.

Another interesting variation of dry-fiber bundle testing would be the influence of changing the gage length of the specimens. The effects of gage lengths were discussed in Chapter 2. Considering Rosen's [2] explanation of a higher probability of long fibers being weaker than short fibers, variation of the gage length could show that shorter specimens withstand higher loads. This could provide more insight to the flaw distributions along the fibers. Variation of the gage lengths would require that alignment rods of appropriate lengths be machined. If the lengths were judiciously chosen, the gage lengths could be varied by about 50 mm (2") using the same alignment rods. The need to try longer gage lengths may not be necessary based on the results herein, but shorter specimens could produce results that lead to recognizable trends.

Experimentation with the impregnation process could lead to interesting results. Variations of pressure and temperatures, as well as length of times that are used to

impregnate the fiber bundles could change the strength characteristics. It would also be important to find if the time between impregnation and curing is critical.

One important recommendation is that any close scrutiny of trends in the lower part of the data should use the raw data. When the data were manipulated to eliminate any offsets in the linear sections from tab slips, some of the lower data points were linearized. This was because some tests had a small amount of initial takeup in the test machine. The takeup caused the initial line to lay flat until the specimen loaded up. These flat areas were shifted to the negative region of the graphs when the aligned data were shifted. It was written into the Matlab® codes to linearize the first ten data points from the origin to align with the rest of the data. Because of these alterations in the lower portions of the data, any important information desired from the very early portions of the tests should be taken from the raw data.

There are several possible applications for the data that has been compiled during this research. Among these are developments for the LLS model, dissipated strain energy density research, and further exploration of the link between dry and impregnated fiber bundle test results.

There are some recommendations for verification of this dry-bundle test method. The first is to research the link between theory and the experimental data from this test method. If the theory has been well substantiated and experimental data match the theory, the test method is further validated. The second is to identify the location and number of fibers broke at the first major failure. If a substantial number of filament breaks were initiated at the tab-fiber interface area, it would be an indication that the test method was introducing error in the data. Acoustic emission measurements could be

used to determine the location of breaks within a fiber bundle and optical techniques could be used to determine the number of filaments broken. Variation of the gage length could be used here to determine if the test method was introducing error. Different gage lengths should yield different results, due to flaw distributions. If all gage lengths yield the same results, then it is likely that the test method is causing bias in the results due to end effects at the tab-fiber interfaces.

REFERENCES CITED

[1] Talreja, R., "Statistical Considerations," *Fatigue of Composite Materials*, Elsevier Science Publishers B.V., 1990.

[2] Rosen, B. W., "Tensile Failure of Fibrous Composites," *AIAA Journal*, Vol. 2, No. 11, 1964.

[3] Gao, Z., Reifsnider, K. L., "Micromechanics of Tensile Strength in Composite Systems," *Composite Materials: Fatigue and Fracture, Fourth Volume*, ASTM STP 1993, pp. 453-470.

[4] Harlow, D. G., Phoenix, S. L., "The Chain-of-Bundles Probability Model For the Strength of Fibrous Materials I: Analysis and Conjectures," *Journal of Composite Materials*, Vol. 12, 1978, pp. 195-214.

[5] Harlow, D. G., Phoenix, S. L., "The Chain-of-Bundles Probability Model For the Strength of Fibrous Materials II: A numerical Study of Convergence," *Journal of Composite Materials*, Vol. 12, 1978, pp. 314-334.

[6] Daniels, H. E., "The Statistical Theory of the Strength of Bundles of Thread.," *Proceedings of the Royal Society, London*, Vol. 183A, 1945, pp. 405-435.

[7] Coleman, B. D., "On the Strength of Classical Fibres and Fibre Bundles," *Journal of the Mechanics and Physics of Solids*, Vol. 7, pp. 60-70.

[8] Beyerlein, I. J., Phoenix, S. L., Chapter 1.19, *Comprehensive Composite Materials*, (A. Kelly and C. Zweben, eds.), Pergamon – Elsevier Science, Vol. 1, 2000

[9] Phoenix, S. L., "Statistical Aspects of Failure of Fibrous Materials," *Composite Materials: Testing and Design (Fifth Conference)*, ASTM STP 674, S. W. Tsai, Ed., American Society for Testing and Materials, 1979, pp. 455-483.

[10] Chiao, T. T., Moore, R. L., "A Tensile Test Method for Fibers," *Journal of Composite Materials*, Vol. 4, January 1970, pp. 118-123.

[11] Hancock, J. R., Swanson, G. D., "A Tension Test for Filamentary Composites," *Journal of Composite Materials*, Vol. 5, July 1971, pp. 414-416.

REFERENCES CITED -- Continued

[12] Wu, E. M., Robinson, C. S., "Computational Micro-Mechanics for Probabilistic Failure of Fiber Composites in Tension," *Composites Science and Technology*, 58, 1998, pp. 1421-1432.

[13] Batdorf, S. B., Ghaffarian, R., "Size Effect and Strength Variability of Unidirectional Composites," *International Journal of Fracture*, 26, 1984, pp. 113-123.

[14] Batdorf, S. B., "Note on Composite Size Effect," *Journal of Composites Technology and Research*, JCTRER, Vol. 11, No. 1, Spring 1989, pp. 35-37.

[15] *Handbook of Composites*, George Lubin, Ed., Van Nostrand Reinhold Company Inc., 1982.

[16] Schimpf, Warren, Meeting at Hexcel Corporation, October, 1998.

[17] Office of Naval Research Interim Progress Report for 7/1999 – 4/2000, for Montana State University-Bozeman research under MSU Contract #290055, Dallas W. Parkins Jr., April, 2000.

APPENDIX

ADDITIONAL SOURCES BIBLIOGRAPHY

ADDITIONAL SOURCES

A.1. Amaniapong, G., Burgoyne, C. J., "Statistical Variability in the Strength and Failure Strain of Aramid and Polyester Yarns," *Journal of Materials Science*, 29, 1994,pp. 5141-5152.

A.2. Bauld, Jr., N. R., *Mechanics of Materials*, 1st Ed., Brooks/Cole Engineering Division, 1982.

A.3. Beyerlein, I. J., Phoenix, S. L., "Stress Profiles and Energy Release Rates Around Fiber Breaks in a Lamina with Propagating Zones of Matrix Yielding and Debonding," *Composites Science and Technology*, 57, 1997, pp. 869-885.

A.4. Chi, Z., Chou, T., Shen, G., "Determination of Single Fibre Strength Distribution from Bundle Testings," Yarns," *Journal of Materials Science*, 19, 1984, pp. 3319-3324.

A.5. Daniel, I. M., Lee, J., "Damage Development in Composite Laminates Under Monotonic Loading," *Journal of Composites Technology and Research*, JCRTER, Vol, 12, No. 2Summer 1990, pp. 98-102.

A.6. Goda, K., Park, J. M., Netravali, A. N., "A New Theory to Obtain Weibull Fibre Strength Parameters from a Single-Fibre Composite Test," *Journal of Material Science*, 30, 1995, pp. 2722-2728.

A.7. *Handbook of Chemistry and Physics*, 72nd Ed., CRC Press, Inc., New York, 1991.

A.8. Hodge, A. J., "A Statistical Comparison of Two Carbon Fiber/Epoxy Fabrication Techniques," *NASA Technical Paper 3179*, National Aeronautics and Space Administration Scientific and Technical Information Program, 1991.

A.9. Juvinall, R. C., "Chapter 17 Statistical Considerations," *Engineering Consideration of Stress, Strain, and Strength*, McGraw-Hill Book Company.

A.10. Kakavas, P. A., Anifantis, N. K., Baxevanakis, K., Datsareas, D. E., Papanicolaou, G. C. "The Effect of Interfacial Imperfections of the Micromechanical Stress and Strain Distribution in Fibre Reinforced Composites," *Journal of Materials Science*, 30,1995, pp. 189-202.

ADDITIONAL SOURCES -- Continued

A.11. Li, Z., Grubb, D. T., "Single-Fibre Polymer Composites; Part I: Interfacial Shear Strength and Stress Distribution in the Pull-Out Test," *Journal of Materials Science*, 29, 1994,pp. 189-202.

A.12. Madhukar, M. S., Drzal, L. T., "Fiber-Matrix Adhesion and Its Effect on Composite Mechanical Properites: II. Longitudinal (0°) and Transverse (90°) Tensile and Flexure Behavior of Grphite/Epoxy Composites," *Journal of Composite Materials*, Vol. 25, August 1991, pp. 959-991.

A.13. Montgomery, D. C., Runger, G. C., Hubele, N. F., *Engineering Statistics*, 1st Ed., John Wiley and Sons, Inc., New York, 1997.

A.14. Perry, R. H. and Green, D. W., *Perry's Chemical Engineers' Handbook*, 6th Ed., McGraw-Hill Inc. New York, 1997.

A.15. Phoenix, S. L., "Clamp Effects in Fiber Testing," *Journal of Composite Materials*, Vol. 6, July 1972, p. 322.

A.16. Phoenix, S. L., Smith, R. L., "Asymptotic Distributions for the Failure of Fibrous Materials Under Series-Parallel Structure and Equal Load-Sharing," *Journal of Applied Mechanics*, Vol. 48, March 1981, pp. 75-82.

A.17. Rosen, B. W., "Mechanics of Composite Strengthening," *Fiber Composite Materials*, American Society for Metals, Metals Park, OH, 1965, pp. 37-75.

A.18. Serway, R. A., *Physics for Scientists and Engineers with Modern Physics*, 3rd Ed., Saunders College Publishing, 1990.

A.19. Strorer, R. A., *1997 Annual Book of ASTM Standards, Section 15: General Products,Chemical Specialties, and End Use Products*, Vol. 15.03 Space Simulation;Aerospace and Aircraft High Modulus Fibers and Composites, 1997.

A.20. *The Student Edition of MATLAB: Version 4: User's Guide*, J. Scordato, Ed., Prentice-Hall, Inc., 1995.

A.21. Vangel, M. G., "Design Allowables from Regression Models Using Data from Several Batches," *Composite Materials: Testing and Design (Twelfth Volume)*, ASTM STP 1274, 1996, pp. 358-370.

ADDITIONAL SOURCES -- Continued

A.22. Weibull, W., "A Statistical Distribution Function of Wide Applicability," *Journal of Applied Mechanics*, 18, 1951, pp. 293-297.

A.23. Wu, H. F., "Statistical Analysis of Tensile Strength of ARALL® Laminates," *Journal of Composite Materials*, Vol. 23, October 1989, pp. 1065-1080.

A.24. Zhang, S. D., Ding, E. J., Numerical Simulations of Burst Processes in Fiber Bundles,"*Journal of Physics A: Mathematics and General*, 28, 1995, pp. 4323-4338.

A.25. Zhang, S. D., Ding, E. J., "Burst-Size Distribution in Fiber-Bundles with Local Load Sharing," *Physics Letters A*, 193, 1994, pp. 425-430.

A.26. Zwillinger, D., *CRC Standard Mathematical Tables and Formulae*, 30th Ed., CRC Press, Inc., 1996.